NIST-GCR-89-566

An Experimental Study of the Pyrolysis of Pure and Fire Retarded Cellulose

Yi Chen

Brown University
Division of Engineering
Providence, RI

May 1989

Issued June 1989

Prepared for
U.S. DEPARTMENT OF COMMERCE
National Institute of Standards and Technology
National Engineering Laboratory
Center for Fire Research
Gaithersburg, MD 20899

NIST-GCR-89-566

An Experimental Study of the Pyrolysis of Pure and Fire Retarded Cellulose

Yi Chen

Brown University
Division of Engineering
Providence, RI

May 1989

Issued June 1989

NIST Grant No. 60NANB8D0851

National Bureau of Standards became the National Institute of Standards and Technology on August 23, 1988, when the Omnibus Trade and Competitiveness Act was signed. NIST retains all NBS functions. Its new programs will encourage improved use of technology by U.S. industry.

Prepared for
U.S. DEPARTMENT OF COMMERCE
National Institute of Standards and Technology
National Engineering Laboratory
Center for Fire Research
Gaithersburg, MD 20899

U.S. DEPARTMENT OF COMMERCE
Robert Mosbacher, Secretary
NATIONAL INSTITUTE OF STANDARDS AND TECHNOLOGY
Raymond G. Kammer, Acting Director

Notice

This report was prepared for the Center for Fire Research of the National Institute of Standards and Technology under Grant Number 60NANB8D0851. The statements and conclusions contained in this report are those of the authors and do not necessarily reflect the views of the National Institute of Standards and Technology or the Center for Fire Research.

An Experimental Study of the Pyrolysis of Pure and Fire Retarded Cellulose

by

Yi Chen

B.S., Beijing Institute of Technology, 1980
M.S., Beijing Institute of Technology, 1982

Thesis

Submitted in partial fulfillment of the requirements of the
Degree of Doctor of Philosophy in the Division of Engineering at
Brown University

May 1989

This dissertation by Yi Chen
is accepted in its present form by the
Division of Engineering as satisfying the dissertation
requirement for the degree of Doctor of Philosophy

Date 17 Jan 1989 Merwin Sibulkin
Merwin Sibulkin

Recommeded to the Graduate Council

Date 19 Jan. 1989 J. M. Calo
Joseph M. Calo

Date 10 January 1989 E. F. Greene
Edward Greene

Approved by the Graduate Council

Date . . . .

VITA

Personal Information

Date of Birth: August 11, 1958
Place of Birth: Shanxi, China

Education

B.S. Mechanical Engineering, Beijing Institute of Technology, 1980
M.S. Mechanical Engineering, Beijing Institute of Technology, 1982
Thesis: "Improvement of Acceleration Response of Turbocharged Diesel Engines"

Professional Societies

Sigma Xi
American Society of Mechanical Engineers

Publications and Presentations

"Pyrolysis of Bulk Samples of Cellulose", with M. Sibulkin and S. S. Tewari, *Proceeding of the International Conference on Physical and Chemical Processes Occurring in a Burning Cigarette*, 311 (1987).

"Heat of Gasification of Pure and Fire Retarded Cellulose", with M. Sibulkin and S. S. Tewari, *The Combined Meetings: Annual Conference on Fire Research of the National Bureau of Standards, and Twentieth Fall Technical Meeting of the Eastern Section of the Combustion Institute*, 1987.

"Improving the Acceleration Response of Turbocharged Diesel Engines with a High Pressure Air Ejection", with Y. Huang, *Transactions of Chinese Society of Internal Combustion Engines*, 2, 293 (1984).

ACKNOWLEDGMENTS

I would like to express my sincere appreciation to Professor Merwin Sibulkin, my thesis advisor, for his help and guidance with this work and throughout my entire graduate career. His encouragement, support, consideration and patience lead him to be generally acknowledged as one of the best advisors in the Division. Due to his direction, my graduate education at Brown University has been a particularly stimulating experience.

I am indebted to Professor Joseph Calo and Professor Edward Greene for their help in reading the manuscript and for many helpful and insightful ideas. Thanks are also due to Professor Eric Suuberg, Professor Richard Dobbins and Professor J. T. C. Liu, for significant information sources and guidance.

I am grateful to Mr. William Lilly, Ms. Jacqueline Groves and Ms. Sandra Spinacci for their help and cooperation. Special thanks to my fellow graduate students of the Fluids and Thermodynamics group, their friendship and comraderie has made graduate life quite enjoyable.

This work was supported by the National Bureau of Standards under Grant Numbers 60NANB6D0629 and 60NANB8D0851. Their support is gratefully acknowledged.

TABLE OF CONTENTS

Vita iii

Acknowledgements iv

Abstract vii

Nomenclature ix

List of Tables xii

List of Figures xiii

Chapter 1. Introduction 1

- 1.1. General Background on Cellulose 1
- 1.2. Previous Work on "Heats" of Pyrolysis 7
- 1.3. Previous Work on Products of Pyrolysis 10
- 1.4. Application to Diffusion Flames 14
- 1.5. The Present Work 16

Chapter 2. Heat of Gasification of Pure and Fire Retarded Cellulose 17

- 2.1. Introduction to Measurements 17
- 2.2. Experimental Apparatus 21
- 2.3. Absorbed Heat Flux Measurement 24
- 2.4. Surface Emissivity Measurement 25
- 2.5. Surface Temperature Measurement 25
- 2.6. Mass Loss Rate Measurement 27
- 2.7. Results and Discussion 27

Chapter 3. Comparison of Experimental and Theoretical Pyrolysis Results 32

- 3.1. Pyrolysis Theory 32
- 3.2. Theoretical Results 37
- 3.3. Comparison of Experimental and Theoretical Results 38

Chapter 4. Noncombustible Gaseous Products of Cellulose Pyrolysis 41

4.1 Introduction to Measurements 41
4.2. Experimental Apparatus 42
4.3. Results and Discussion 45

Chapter 5. Products of Cellulose Pyrolysis 49

5.1. Introduction to Analysis 49
5.2. Results and Discussion 54

Chapter 6. Summary of Retardant Effect on Burning of Cellulose 58

Appendix A. Sample Preparation 61

Appendix B. Data Acquisition and Processing 65

B.1. Temperature Signal Conditioning 65
B.2. Temperature and Mass Sampling 67
B.3. Temperature and Mass Data Processing 68

Appendix C. DSC Measurement of Heat of Reaction 70

Appendix D. Calibration of Gas Chromatograph 72

References 77

Tables 82

Figures 91

ABSTRACT

The pyrolysis of pure and fire retarded bulk cellulose samples in a nitrogen atmosphere is studied. Sodium hydroxide is used as the fire retardant. The study is directed toward determining the effects of the solid phase fire retardant on the burning of cellulose. The material property of pure and fire retarded cellulose which most directly affects its burning behavior, the heat of gasification, is measured by using a specially designed pyrolyzing chamber. Theoretical results are obtained for a one-dimensional pyrolysis wave propagating into cellulose by using a finite-difference calculation. The experimental results are in qualitative agreement with the computations, but give a lower value for the heat of gasification. The mass fraction of noncombustible volatiles in the total volatile products of pyrolysis, the stoichiometric oxygen/fuel ratio of the combustible volatiles and the heat of combustion per unit mass of combustible volatile are also obtained as experimental results. These data have been obtained because they are needed as inputs in diffusion flame calculations. The experimental data show that sodium hydroxide acts as a catalyst in the pyrolysis of cellulose. Its addition leads to decreases in the heat of gasification and the mass fraction of noncombustible volatiles in the total volatiles, and to increases in the stoichiometric ratio and the heat of combustion of combustible volatiles, thereby has a dual effect on cellulose burning.

The experimental techniques developed for the study will be useful in measuring the combustion properties of other charring materials and will

assist in the development of scientifically based test methods. The experimental results are useful in determining the physical mechanisms by which solid phase fire retardants act to suppress flaming combustion, and will help to provide a rational basis for the design of materials with improved fire safety characteristics.

NOMENCLATURE

A: Preexponential factor

B_h: Blowing parameter

c: Counts

C_p: Specific heat

d: Diameter

E: Activation energy

F: Calibration factor

Gr_d: Average Grashof number based on diameter

h_o: Average zero mass flux heat transfer coefficient

$\bar{h}$: Average value of heat transfer coefficient over surface area

h: Enthalpy

h_c: Heat of combustion

h_g: Heat of gasification

h_p: Heat of pyrolysis

h_r: Heat of reaction

k: Thermal conductivity

k^*: Temperature coefficient of thermal conductivity

m: Mass

$\dot{m}$: Mass flow rate

M: Molecular weight

$\bar{Nu}_d$: Average Nusselt number based on diameter

P: Pressure

P_r: Prandtl number

P_{sat}: Saturated vapor pressure

q: Heat flow per unit mass

$\dot{q}_{ab}$: Absorbed heat flux per unit time

$\dot{q}_{c}$: Convective heat flux per unit time

$\dot{q}_{emit}$: Emitted heat flux per unit time

$\dot{q}_{net}$: Net heat flux per unit time

R: Gas constant

t: Time

T: Temperature

V: Volume

$\dot{V}$: Volume flow rate

V_p: Velocity of pyrolysis wave

x: Coordinate

X: Mole fraction

Y: Mass fraction

Greek

α Absorptivity

ϵ: Emissivity

λ: Wave length

ν: Kinematic viscosity

ν_s: Stoichiometric ratio

ρ: Density

σ: Boltzmann constant

ϕ: Relative humidity

Superscripts

" Per unit area

Subscripts

A: Air

C: Char

cell: Celllulose

cv: Combustible volatiles

d: Diameter

G: Gaseous volatiles

i: Species

inert: Inert gases

m: Mixture of air and N_2

r: Reference

s: Surface

S: Solid fuel

vol: Total volatiles

∞: Ambient

LIST OF TABLES

2.1 Reflectance of Sample Surface

3.1 Material Properties Used in Pyrolysis Calculations

5.1 Mass Fractions of Char from Cellulose Pyrolysis

5.2 Elemental Composition of Cellulose

5.3 Elemental Composition of Char

5.4 Elemental Composition of Total Volatiles

5.5 Mass Fractions of Noncombustible Gases in Total Volatiles

5.6 Elemental Composition of Combustible Volatiles and Stoichiometric Ratio

5.7 Major Products of Cellulose Pyrolysis

6.1 Material Properties Used in Diffusion Flame Calculations

LIST OF FIGURES

1.1 General scheme for cellulose pyrolysis

2.1 Schematic drawing of the apparatus used in heat of gasification measurements

2.2 Schematic drawing (top view) of set-up for cellulose pyrolysis measurements

2.3 Heat flux gauge calibration curve

2.4 Vertical variation of absorbed heat flux over the sample height

2.5 Voltage outputs of thermocouple and pyrometer vs. time

2.6 Calibration of surface temperature vs. pyrometer output voltage, the data is fitted by the polynomial $T = -116 + 641V - 157V^2 + 14.6V^3$

2.7(a) An example of computer output of surface temperature vs. time $Y_R=0$; $\dot{q}''_{ab,s}=40$ kW/m^2

2.7(b) An example of computer output of mass loss rate vs. time; $Y_R=0$; $\dot{q}''_{ab,s}=40$ kW/m^2

2.7(c) An example of computer output of heat of gasification vs. time; $Y_R=0$; $\dot{q}''_{ab,s}=40$ kW/m^2

2.8 Surface temperature vs. time for different absorbed heat fluxes; $Y_R=0$

2.9 Mass loss rate vs. time for different absorbed heat fluxes; $Y_R=0$

2.10 Heat of gasification vs. time for different absorbed heat fluxes; $Y_R=0$

2.11 Surface temperature vs. time for pure and retarded samples; $\dot{q}''_{ab,s}=40$ kW/m^2

2.12 Mass loss rate vs. time for pure and retarded samples; $\dot{q}''_{ab,s}=40$ kW/m^2

2.13 Heat of gasification vs. time for pure and retarded samples; $\dot{q}''_{ab,s}=40$ kW/m^2

2.14 Surface temperature vs. retardant concentration; $\dot{q}''_{ab,s}=40$ kW/m^2: t=200s.

2.15 Mass loss rate vs. retardant concentration; $\dot{q}''_{ab,s}=40$ kW/m^2 ; t=200s.

2.16 Heat of gasification vs. retardant concentration; $\dot{q}''_{ab,s}=40$ kW/m^2 ; t=200s.

3.1 Control volume used in pyrolysis analysis of a charring fuel

3.2 Theoretical surface temperature vs. time for pure and retarded cellulose

3.3 Theoretical mass loss rate vs. time for pure and retarded cellulose

3.4 Theoretical heat of gasification vs. time for pure and retarded cellulose

3.5 Experimental and theoretical mass loss rate vs. time for pure cellulose; $Y_R=0$

3.6 Experimental and theoretical mass loss rate vs. time for retarded cellulose; $Y_R=0.03$

4.1 Schematic drawing of apparatus used in measurements of gaseous products

4.2 Schematic drawing of GC flow system

4.3 An example of output of GC analysis; $Y_R=0.03$; $t=180s$.

4.4 Mass fraction of CO_2, H_2O and CO vs. time for pure and retarded cellulose samples; $\dot{q}''_{ab,s}=40\ kW/m^2$

4.5 Mass fraction of CO_2, H_2O and CO vs. retarded concentration; $\dot{q}''_{ab,s}=40\ kW/m^2$; $t=180s$.

5.1 Effects of retardant concentration on major products of cellulose pyrolysis.

A.1 NaOH retardant concentration in the sample, Y_R, as a function of retardant concentration in the cellulose slurry, Y_A

A.2 Schematic drawing of the apparatus for making cellulose samples

B.1 Sequence of temperature and mass sampling times

C.1 An example of DSC output of differential heat flow vs. temperature

C.2 Comparison of DSC results for pure and retarded samples

D.1 Calibration curve of water mass vs. integrator count

CHAPTER 1

INTRODUCTION

1.1 General Background on Cellulose Pyrolysis

Cellulose is a major constituent of combustible materials available as fuel in fires, for example, Fremy (1868) showed that wood is 40% cellulose. The combustion of cellulose, therefore, has always been closely associated with the development of mankind. An essential feature of the combustion of cellulose is its pyrolysis, or thermal degradation. Considerable effort has been expended in the study of cellulose pyrolysis because of its central importance in fire research and cellulosic materials utilization. The study of cellulose pyrolysis is closely associated with practical problems such as textile flame-retardancy, energy and chemical production from thermal conversion of biomass and air pollution research.

A cellulose molecule consists of long chains of repeating glucosan units, each having a formula of $C_6H_{10}O_5$. Cellulose seems to be divided up into periodically spaced crystalline or highly ordered regions, in which the molecules are linked together by hydrogen bonds, and into amorphous or highly disordered regions, where this kind of bonding is mostly absent.

The literature on cellulose is mainly concerned with its thermal degradation, although some burning studies have also been reported. An extensive survey of this literature is given by Shafizadeh (1968); more recent work is discussed in Lewin and Basch (1978).

Pyrolysis encompasses the processes by which gaseous fuel is liberated to support fire by the breakdown of the fuel constituents under the influence of heat. The chemistry of cellulose pyrolysis is very complex. Different mechanisms have been suggested by numerous investigators. The one pointed out by Kilzer and Broido (1965) has been generally accepted. It maintains that pyrolysis of cellulose proceeds by two distinct competing paths, which involving at least three concurrent and consecutive processes, each including one or more reactions. As illustrated in Fig. 1.1., the two paths include: (1) the dehydration and char-forming reactions, which are initiated at lower temperatures and continue at elevated temperature; and (2) depolymerization and levoglucosan or tar-forming reactions, which gather momentum at temperatures above 250°C and result in rapid volatilization. The first process, which is slightly endothermic, is attributed to an inter-molecular reaction with loss of water to form a "dehydrocellulose". During the second endothermic process, which competes with the first process for native cellulose, levoglucosan, the major constituent of the tar, is postulated to arise from the rearrangement of 1, 4-anhydro-α-D-glucopyranose formed in an "unzipping" reaction. The tar then breaks down into highly flammable volatiles, which support flaming combustion, and into char. Finally, the exothermic process is ascribed to reactions of the "dehydrocellulose", which experiences carbon-carbon and carbon-oxygen bond ruptures and hydride ion transfers to produce volatile carbon-containing compounds and hydrogen, and inter-molecular condensations to produce char.

Although the nature and extent of many individual reactions involved in cellulose pyrolysis are not known, or sufficiently defined, it has been found by Lipska et al. (1966), McCarter (1972), Lee et al. (1977 and 1981), Kashiwagi et al. (1981), Cullis et al. (1983), Mok et al. (1983), Nunn et al. (1985) and Ohlemiller (1987) that these reactions are highly influenced by temperature, external radiant flux, external heating rate, total time of heating, sample type, amibient oxygen concentration, water content, and pressure. Lipska and Parker (1966) studied the isothermal pyrolysis of cellulose in nitrogen over a temperature range of 250 - 300°C, and found that decomposition and volatilization occuring during pyrolysis, increases with increasing temperature. McCarter (1972) performed pyrolysis studies of cellulose at rates approaching those in burning, and found that the activation energy at high temperature differs from that previously reported at lower temperature. Mok et al. (1983) investigated the effects of pressure on cellulose pyrolysis and found that increased pressure favors char formation.

Fire retardation is essentially an interruption or suppression of the burning process. Research on the fire retardation of cellulose has had a long history with the aim of preventing destructive fires. There is a voluminous literature on the effects of fire-retarding additives on the thermal degradation of polymeric materials. An extensive discussion of fire retardancy is given in the Encyclopedia of Polymer Science and Technology (1967). Systematic coverage of fire retardants is presented in Fire Safety Aspects of Polymeric Materials, Vol. 1. (1977). Current commercial fire-retarded materials have been reviewed by Bauer (1978). The previously mentioned reviews by Shafizadeh (1968) and Lewin and Basch (1978) also discuss effects of fire retardents on cellulosic materials.

The theories, which have been advanced to explain the effect of fire retardants on cellulose are categorized by Shafizadeh (1968) and Mark et al. (1975) as follows.

(1) Coating therories. These attribute the retardant action to a coating of the fibers by the melted or foamed retardant, or both, restricting the escape of volatile products of cellulose pyrolysis and the access of atmospheric oxygen to the reaction zone.

(2) Thermal theories. These attribute the retardant action to a lowering of cellulose temperature, brought about by: (a) insulating cellulose by a coating of melted or foamed chemical, or both; or (b) absorbing the heat, which would otherwise reach cellulose, by endothermic reaction in the retardant; or (c) increasing thermal conductivity of cellulose and thus slowing down the temperature rise.

(3) Chemical theories. These attribute the retardant actions to a modification of the initial pyrolytic reactions in cellulose pyrolysis through: (a) catalysis of decomposition reactions leading to dehydration and char formation, thus increasing the production of CO_2, H_2O and char; and (b) inhibition of decomposition reactions leading to tar formation, and thus decreasing the production of flammable volatiles.

(4) Gas phase theories. These attribute the retardant action to modification of the volatiles from cellulose pyrolysis by gases evolved during decomposition of the retardant, such as (a) diluting the flammable volatile decomposition products with nonflammable gases, such as CO_2 and H_2O; and (b) introducing decomposition products from the retardant that act as chain breakers to terminate free-radical chain reactions in the flame.

Many researchers, such as Kilzer et al. (1965), have believed that the two competitive paths feature of pyrolysis, as shown in Fig. 1.1., applies to fire-retarded cellulose as well, but McCarter (1972) believes that the two main paths are sequential, not competitive, for retarded cellulose. Tang et al. (1964), Kilzer et al. (1965), McCarter (1972) and Shafizadeh (1968 and 1975) believe that fire retardants work by catalysis of the dehydration path, thus increasing the production of char, water and CO_2 at the expense of tar, which releases the flammable volatiles.

A notable early study on the effect of flame retardants on cellulose was performed by Tang and Neill (1964). They found an increase in the yield of char, and a decrease in the heat of pyrolysis when fire retardants are added. In another study of cellulose pyrolysis, Lipska and Martin (1971) found strong effects of acid treatment on the isothermal pyrolysis rate. These types of studies are continuing; a recent example is Rogers and Ohlemiller (1981) who investigated the degradation of cellulosic material of the type used in home insulation. Paker and Lipska (1969) and Mok et al. (1983) believe that some of the char is produced by the action of retardants on levoglucosan. Drews and Barker (1974) found that the chemical nature of the char produced by pyrolyzing cellulose was independent of the different types of organophosphorous compounds added as retardants. Woodley (1971) found that a retardant such as $KHCO_3$ causes changes in pyrolysis vapor products of cellulose. The pyrolysis products depend on the concentration, rather than the type of retardants. Kilzer et al. (1965) speculated that water helps cool down the condensed phase to a temperature at which it no longer supplies flammable volatiles. Mok et al. (1983) believe that retardants tend, overall, to lower the decomposition temperature of cellulose, and thereby modify its pyrolysis so that char residues are increased, and the amount and/or flammability of the evolved vapors are decreased.

A number of fire retardants, primarily inorganic salts, have been studied in the literature cited above. The most comprehensive comparative study of fire retardant effects on cellulose was made by Shafizadeh et al. (1975) who ranked 21 retardants on the basis of their effect on char production and on the heat of combustion of the gaseous pyrolysate. The retardants which span the range of effectiveness given by Shafizadeh, in order of increasing effectiveness, are $(NH_4)_2\ CO_3$, $NaHCO_3$, Na_2CO_3 and NaOH.

Lipska and Martin (1971) studied retarded cellulose in a nitrogen atmosphere and found that the presence of oxygen, even in low concentrations, will increase the rate of decompostion in the initial period of pyrolysis. They also found that the overall pattern of decomposition of pyrolyzed cellulose treated with basic and neutral additives is similar to that of the untreated cellulose, but the pyrolytic decomposition of cellulose treated with acidic retardants takes on different characteristics. They suggested that the extremely rapid decomposition rates of the acidic-salt-treated samples may be caused by the combined efforts of hydrolysis and pyrolysis.

As a result of rapidly developing computational techniques, theoretical modelling of cellulose pyrolysis has become popular. Kanury and Blackshear (1970) proposed a simple linear model to compute the thermal properties of partially charred, woody solids, given information about thermal conductivity and specific heat as a function of the extent of charring. Roberts (1971) conducted a thermal analysis of wood pyrolysis and concluded that the conventional assumption of constant thermal diffusivity and no internal convective heat transfer cannot be justified for the entire wood pyrolysis processes. In the model developed by Kung (1972) for wood pyrolysis, thermal decomposition was assumed to occur by a first order reaction with an Arrhenius temperature dependence. A parametric study was made of the sensitivity of such results as temperature-dependent mass loss rate to changes in the assumed values of the kinetic constants and heat of gasification. This type of analysis was extended by Kansa et al. (1977) to include a momentum equation for the motion of the pyrolysis gases in the interior of the solid, thus allowing the build-up of internal pressure to be calculated. Even though numerous models have been developed to study cellulose pyrolysis and predict its results, at present there is no model which accurately describes the entire cellulose pyrolysis process. However, most researchers agree that the thermal properties of cellulose and char, and the "heats" of pyrolysis are the factors which most strongly affect cellulose pyrolysis, and thus need to be studied further.

1.2 Previous Work on "Heats" of Pyrolysis

In the literature, several kinds of "Heat" terms have been used to describe the energy changes occuring during cellulose pyrolysis. These are: (1) the heat of pyrolysis, h_p, which is defined as the difference in enthalpy between the pyrolysis products (volatiles plus char) at the cellulose sample surface temperature and the original cellulose at ambient temperature; (2)

the heat of reaction, h_r, which is defined as the difference in enthalpy between the products and reactants at ambient temperature; and (3) the heat of gasification, h_g, which is defined as the ratio of the net surface heat flux to the volatile generation rate due to pyrolysis. Whereas h_p and h_r are thermodynamics quantities, h_g is not. While h_p and h_r can be calculated from other thermodynamic quantitites, h_g must be obtained by measurement. By conventions, h_p, h_r and h_g are positive for an endothermic reaction.

Experimentally, DTA (Differential Thermal Analysis) and DSC (Differential Scanning Colorimetry) are usually used to obtain the heat of pyrolysis and the heat of reaction. Tang and Neill (1964) used DTA to measure the heat of reaction for both unretarded and retarded cellulose samples. They found that retarded samples have lower heats of reaction than unretarded samples, and give a value of 368±15 J/g (endothermic). They speculated that this is the result of the endothermic depolymerization and dehydration of cellulose and the exothermic polymerization and aromatization of pyrolysis products. Roberts (1971) conducted a survey on the heat of reaction during the pyrolysis of cellulose. The data reported, which are from DTA and other experiments, cover a range from 370 J/g (endothermic) to -80 J/g (exothermic). It was concluded that the width of the range of results is due to variations in experimental method and in the conditions of pyrolysis. Mok et al. (1983) used DSC to investigate the effects of pressure and purge gas flow rate on the heat of cellulose pyrolysis. It was found that the heat of pyrolysis decreases with increasing pressure and decreasing flow rate, and that preheating of cellulose samples produces a lower heat of pyrolysis.

Lee et al. (1977) performs experiments on wood pyrolysis at fire-level surface heat fluxes using laser simulation, and found that the overall heat of reaction varies from endothermic in the case of low heating rate to exothermic for high heating rate, ranging from 610 J/g to -1714 J/g. Tewarson (1980) obtained experimental data on the heat of gasification for oak which gave 1700 J/g for external heat flux ≤ 46 kW/m^2, and 5500 J/g for external heat flux > 46 kW/m^2.

Kung et al. (1973) developed a mathematical model for the pyrolysis of a wooden cylinder, which, in addition to the usual consideration of transient heat conduction and Arrhenius reaction rate, included terms allowing for internal heat convection of volatiles and variable thermal properties. The model was used together with experimental values from Roberts and Clough's (1963) work to yield a heat of reaction of 202 J/g (endothermic). Calculated results from the model also show that the pyrolysis rate increases with an assumed increase of heat of reaction. The heat of reaction is deemed as one of the important parameters in wood pyrolysis. Sibulkin (1986) examined the relationships between the heats of reaction, pyrolysis and gasification for vaporizing and charring materials. It was shown that the heat of pyrolysis, h_p, is equal to the heat of gasification, h_g, only for steady burning of thermally thick, vaporizing material, such as PMMA (polymethyl methacrylate); for charring materials, such as cellulose, there is no simple relationship between h_g and h_p. Solutions for pyrolysis of cellulose were also obtained by him using a one-dimensional numerical model with material properties estimated from the literature. It was found that after an initial transient, h_g is about twice h_p. For a semi-infinite slab the value of h_g remains nearly constant; while for a finite slab the value of h_g decreases with time to values less than h_p. Changes in the assumed chemical reaction rate and the incident heat flux are found to have a minor effect on h_g. The heat of gasification is also relatively insensitive to changes in the char density and thermal conductivity. The variation of h_g with time is nearly independent of the assumed heat of reaction, h_r, but the magnitude of h_g varies almost directly with the value of h_r.

1.3 Previous Work on Products of Pyrolysis

In order to understand pyrolysis mechanisms and develop more effective fire retardants, many studies have been done on the pyrolysis products of wood and pure and retarded cellulose. Generally, pyrolysis products of cellulose include char, tar, CO, CO_2, H_2O and other volatiles according to the mechanism described in Section 1.1.

Instruments such as GC (Gas Chromatograph) and MS (Mass Spectrometer) are extensively used in the experiments for pyrolysis products measurements. Lipska and Martin (1971) performed GC analyses of the pyrolysis of cellulose in nitrogen and found a complex range of products produced. Wodley (1971) used GC and MS to measure the pyrolysis products of both unretarded and retarded cellulose and levoglucosan. The results indicated that fire retardants decrease the number of compounds formed during pyrolysis. The comparison of the pyrolysis products generated under different atmospheres (N_2 and air) in the temperature range of 330-400°C showed that the formation of pyrolysis products is independent of either atmosphere or temperature. The pyrolysis products formed for different fire retardants and concentrations indicated that the products depend more on the concentration than on the type of retardant. Drews and Barker (1974) investigated the chars produced from the burning of a series of cotton fabrics treated with different types of phosphorus compounds, and found that the chemical nature of the char formed seems to be independent of the chemical structure of the phosphorus compound. Kashiwagi et al. (1981) measured the pyrolysis products of thermally thick white pine using GC. The experiments were done for different radiant fluxes in both nitrogen and nitrogen-oxygen atmospheres. The results indicated that the yields of char, CO, CO_2 and THC (total hydocarbon) increase with increasing radiant flux in a nitrogen atmosphere. In oxygen-containing atmospheres, the effects of the radiant flux on the evolved gaseous products are different. CO_2 production increases significantly with increasing radiant flux, whereas CO evolution does not. It was pointed out that ambient oxygen also significantly increases char depth and changes the volatile products distribution during pyrolysis. It was concluded, therefore, that the effects of ambient oxygen on the gasification process cannot be ignored. are different. The CO_2 production increases significantly with increasing radiant flux, but CO evolution does not change significantly at different radiant fluxes. It was pointed out that ambient oxygen also significantly increases char depth and changes the volatile products distribution during pyrolysis. It was concluded, therefore, that the effects of ambient oxygen on the gasification process cannot be ignored.

Chan et al. (1985) performed experiments on product formation in the rapid pyrolysis of thermally thick wood particles. The results show that the thermal properties, heat flux, and particle size, interact in a nonlinear way to alter the ultimate yields, which include char, tar, water, and gases such as CH_4, C_2H_4, CO, CO_2, and H_2O. It was also found that as particle size and heat flux are varied in the experiments, the gas products contain changing proportions of chemicals such as CH_4 and C_2H_4 as functions of time, which indicates a potential for optimization of product distribution from thermally thick biomass particles in the event that costly size reduction must be avoided. Roy et al. (1985) studied pyrolysis of aspen poplar under vacuum. The pyrolysis products obtained are char, water, gases such as CO, CO_2, CH_4, and pyrolytic oils which contain liquid phase organic compounds, such as acetic and formic acids. Parameters such as temperature, particle size, heating rate, total pressure, and residence time of gases and vapours in the reactor were examined. Low pressure, short residence time and high heating rate were found to favour the pyrolytic oil yield, and the yield of char was correspondingly low. Nunn et al. (1985) studied the effect of temperature on the yields, composition and rates of evolution of major products from the rapid pyrolysis of sweet gum hardwood. It was found that the pyrolysis products include char, tar, CO, CO_2, H_2O, CH_4, C_2H_4, HCHO, and acetic acid. The experimental results indicated that tar is the major pyrolysis product at temperatures above 800K; secondary cracking of this tar contributes significantly to the yields of CO, CH_4, C_2H_4 and most of the other light gaseous products at temperatures above 900 - 950K. On a weight basis, CO is the dominant gaseous product above 850K, while CO_2 and water dominate the gaseous products below 850K. Total gas production (including water) increases monotonically with increasing temperature, where light hydrocarbon gases such as CH_4, C_2H_4 and C_3H_6 are relatively minor products. Ohlemiller et al. (1987) did experiments on wood pyrolysis at fire-level heat fluxes in atmospheres of varying oxygen concentration. The results show that the major pyrolysis products, which include CO, CO_2, water, tar and THC vary rapidly with time only in the first 2 or 3, minutes but their rate of emission continues to vary more slowly with prolonged heat exposure. It was also indicated by GC and MS measurements that the organic condensate or tar is extreamely complex in composition, probably exceeding 700 constituents.

On the other hand, theoretical work on predicting pyrolysis products is in steady progress as well. Chan et al. (1985) developed a one-dimensional model to predict volatiles release rate and composition as a function of biomass physical properties. The predicted shape and amplitude compare favorably with the experimental data. However, further refinement of the current kinetic mechanism and thermal property variation with temperature in the model is needed. Nunn et al. (1985) did a linear simulation of whole wood pyrolysis behavior based on kinetic data for the pyrolysis of cellulose and lignin. It was found that the model predicts total weight loss (i.e. total weight of products), quite satisfactorily, but breaks down for individual products and total gas yield. Therefore, further model improvement is needed.

1.4 Application to Diffusion Flames

Flames are broadly classfied as pre-mixed and diffusion flames. A pre-mixed flame occurs if fuel and oxidizer are homogeneouly mixed. This is possible if the rate at which fuel and oxidizer diffuse into each other is greater than the rate at which they chemically react with each other. On the other hand, a diffusion flame occurs if the diffusion rate of fuel and oxidizer is slow compared to their reaction rate. In such a situation, the flame exists only in a "reaction zone", where the fuel and oxidizer, which are initially separated, mix together through molecular diffusion and turbulent dispersion.

Natural fires are free convection, diffusion flames; their analysis involves both solid and gas phase phenomena. After the ignition from an external source the combustion in the gas phase feeds heat by radiation and conduction to the solid fuel, which in response, generates fuel volatiles, which in turn, sustain the combustion. This conversion of a solid phase into gaseous volatiles involves the phenomenon of pyrolysis. According to Emmons (1980) and Atreya (1983), pyrolysis is one of the three separable components in fire phenomena, with other the two being ignition and fire spread. Moreover, cellulose maintains its dimensional stability while burning, which results in a "classical" diffusion flame enveloping the sample. The study of cellulose pyrolysis is necessary in order to understand diffusion flames, and the results can be readily applied to diffusion flame theory.

One of the modern developments in fire science has been the use of mathematical models. Such models are used to gain a more fundamental understanding of fire phenomena, to interpret standard fire tests, and to design fuel materials or buildings with a prescribed degree of fire safety. Diffusion flame models, e.g. Pagni (1980) and Sibulkin et al. (1982), have been developed to predict burning behavior such as burning rate and extinction limits for a solid fuel with simple geometry such as a vertical wall or a stagnation region. These models have also identified the material properties which most affect burning.

Most diffusion flame analyses to date have modeled a simple fuel, such as PMMA. For these fuels there is no accumulation of char at the fuel surface. Consequently, it can be shown that after an initial transient the surface temperature, heat of gasification and burning rate are independent of time, as long as the fuel remains thermally thick. On the other hand, materials which char, such as wood, show a dependence on time related to the growth of the char layer. Sibulkin and Tewari (1985) have studied the burning of cellulose, a particularly simple charring material.

In order to obtain quantitative results from diffusion flame models for the combustion of cellulose, a number of materials properties of the fuel-oxidizer system must be known. Two of these parameters, which most affect burning, are the heat of combustion and the heat of gasification, and their ratio is a key factor in burning rate calculation. It is the need for these data that make the study of cellulose pyrolysis very important to diffusion flame theories. Pyrolysis and combustion of cellulose have become closely coupled topics in fire research.

1.5 The Present Work

It has been revealed by the literature reviewed in the previous sections that most research on the pyrolysis of cellulosic materials is primarily concerned with details of the chemical processes which occur as the materials are heated. For this type of work, the appropriate experimental techniques are those of thermal analysis such as TGA and DSC, and the typical sample is a powdered material weighing on the order of milligrams. Although detailed chemical studies are necessary to obtain workable pyrolysis mechanisms, they are of little help in actual design of a flame resistant material.

In the present work, pyrolysis of bulk cellulose in a nitrogen atmosphere is studied. Sodium hydroxide is used as a fire retardant. The materials property of pure and fire retarded cellulose which most directly affect its burning behavior, the heat of gasification, is measured, with concurrent numerical analysis of one-dimensional pyrolysis. The heat of combustion of the volatiles, their stoichiometric ratio and the mass fraction of noncombustible volatiles produced in pyrolysis are also obtained as experimental results. These data can be used as inputs to a diffusion flame model, and the calculated results can be compared with previous cellulose burning measurements. The major objectives of the work are: (1) to develop techniques which will be useful in measuring the combustion properties of charring materials and which will assist in the development of scientifically-based test methods; and (2) to use the experimental results to determine the physical mechanisms by which solid phase fire retardants act to suppress flaming combustion, which will help to provide a rational basis for the design of materials with improved fire safety characteristics.

CHAPTER 2

HEAT OF GASIFICATION OF PURE AND FIRE-RETARDED CELLULOSE

2.1 Introduction to Measurements

As described in Section 1.5., most research on the pyrolysis of cellulosic materials has been primarily concerned with the chemical processes which occur as the material is heated, and the typical sample for this type of work is a powered material weighing on the order of milligrams. Another motivation of the study of pyrolysis is related to its role as one of the processes in the burning of solid fuels. The burning of a solid fuel, such as cellulose, can be predicted by diffusion flame theory for several simple geometries, such as a vertical wall or a stagnation region. In order to obtain quantitative results, a number of combustion-related material properties must be known. In the present study, a new type of experiment is developed, and one of the material properties which most affects burning, the heat of gasification, is measured for bulk pure and retarded cellulose samples. The measured data will be used as inputs to a diffusion flame model. The results of the numerical calculations will then be compared with the previous combustion measurements in order to understand how the retardants act to suppress fires.

A heat of gasification is defined as the ratio of the net surface heat flux resulting from flaming combustion to the volatile generation rate due to pyrolysis.

In the h_g measurements, the basic theory is as follows. The definition of the heat of gasification is

$$h_g = \frac{\dot{q}''_{net}}{\dot{m}''} \tag{2-1}$$

where: $\dot{m}''$ = sample mass loss rate per unit area; i.e., the mass flux of gaseous products leaving the surface.

$\dot{q}''_{net}$ = net heat flux going into the sample through the front surface per unit area and time

$$= \dot{q}''_{ab,s} - \dot{q}''_{emit,s} - \dot{q}''_{c,s} \tag{2-2}$$

where: 1) $\dot{q}''_{ab,s}$ = heatflux absorbed by sample front surface.

2) $\dot{q}''_{emit,s}$ = heatflux emitted from sample front surface per unit area and time.

The radiation heat transfer theory for a grey body is used to estimate the term:

$$\dot{q}''_{emit,s} = \epsilon_s \sigma \left(T_s^4 - T_\infty^4\right) \tag{2-3}$$

where: ϵ_s = emissivity of sample front surface = 0.96

σ = Boltzmann constant = 5.67×10^{-8} W/m^2 K^4

T_s = temperature of sample front surface .

T = ambient temperature = 298K

3) $\dot{q}''_{c,s}$ = heat flux due to convection through sample front surface per unit area and time.

The convective heat loss $\dot{q}''_c$ could not be measured and therefore, the natural convective heat transfer theory for vertical planes is followed to estimate the term:

$$\dot{q}''_{c,s} = \bar{h}(T_s - T_\infty) \tag{2-4}$$

where: $\bar{h}$ = average value of heat transfer coefficient over sample front surface area.

The effect of "blowing" is approximated by

$$\bar{h} = \frac{\bar{h}_o \ell n(1+B_h)}{B_h}$$

where B_h = blowing parameter

$$B_h = \frac{C_p \dot{m}}{\bar{h}_o}$$

$\bar{h}_o$ = average zero mass flux heat transfer coefficient = $\frac{k_r}{d} \overline{Nu}_d$

$\overline{Nu}_d$ = average Nusselt number based on sample diameter d

$$\overline{Nu}_d = 0.68 + 0.67\, Gr_d^{1/4} Pr^{1/4} \left[1 + \left(\frac{0.492}{Pr} \right)^{9/16} \right]^{-4/9}$$

$\overline{Gr}_d$ = average Grashof number based on sample diameter d

$$\overline{Gr}_d = \frac{g(T_s - T_\infty)\, d^3}{T_\infty\, \nu_r^{\,2}}$$

The values of C_p, k_r, Pr, and ν_r are taken as constants at T_r from the physical property table for N_2.

i.e. T_r = reference temperature = $\dfrac{T_s + T_\infty}{2}$ = 700K

C_p = specific heat capacity = 1097 J/kgK

k_r = thermal conductivity = 0.051 w/mK

Pr = Prandtl number = 0.69

ν_r = kinematic viscosity = 65×10^{-6} m^2/s.

From the equations (2-2), (2-3) and (2-4), the expression for net heat flux into the sample front surface is:

$$\dot{q}''_{net} = \dot{q}''_{ab,s} - \epsilon_s \sigma (T_s^4 - 298^4) - \bar{h}\,(T_s - 298) \qquad (2\text{-}5)$$

Thus, the basic measurements needed to obtain the heat of gasification are the absorbed heat flux, the surface emissivity, the surface temperature and the mass loss rate. Detailed descriptions of $\dot{q}''_{ab,s}$, ϵ_s, T_s and $\dot{m}''$ measurements are presented in Sections 2.3, 2.4, 2.5, and 2.6.

2.2 Experimental Apparatus

A schematic side view of the apparatus developed to measure the heat of gasification of pure and fire-retarded cellulose is shown in Fig. 2.1, while a schematic drawing of the top view of the experimental set-up shown in Fig. 2.2 gives more detailed information about the apparatus.

The pyrolysis chamber is an extensively modified glass draft shield of a top-loading electronic balance. The top of the pyrolysis chamber has an added cone through which the gases exhaust. The cellulose sample, in the form of a horizontal 2.5 cm diameter cylinder, is held by a sample holder made of ceramic foam. The sample and the holder are mounted inside the chamber. Because the sample must be enclosed in a chamber having a front window, a combination of a quartz plate (acting as an intermediate window), radiation shields and cooling coils were added to prevent breakage of the front window and to reduce heat flow to the electronic balance. In addition, air cooling (not shown) is used to keep the temperature of the chamber window and quartz plate below 200 °C so that the thermal radiation from these surfaces does not affect the measurements. An opaque shutter is used to begin the experiment at a well defined time.

A 2-stage nitrogen supply system is attached to the weighing chamber. A valve and tubing arrangement allows the chamber to be purged with pure N_2 at about 175 ℓ/min in order to remove air before the pyrolysis experiments, and to supply the chamber with pure N_2 at about 25 ℓ/min during pyrolysis to exclude oxygen from the atmosphere. An inclined tube, water manometer is used to monitor the pressure inside the weighing chamber to make sure no outside air is leaking into chamber, which shows positive pressure (in the orfer of 1mm H_2O) during pyrolysis.

The reason for using a nitrogen atmosphere during pyrolysis is related to the desire to simulate the burning of diffusion flames. Both experiment (Seshadri and Williams, 1978) and calculations (Sibulkin et al., 1982) have shown that for many types of diffusion flames the oxygen concentration between the flame and the fuel surface is close to zero. Thus the gas composition at the fuel surface during burning in air is made up of nitrogen and products of combustion (primarily H_2O, CO_2 and CO), plus possible traces of oxygen. This atmosphere is simulated by pure nitrogen in this experiment. In order to prevent air leaking in, the pyrolysis chamber is sealed at the sides by duct tape and platic sheets. The absence of oxygen in the chamber was checked periodically by gas chromatograph measurements.

In the experiments, the heat flux from the flame to the fuel surface is simulated by a pair of infrared lamps (Research Inc, Model 5305-5A). Tungsten filament, quartz envelope lamps giving a blackbody spectral distribution of energy are used. The lamps are connected electrically in series, and supplied with up to a total of 480 volts (240 volts for each lamp) through a power controller (Research Inc., Model 646). A control panel is set between the power controller and the lamps to control the heat flux and the water cooling system. A special mounting holds the lamps at an optimum angle (approximately 32° from horizontal) to provide a nearly uniform heat flux over the sample front surface. Two heat flux gages (Medtherm, 64-20-20T and 64-20-20) are used in absorbed heat flux measurement (details are given in Section 2.3).

A spectrophotomer (CARY, Model 17) and a Fourier-Transform Infrared Spectroscopy (Nicolet, Model 60SX) were used to measure the surface emissivity measurement (for details see Section 2.4). An infrared pyrometer (Raytek, series SL-300 CC) is used to measure the sample surface temperature (for details see Section 2.5). The output of the pyrometer is sent to a microcomputer (Apple IIe) for processing. An instrumentation amplifier (Interactive Microwave Inc., ADA-AMP) is used for signal conditioning of the voltage output of the pyrometer, and then connected to the data acquisition interface (Interactive Microwave Inc., ADA-LAB) of the computer. Temperature readings are taken every 0.2 seconds (for details see Appendix B).

For the mass loss rate measurements, (for details see Section 2.6), an electronic balance (Mettler, PC220) was used. The signal from the balance is sent to the computer for data processing through a special interface (Microsystems Research Corp. SOFTWEIGH). Mass readings are taken every 3 seconds.

In order to run the experiments under the same conditions, the apparatus was checked regularly at specific time intervals.

The monthly apparatus icluded: (1) heat flux gauge A and B (Medtherm, 64-20-20T and 64-20-20) versus multimeter (Fluke, 8840A) at 25 kW/m^2 to 40 $kW/^2$ using 5 kW/m^2 interval; (2) electrical balance (Mettler, PC 220) versus standard weight of 50 g; (3) blackbody (Infrared Industries Inc., Model 463) with temperature controller (Infrared Industries Inc.. Model 101B), versus its own thermocouple (Platinum/Platinum 10% Rhodium, Type S) at 400°C to 800°C at 50°C interval; (4) ADA-LAB (Apple IIe computer data acquisition interface) reading versus standard voltage source (Analogic, Model 3100) at zero to maximum pyrometer voltage output of 4 volts using 0.5 volt interval; (5) computer (Apple IIe) disk driver speed check.

The daily apparatus checking included: (1) pyrometer (Raytek, SL-300) versus blackbody (IR, Model 463) set at 500°C through ADA-LAB to both the computer and multimeter (Fluke, 8840 A). (2) the $\dot{q}''_{ab,s}$ value against the power input to the IR lamps (Research, Inc., Model 5305-5A), through multimeter (Fluke, 8840A), by placing het flux gauge A (Medtherm, 64-2020T) at the sample location, to make sure the input power indicator, RUN POT SETTING, in the control panel corresponds to the desired heat flux.

2.3 Absorbed Heat Flux Measurement

Heat flux absorbed by the sample front surface is measured using the heat flux gauge A (Medtherm, 64-20-20T). The water-cooled radiation flux gauge can be placed precisely at the sample location by means of a specially made jig. From the slope of the calibration curve supplied by the manufacturer, shown in Fig. 2.3., the output of the gauge in mV is converted into the heat flux absorbed using the following calibration factor: gauge constant = 2.295 W/cm^2 mV. The heat flux gauge B (Medterm, 64-20-20) is used as a cross-check of the working gauge.

A routine check of the heat flux (heat flux gauge A output) versus sample height was performed prior to each run using heat flux gauge A and multimeter (Fluke, 8840 A). A typical distribution curve of heat flux (gauge A output) versus sample height is presented in Fig. 2.4, which shows the sample center absorbs the desired heat flux, which is 40 kW/m^2, while the lower part of the sample gets more than 40 kW/m^2, and the upper part of the sample gets less than 40 kW/m^2. The resultant distribution gives ±4% of heat flux variation over the sample height. (Previous checks showed the heat flux was uniform in the horizontal direction, i.e., parallel to the filaments of the lamps.)

2.4 Surface Emissivity Measurement

According to the radiative heat transfer theory for grey bodies, the emissivity, ϵ, is equal to absorptivity, α, while the absorptivity is equal to one minus the reflectivity, ρ, i.e., $\epsilon = \alpha = 1 - \rho$. Thus, the sample surface emissivity is obtained by measuring the reflectivity of the sample surfaces.

A spectrophotometer (CARY, Model 17) and a Fourier-Transform Infrared Spectrometer (Nicolet, Model 60SX) were used to measure the surface relectivity of unretarded ($Y_R = 0$) and retarded ($Y_R = 0.03$) samples after different pyrolysis times such as 0, 50 and 300 s. The spectral ranges of the two instruments are $\lambda = 0.2 \sim 3.5$ μm and $\lambda = 2.5 \sim 25$ μm, respectively, which cover a sufficient range of infrared light. The data from the sample surface reflectivity measurements are summarized in Table 2.1, from which the average value of 0.04 is obtained. The sample surface emissivity is therefore taken to be 0.96.

2.5 Surface Temperature Measurement

An infrared pyrometer (Raytek, Series SL 300 CC) is used in the sample surface temperature measurement. The pyrometer provides a linear output of 2 to

10 volts for a temperature range of 450°C to 1000°C_0. A black body versus pyrometer voltage test produced a linear reading of 2 to 10 volts on a multimeter (Hewlett Packard, Model #3466A). The spectral response of the detector is 2.1 to 2.3 μm. Before measurements by the pyrometer are begun, a check is made on its reproducibility by focusing it on it on a standard source of black body radiation (Infrared Industries Inc., black body radiation source, Model 463). The black body itself is checked at 500°C both by its own thermocouple (for details see Section 2.3) and by inserting a thermocouple (Type K, d = 0.003 in.) into its cavity.

In order to obtain accurate temperature measurement results, a calibration curve of the pyrometer voltage output versus sample surface temperature measured by a thermocouple is needed. (Direct measurement of temperature using thermocouples were not done because attachment of the thermocouples interfered with the pyrolysis process.) A series of special runs was made for this purpose at $\dot{q}''_{ab,s} = 40$ kW/m^2, following the standard procedure, except that the samples were not painted with black heat resistant enamel because of the desire of obtaining a low surface temperature. Many difficulties were encountered while trying to attach the thermocouple to the sample surface. Several kinds of cements, such as 5 minute Epoxy, 732 RTV, Sauereisen, and Duco cement, were tried on cellulose samples and failed in use because of either thermal or mechanical weaknesses. It was decided finally to use Omega CC high temperature cement (mix 3 parts filler to 1 part liquid by weight, or 2 parts filler to 1 part liquid by volume) to glue the thermocouples (Chromel-Alumel, Type K, d = 0.003 in.) at the centers of surfaces of unretarded ($Y_R = 0$) and retarded ($Y_R = 0.03$) samples respectively. The voltage outputs of both the thermocouple and the corresponding pyrometer are simultaneously recorded on a strip chart recorder (Hewlett Packard, Model 7100 B). A schematic drawing of a recording is shown in Fig. 2.5. Using a 3rd order polynomial curve fit generated on a computer, the calibration curve of sample surface temperature versus the pyrometer voltage output shown in Fig. 2.6, is obtained. The voltage-temperature polynomial expression corresponding to the curve is used in the main computer program to convert the pyrometer voltage output into sample surface temperature.

2.6 Mass Loss Rate Measurement

The mass loss rate of samples during pyrolysis is measured by an electronic balance (Mettler, PC 220). The sample is put in the sample holder, mounted on the balance and aligned with the pyrometer. The weighing chamber is then sealed at its sides using Scotch masker tape. The balance is then tared. Once pyrolysis is initiated, the signal from the balance is sent to the computer for processing. In this manner, the mass loss rate data are obtained (for details see Section 2.6).

2.7 Results and Discussion

Heat of gasification measurements were primarily made at an absorbed heat flux of $\dot{q}_{ab,s}$ of 40 kW/m^2. This heat flux gives mass loss rates which are comparable to those found by Tewari (1985) for cellulose samples burning in air. The typical computer outputs of surface temperature, mass loss rate and heat of gasification versus time for an unretarded sample at the absorbed heat flux of 40 kW/m^2 are shown in Fig. 2.7 (a), (b) and (c), respectively. It is obvious that surface temperature increases rapidly during the first 100 seconds of pyrolysis and then but at a slower rate. The surface temperature increases from 700K(427°C) to 850K(577°C) during the run. The mass loss rate increases rapidly during the first 55 seconds of pyrolysis, reaches the maximum value of 10×10^{-3}kg/m^2.s, and then decreases afterwards at a slower rate. The resulting curve for heat of gasification drops rapidly at first and then approaches a nearly constant value of $h_g = 1 \times 10^6$ J/kg.

Additional measurements were made at absorbed heat fluxes of 25, 30, and 35 kW/m^2 for unretarded samples. The results for different heat fluxes are shown in Fig. 2.8, Fig. 2.9 and Fig. 2.10. As the heat flux decreases, the values of surface temperature and mass loss rate decrease and heat flux decreases, the values of surface tmperature and mass loss rate decrease and heat of gasification values increase. While T_s, $\dot{m}''$ and hg kW/m^2 to 25 kW/m^2 makes the biggest quantitive difference for the T_s, $\dot{m}''$ and h_g values. Also, the time needed to achieve the maximum mass loss rate is affected by the absorbed heat flux; the lower the flux, the longer the time.

In order to study how a solid phase fire retardant affects the heat of gasification h_g, runs were made with cellulose samples retarded with sodium hydroxide at mass concentrations of 0 to 0.03 (i.e., $Y_R = 0$ to 0.03).

Fig. 2.11, Fig. 2.12 and Fig. 2.13 show the measured values of surface temperature, mass loss rate and heat of gasification as functions of time for $Y_R = 0$ and $Y_R = 0.03$. Fig. 2.11 indicates that the surface temperature for $Y_R = 0$ and $Y_R = 0.03$ increases continuously with time.

The difference between the temperatures decreases with time and reaches a constant value after 150 s. Fig. 2.12 shows that for both Y_R = 0 and 0.03, the mass loss rates increase to peak values and then decline. On the other hand, this figure indicates that retardant addition results in a much higher mass loss rate value and a faster changing rate of mass loss rate with time. The mass loss rate for Y_R = 0.03 reaches its peak value at 40 s, while the one for Y_R = 0 reaches its peak value, which is about 60% of the retarded one, at a later time, say 60 s. Also the difference between the two mass loss rate values decreases with time rapidly, especially after the peak. Fig. 2.13. shows that the retardant reduces the value of the heat of gasification significantly. While the values of heat of gasification for Y_R = 0 and Y_R = 0.03 both decrease to one-third of their initial values by the end of the pyrolysis, the ones for Y_R = 0.03 are about 2 times lower than the one for Y_R = 0. The difference between the two h_g values decreases with time rapidly, and approaches a nearly constant value after 150 s. As a whole, the results show that retardant addition causes increases in surface temperature and mass loss rate (or pyrolysis rate), and a decrease in the heat of gasification. It can be seen from the figures that the curves for T_s for both Y_R = 0 and 0.03 have nearly the same shape and are parallel to each other except at the very beginning. This is also true for h_g, but not for $\dot{m}''$. The $\dot{m}''$ curves show a significant difference in the peak value region; the one for Y_R = 0.03 is much steeper than the one for Y_R = 0. Therefore, the increase of mass loss rate plays an important role in the reduction of heat of gasification upon retardation.

Measured values of surface temperature, mass loss rate and heat of gasification as functions of retardant concentration at t = 200 seconds and an absorbed heat flux of 40 kW/m^2 are shown in Fig. 2.14, Fig. 2.15 and Fig. 2.16. It can be seen from Fig. 2.14 that the surface temperature T_s increases with retardant concentration Y_R. On the other hand, T_s changes with Y_R in a nonlinear manner. It increases with Y_R rapidly at first, and then keeps increasing but at a much lower rate. In other words, T_s becomes insensitive to Y_R beyond a certain extent. This implies that NaOH is acting as a catalyst during pyrolysis, and that only a small amount of NaOH is very effective. Fig. 2.15 shows the mass loss rate $\dot{m}''$ also increases with retardant concentration. Similar to the case for T_s, the initial small amount of retardant addition indicates a significant influence on $\dot{m}''$. As a result, the heat of gasification, h_g, decreases with Y_R, as shown in Fig. 2.16. Again, a small concentration of retardant causes a large decrease in h_g. When Y_R changes from 0 to 0.03, h_g decreases to nearly one-third of its initial value. Such a major reduction in the heat of gasification with retardant addition is caused by the combination of the increase in mass loss rate and the increase in surface heat loss. While the increase in T_s from 830K at Y_R = 0 to 860K at Y_R = 0.03 is not large, it increases the radiative heat loss from the sample surface enough to have a significant effect on $\dot{q}''_{net}$ and h_g (for details see Section 2.1).

The experimental results are contrary to what might have been expected, because retardant addition is known to increase the char density and presumably the char conductivity. Heat transfer analysis would therefore predict a decrease in surface temperature with retardant addition.

This question led to the next phase of the project which was directed at measuring noncombustible gaseous products of cellulose pyrolysis (i.e., Chapter 4).

CHAPTER 3

COMPARISON OF EXPERIMENTAL AND THEORETICAL PYROLYSIS RESULTS

3.1 Pyrolysis Theory

From a conceptual viewpoint, flaming combustion can be divided into two parts: the gas-phase combustion region (the flame) where the fuel volatiles are consumed, and the solid phase pyrolysis region where the fuel volatiles are generated. The energy released by combustion is transferred to the fuel surface as a convective heat flux and a radiant heat flux. The sum of the two fluxes, minus a significant heat loss from the hot fuel surface due to re-radiation, gives the net heat flux into the fuel. It is this net heat flux which causes the fuel to pyrolyze, leading to the production of fuel volatiles at a mass flow rate $\dot{m}''_{G,W}$, i.e., the mass loss rate during pyrolysis.

Three terms are used in the literature to describe the energy changes which occur during pyrolysis, they are heat of reaction, heat of pyrolysis and heat of gasification.

The heat of reaction $h_{r,\infty}$ is defined as the enthalpy of reaction per unit mass of volatiles at an ambient temperature T_∞ for the reaction

Solid (S) → Char (C) + Gaseous volatiles (G)

so that

$$h_{r,\infty} \equiv h_{G,\infty} + h_{C,\infty}\left[\frac{\rho_C}{\rho_S - \rho_C}\right] - h_{S,\infty}\left[\frac{\rho_S}{\rho_S - \rho_C}\right] \tag{3-1}$$

The definition for the heat of pyrolysis h_p is the difference between the enthalpy of the products at the surface temperature T_w and the reactants at the ambient temperature T_∞ per unit mass of volatiles so that

$$h_p \equiv h_{G,w} + h_{C,w}\left[\frac{\rho_C}{\rho_S-\rho_C}\right] - h_{S,\infty}\left[\frac{\rho_S}{\rho_S-\rho_C}\right] \qquad (3\text{-}2)$$

Thus h_p is equal to $h_{r,\infty}$ plus the sensible heat needed to raise the temperature of the products from T_∞ to T_w.

For pure cellulose, $h_{r,\infty}$ should not depend on the type of sample (powered vs. bulk). However, the value of $h_{r,\infty}$ may vary with the heating rate, since the products of pyrolysis are heating rate-dependent. The value of h_p may well depend on the type of sample since for a bulk sample, as shown in Fig. 3.1, the initial products of pyrolysis may undergo additional chemical reactions as they flow through the hot char layer to the sample surface.

The definition of h_g for use in diffusion flame theory is the ratio of the net surface heat flux resulting from flaming combustion to the volatiles generation rate due to pyrolysis, that is

$$h_g \equiv \frac{\dot{q}''_{net}}{\dot{m}''_{G,W}} \qquad (3\text{-}3)$$

where $\dot{m}''_{G,W} = \dot{m}''$.

An analysis of pyrolysis in a charring material, such as cellulose, resulting from an external heat flux (Sibulkin, 1986) shows that the heat of gasification is not simply related to the standard heat of reaction during pyrolysis. The semi-infinite control volume used in the analysis for a charring fuel such as cellulose is shown in Fig. 3.1. The coordinate x = 0 represents the fuel surface, and the positive direction of x is taken into the fuel. In this analysis, it is assumed that the flame is established at time t = 0, when heat flux $\dot{q}''_{net}$ begins to go into the fuel. As time increases, a As time increases, a pyrolysis wave moves into the fuel converting th original solid material (S) into char (C) with the release of gaseous volatiies (G). The velocity of the pyrolysis wave, V_p, is related to the mass pyrolysis rate $\dot{m}''_{G,w}$ by

$$V_p = \dot{m}''_{G,W}/[\rho_S - \rho_C] \qquad (3\text{-}4)$$

An outline of the analysis is as follows: Applying the conservation of mass to a differential element of length dx and unit cross-sectional area (see Fig. 3.1) gives

$$\frac{d\dot{m}''_G}{dx} = -\frac{\partial \rho}{\partial t} \qquad (3\text{-}5)$$

where $\dot{m}''_G$ is taken as positive in the negative x direction.

And applying conservation of energy to the same element gives

$$\frac{\partial}{\partial t}[\rho h] = \left[\frac{\partial \rho}{\partial t}\right] h_{r,\infty} + \frac{\partial}{\partial x}\left[k\frac{\partial T}{\partial x}\right] + \frac{\partial}{\partial x}\left[\dot{m}''_G h_G\right] \qquad (3\text{-}6)$$

Integration of Eq. (3.6) from x = 0 to ∞ and use of Eq. (3-5) gives

$$\int_0^\infty \frac{\partial}{\partial t}[\rho h]dx = -\dot{m}''_{G,W}h_{r,\infty} + \dot{q}''_W - \dot{m}''_{G,W}h_{G,W} \qquad (3\text{-}7)$$

where $\dot{q}''_W = \dot{q}''_{net}$.

After relating the local density, ρ, and enthalpy, h, to the corresponding values for the solid and char, the results can be combined with Eq. (3-3) to give as a general result for the heat of gasification

$$h_g = h_{r,\infty} + h_{G,W} + \frac{1}{\dot{m}''_{G,W}}\int_0^\infty \left(-\frac{\partial\rho}{\partial t}\right)\left[\left(\frac{\rho_C}{\rho_S-\rho_C}\right)\left(h_C - h_{C,\infty}\right) - \left(\frac{\rho_S}{\rho_S-\rho_C}\right)\left(h_S - h_{S,\infty}\right)\right]dx +$$

$$\frac{1}{\dot{m}''_{G,W}}\int_0^\infty \left(\rho c\right)\frac{\partial T}{\partial t}dx \qquad (3\text{-}8)$$

In Eq. (3-8) the first integral on the RHS of the equation gives the change in sensible enthalpy between the char and solid while the second integral is an unsteady, energy storage term. The analysis thus shows that the relationship between the heat of gasification and the heat of reaction (or the heat of pyrolysis) is not a simple one.

In order to gain more understanding of the pyrolysis mechanism and as a "check out" of the experiments, a numerical analysis of the pyrolysis of pure and fire retarded cellulose was made. A computer program based on the method of finite differences has been used to solve Eqs. (3-5) and (3-6) to obtain numerical results. The program was developed by Kung (1972) and modified by Tamanini (1976). The complex pyrolysis chemistry is replaced by a single global reaction with a rate law given by

$$-\frac{\partial \rho}{\partial t} = [\rho - \rho_C] \; A \; \exp[-E/RT] \qquad (3\text{-}9)$$

A number of thermal and material properties of cellulose and char are needed as the inputs to the program. The results of the calculations depend on the values used for the properties. However, accurate values of many of these properties are not known. The set of property values used in the calculations are given in Table 3.1; they are taken as best estimates from the literature. The thermal conductivities of cellulose and char are both taken as the linear functions of local temperature given by

$$k = k_\infty + k^* \, (T - T_\infty) \qquad (3\text{-}10)$$

The values of materials properties, such as the density of char, ρ_C, the thermal conductivity of char at the ambient temperature, $k_{C,\infty}$, and the heat of reaction at the ambient temperature, $h_{r,\infty}$, are tabulated in Fig. 3.2 , Fig. 3.3, and Fig. 3.4, because these properties have proved to be the ones which cause the difference between pure (Y_R = 0) and retarded (Y_R = 0.03) cellulose in the calculations. The values of ρ_C came from direct measurement, the value of $k_{C,\infty}$ was taken from the literature, and the $h_{r,\infty}$ value came from the DSC measurement results (for details see Appendix C).

With these inputs, the program can then be used to calculate the fuel surface temperature, T_s, the mass loss rate, $\dot{m}''$, and the heat of gasification, h_g, under different net heat fluxes into the fuel surface, $\dot{q}''_{net}$

(or absorbed heat fluxes $\dot{q}''_{ab,s}$). In order to compare the numerical results with experimental data, the heat flux absorbed by the fuel surface was taken to be constant at a value of 40 kW/m^2 (see Section 2.7), so that

$$\begin{aligned} \dot{q}''_{net} &= \dot{q}''_{ab,s} - \dot{q}''_{emit,s} - \dot{q}''_{c,s} \\ &= 40 - \epsilon_s \sigma (T_s^4 - T_\infty^4) - h(T_s - T_\infty) \qquad (3\text{-}11) \end{aligned}$$

which is the same as Eq. (2-5) in Section 2.1. As final results, the values of T_s, $\dot{m}''$ and h_g as functions of time were printed and plotted.

3.2 Theorctical Results

By using the computer program described in Section 3.1, the theoretical results for the pyrolysis of pure and fire retarded cellulose at $\dot{q}''_{ab,s}$ = 40 kW/m^2 cellulose are obtained.

Figure 3.2 shows the numerical results of surface temperature T_s as a function of time for pure cellulose (Y_R = 0) and retarded cellulose $_R$ (Y_R = 0.03). It can be seen that the values of T_s for both pure and retarded cellulose increase with time, and the T_s of retarded cellulose is higher than that of pure cellulose, which is qualitatively consistent with the experimental results. However, the difference of T_s between pure and retarded cellulose is much smaller than the experimental one shown in Fig. 2.11. A very important phenomenon uncovered by the calculations is that the value of the heat of reaction is different in the two cases. The dominant reactions for pure and retarded cellulose are endothermic and exothermic respectively (see Appendix C). This result can be used to explain why the value of T_s increases with retardant addition (because of the exothermic reaction), which is contradictory to the prediction by heat transfer analysis as mentioned in Section 2.7.

Figure 3.3 presents the numerical results of mass loss rate vs. time for pure cellulose ($Y_R = 0$) and retarded cellulose ($Y_R = 0.03$). The qualitative shape of the curves, a rapid rise to a peak mass loss rate followed by a steady decline, is similar to experimental data (see Fig. 2.12). It was confirmed that the addition of the retardant leads to an increase in the mass loss rate. A detailed comparison of the theoretical and experimental results for the mass loss rate is present in the next section.

Figure 3.4 gives the numerical results for the heat of gasification as a function of time for pure cellulose ($Y_R = 0$) and retarded cellulose ($Y_R = 0.03$). It shows that addition of the retardant lowers the heat of gasification, which is qualitatively in agreement with the experimental data (see Fig. 2.13). However, the calculated h_g values decrease faster than the experimental ones, and become constant thereafter. Diffusion flame theory predicts that a decrease in h_g would promote burning. It was expected, therefore, that char-promoting retardants would increase h_g. Since the opposite trend was found, further work was carred out (for details see Chapter 4).

3.3 Comparison of Experimental and Theoretical Results

From Fig. 3.2, Fig. 3.3 and Fig. 3.4, it is obvious that the theoretical results for both pure and retarded samples agree qualitatively with the experimental results; that is, the surface temperature T_s increases with time, $\dot{m}''$ first increases rapidly to a peak, and then decreases with time, and heat of gasification, h_g, decreases with time first rapidly and then slowly. On the other hand, the addition of retardant leads the higher T_s and m" values and the lower h_g value.

There are recognizable quantitative differences between the numerical and experimental results. The values of surface temperature T_s from the calculations, shown in Fig. 3.2, are smaller than those from the experimental data. The calculated h_g values in both pure and retarded cases are 2 to 4 times higher than the experimental data. A more detailed comparison between theoretical and experimental values of the mass loss rate for pure (Y_R = 0) and retarded (Y_R = 0.03) cellulose is shown in Fig. 3.5 and Fig. 3.6. As mentioned in Section 3.1, the thermal conductivities of cellulose and char and the heat of reaction at the ambient temperature, $h_{r,\infty}$, are the parameters which most affect the pyrolysis calculations, therefore, the calculations have were performed for both constant and variable k and $h_{r,\infty}$ values. It can be seen from Fig. 3.5 and Fig. 3.6 that for both pure and retarded cellulose, the constant values of thermal conductivity and heat of reaction lead to results that divergent the most from the experimental ones. For the thermal conductivities which vary with the surface temperature linearly, in the pure cellulose case shown in Fig. 3.5, the $h_{r,\infty}$ value of 0.5×10^6 J/kg leads to a peak value which is very close to the experimental one, while the $h_{r,\infty}$ value of 0.23×10^6 J/kg results in a much higher peak value but narrows the differences between the "downhill" theoretical and experimental data. Similarly, in the retarded cellulose case shown in Fig. 3.6, the $h_{r,\infty}$ value of -0.10×10^6 J/kg leads to the $\dot{m}''$ values lower than the experimental data, while the $h_{r,\infty}$ value of -0.30×10^6 J/kg leads to a higher peak value and lower "downhill" values, which indicates a better simulation of the experimental results as a whole.

The $h_{r,\infty}$ values used in both comparisons are the best possible estimated values available. The comparisons show that for the pyrolysis theory used, variable thermal conductivities yield a better simulation of the experimental results.

The numerical calculations confirm the experimental results and show that retardant addition increases the surface temperature (this leads to a decrease in $\dot{q}''_{net}$) and the mass loss rate, and decreases the heat of gasification. This is contrary to the known fact that retardation increases char production, density and presumably the char conductivity; thus there should be decreases in both surface temperature and volatile production and an increase in heat of gasification. Although it was discovered that the value of the heat of reaction is different for pure and retarded cellulose, which can be used to explain the increases in T_s by retardant addition, more information is needed in order to completely understand the phenomena.

CHAPTER 4

NONCOMBUSTIBLE GASEOUS PRODUCTS OF CELLULOSE PYROLYSIS

4.1 Introduction to Measurements

Diffusion flame theory predicts that a decrease in h_g would promote burning. Therefore, it had been expected that char promoting retardants would increase h_g. However, our experiments show that retardant addition increases the surface temperature and the volatile production rate (i.e., mass loss rate), and thus decreases the heat of gasification of cellulose samples. In order to explain the contradiction between the theoretical prediction and the experimental results, and to explore the mechanism of fire retardation, measurements of noncombustible gaseous products of cellulose pyrolysis were made.

An analytical gas chromatograph was used to measure the inert fraction of the total volatiles. The amounts of noncombustible gaseous products, CO_2 and H_2O, in the total volatiles are obtained (the amount of CO is also obtained at same time because of the column used). With the known inert fraction of the volatiles, the combustible fraction of the total volatiles can be calculated, and then used to obtain the heat of combustion and stoichiometric ratio of the "fuel", (i.e. the combustible fraction of the volatiles). These property values can then be used in combustion calculations for burning rates and flammability limits.

4.2 Experimental Apparatus

A schematic side-view of the basic apparatus used in noncombustible gaseous products measurements is shown in Fig. 4.1.

In this experiment, as in the previous heat of gasification measurements, a pair of infrared radiant lamps (Research Inc., Model 5305-5A) are used as the external heat flux source simulating the heat flux from the flame to the fuel surface. The same extensively modified glass draft of a top-loading electronic balance (Mettler, PC220) is used as the weighing chamber, together with the same water-air cooling system and 2-stage nitrogen supply system. The electronic balance is connected to the computer (Apple IIe) to acquire and process the mass data to give the total volatiles production rate, i.e. the mass loss rate, as a function of time.

An analytical gas chromatograph, i.e. GC, (Carle Instruments, Inc., Model 111) is used, together with an integrator (Hewlett Packard, Model 3380A), to measure the noncombustible gaseous products of cellulose pyrolysis. In order to obtain reliable GC results, a special sampling system was designed. First of all, based on Heskestad's study (1981), a system was designed to mix the volatile gases which come out from the weighing chamber. As shown in Fig. 4.1, the weighing chamber is connected to a glass tube where the volatiles are mixed. In order to obtain good mixing, an annular metal washer is put at the entrance to the mixing tube. The ratio of the washer inner diameter to tube inner diameter is 0.5 as recommended by Heskestad for the optimum mixing.

After mixing, the flow is split in two; i.e., to the GC sampling loop, and to a rotameter (Gilmont Instruments, Inc., Flowmeter Catalog No. F1500) used to measure the volumetric flow rate of the volatiles. The rotameter is then connected to the main exhaust system through a flexible tube.

In order to accurately measure the volatile flow rate, a thermocouple (Chromel-Alumel, Type K, d = 0.003 in) is inserted into the mixing tube. The thermocouple is connected to a digital temperature indicator (Omega Engineering, Inc., Model 199) which reads the temperature of the volatiles passing through the rotameter. These temperature data are then used in the calculation of the volatiles flow rate. (The flow rate cannot be read directly from the calibration chart, because the volatiles temperature, ranging from 56°C to 72°C is far above the standard temperature, i.e. 21°C, at which the calibration chart is obtained.)

A vacuum pump (Cole-Parmer Instrument Co., Air Cadet, Model No. 7530-40) is used to create the pressure difference needed to draw the volatile gases through the GC sampling loop. (Before injecting volatiles sample into GC columns, the pump is turned off to let the pressure inside the GC sampling loop recover.) The pressure in the GC sampling loop is monitored by a mercury manometer. The volatiles flow rate through the sampling loop is measured by a rotameter (Emerson Electric Co., Sho-Rate 150, Model 1355). A pump bypass is used to adjust the flow rate through the sampling loop to a value of 180 mℓ/min during GC sampling. The time needed for volatiles to move from pyrolyzing sample surface to GC sampling valve has been estimated so that during the experiment, the volatiles inside the sample loop can be injected into the GC column at the proper time, which is directly related to the time used for the mass loss rate measurements. The GC used helium as the carrier gas. The helium flow was 22 mℓ/min at a pressure of 42 psig. Before the measurements, the helium flow was run through the GC columns by using the valve switch to get air out of the sampling loop (because of a possible overnight leakage). The column temperature was set at 60°C. A schematic drawing of GC valves and columns is shown in Fig. 4.2. There are 3 columns in the GC, column 1 (6'-80/100 Porapak Q) is used to measure the noncombustible volatiles, CO_2 and H_2O, while column 2 (5'-80/100 Molecular Sieve 5A) is used to measure O_2, N_2, and CO and column 3 is used as the reference column.

The amount of volatiles injected into the GC columns is 1 mℓ. After injection, the positions of the GC valves are controlled by a timer. The volatile sample is sent either through column 1, or column 2 or column 1 plus column 2. The timing sequence has been chosen so that CO_2 and H_2O are separated by column 1, and O_2, N_2 and CO are separated by column 2. A TCD (thermal conductivity detector) was used. The output of the GC is sent to the integrator which obtains the area of the sample peak and calculates the area percentage of each peak. The total time of analysis was 30 minutes per sample. The GC was calibrated using a bottle of calibration gas and a mixture of laboratory air and N_2. Details of the GC calibration are presented in Appendix D.

In this experiment, as in the previous one, some of the apparatus were checked regularly in order to keep the experimental conditions consistent.

The monthly apparatus checks included: (1) heat flux gauge A (Medtherm, 64-20-20T) versus heat flux gauge B (Medtherm, 64-20-20); (2)

electronic balance (Mettler, PC 220) versus standard weight of 50 grams; and (3) computer (Apple IIe) disk driver speed checking by using the Master disk.

The daily apparatus check was made of the IR lamps against the heat flux gauge A by using a multimeter before and after each run. The purpose of this was to insure that the RUN POT SETTING in the control panel corresponds to the desired heat flux, and that the heat flux is uniformly distributed over the entire sample surface (for details see Section 2.2).

Since the total GC measuring time is 30 minutes per sample while the total cellulose pyrolysis time is 5 minutes, only one GC sample can be taken during each run. Based on the h_g measurement results, it was decided that the volatile products of cellulose pyrolysis at 90, 180 and 270 seconds will be measured by the GC. (The time needed for volatiles to move from the pyrolyzing sample surface to the GC sampling valve, estimated as 15 seconds, was taken into account.)

4.3 Results and Discussion

A series of runs were made to measure the noncombustible gaseous products of pyrolysis for pure (Y_R = 0) and fire retarded (Y_R = 0.03) cellulose samples. The volatiles coming out from the sample surfaces were sampled by the GC at 90, 180 and 270 seconds. The GC results were recorded by the integrator.

For pure cellulose samples, the GC analysis showed peaks for CO_2, H_2O, O_2 and N_2, while for fire-retarded samples, the GC results included CO. An example of the GC output from the integrator is shown in Fig. 4.3 for a fire retarded (Y_R = 0.03) sample at 180 s. It can be seen that the integrator starts recording at the moment the volatile sample is injected into the GC columns. It is known from the GC calibration run that the peaks recorded at 2.19, 5.82, 14.05, 14.74 and 20.72 minutes represent CO_2, H_2O, O_2, N_2 and CO, respectively. The other small peaks are just the responses to the GC valve switches from clockwise to counterclockwise. The GC analysis is completed at 30 minutes as preset by the GC operating program. After the recording is stopped, the GC results are tabulated to give the recording time (RT), area (in counts) and area % (in count %), where the column "Type" explains the characteristics of the individual peaks . The "T" means a peak with "tangent skimmed base", and the "M" means a peak which "merged with the preceding peak". It can be seen from the data that among the total volatiles, the area % of CO_2, H_2O and CO are 0.21%, 0.44% and 0.14%, respectively. Also, there is 99% N_2 in the volatiles, which agrees with the estimated value. The peak representing N_2 is chopped off, because it has exceeded the recording limit. The amount of O_2, 0.02% is negligible, which shows that within the acceptable experimental error, the cellulose sample surface can be considered surrounded by nitrogen, as in the "real" diffusion flame situation. The density of the total volatiles can be approximated by the density of nitrogen.

As described in the previous section, the masses of CO_2, H_2O and CO are calculated from the GC analysis results, which then is divided by the total volatiles production rate which is measured simultaneously, leading to the results for mass fractions of CO_2, H_2O and CO. The final results of the measurements of noncombustible gaseous products of cellulose pyrolysis are summarized in two figures.

The mass fractions of CO_2, H_2O and CO vs. time for pure and fire retarded samples at $\dot{q}''_{ab,s} = 40$ kW/m^2 are shown in Fig. 4.4. In this figure, the values of Y_{CO2}, Y_{H2O} and Y_{CO}, with the error bars, are plotted against the pyrolysis time for both the $Y_R = 0$ and $Y_R = 0.03$ cases. The values of Y_{CO2} increase with time at about the same rate for Y_R=0 and 0.03. For Y_{H2O}, the values for $Y_R = 0$ increase with time at a faster rate than those for $Y_R = 0.03$. The values of Y_{CO} for $Y_R = 0.03$ increase very slowly with time, while there is no measurable amount of CO for $Y_R = 0$. The most significant results of the measurements are the effects of the retardant on the amounts of CO_2 and H_2O produced. The figure shows that the values of Y_{CO2} for $Y_R = 0.03$ are about 4 times higher than those for $Y_R = 0$. Also the values of Y_{H2O} for $Y_R = 0.03$ are about twice those for $Y_R = 0$.

The mass fractions for CO_2, H_2O and CO vs. retardant concentration at $\dot{q}''_{ab,s} = 40$ kW/m^2 are shown in Fig. 4.5. In this figure, the values of Y_{CO2}, Y_{H2O} and Y_{CO} with error bars are plotted against retardant concentration for a pyrolyzing time of 180 seconds. Fig. 5.6, shows that the values of Y_{CO2}, Y_{H2O} and Y_{CO} increase with the retardant concentration. It also shows that Y_{CO2}, Y_{H2O} and Y_{CO} all increase very rapidly as Y_R changes from 0 to 0.01. Over this Y_R range, Y_{CO} nearly increases to its maximum value and remains almost constant thereafter. The value of Y_{CO2} increases to 80% of its value for $Y_R = 0.03$ and then increases at a much slower rate. On the other hand, Y_{H2O} increases to its maximum value at about $Y_R = 0.015$, and then starts to decrease. These results imply that the most significant changes in Y_{CO2}, Y_{H2O} and Y_{CO} are caused by a small amount of retardant addition. Therefore the retardant NaOH is speculated to be acting as a catalyst.

Both figures show that the Y_{H2O} values have larger errors than the Y_{CO2} and Y_{CO} values. From the Fig. 4.3, it can be seen that the peak of the H_2O curve has a long tail which is significantly different from the other peaks. Therefore, cutting off the H_2O peak tail, which is executed by the integrator automatically during the GC analysis, can be considered as a possible source of error in the H_2O measurements.

The results for Y_{CO2} and Y_{H2O} are very valuable in explaining the puzzle left by the h_g measurements, because even though the addition of retardants decreases the h_g values unexpectedly, it also increases the noncombustible gaseous products, CO_2 and H_2O, significantly during the cellulose pyrolysis. The physical mechanism by which the fire retardant NaOH acts to suppress flaming combustion has to be explained by the combination of the two aspects.

CHAPTER 5

PRODUCTS OF CELLULOSE PYROLYSIS

5.1 Introduction to Analysis

Diffusion flame theory shows that the fuel-related material properties which must be determined to predict burning behavior are: (1) h_g, the heat of gasification; i.e., the heat input per unit mass of volatiles produced; (2) Y_{FT}, the mass fraction of combustible volatiles in the total volatile products of pyrolysis; (3) ν_s, the stoichiometric oxygen/fuel ratio of the combustible volatiles; (4) $h_{c,cv}$, the heat of combustion per unit mass of combustible volatiles. Of these four properties, h_g has been measured, as described in Chapter 3. The other three quantities, Y_{FT}, ν_s and $h_{c,cv}$ can be determined as follows from using the experimental results.

The mass fraction of combustible volatiles in total volatiles, Y_{FT}, is defined as:

$$Y_{FT} = 1 - \frac{\dot{m}_{(CO_2 + H_2O)}}{\dot{m}_{vol}} = 1 - Y_{CO_2} - Y_{H_2O} \qquad (5\text{-}1)$$

therefore, once the values of Y_{CO2} and Y_{H2O} are calculated from the GC analysis results, the values of Y_{FT} are known. In order to obtain the stoichiometric oxygen/fuel ratio of the combustible volatiles, ν_s, the C, H, O composition of the combustible volatiles are calculated first from the following:

$$Y_{i,cv} = \frac{\dot{m}_{i,cv}}{\dot{m}_{cv}} = \frac{Y_{i,vol} - Y_{i,CO2}\ Y_{CO2} - Y_{i,H2O}\ Y_{H2O}}{Y_{FT}} \qquad (5\text{-}2)$$

where: $Y_{i,cv}$ = mass fraction of species i in the combustible volatiles. The subscript i represents C, H, O, respectively in this section.

$\dot{m}_{i,cv}$ = mass of species i in the combustible volatiles per unit time.

$\dot{m}_{cv}$ = mass of the combustible volatiles per unit time.

$Y_{i,vol}$ = mass fraction of species i in the total volatiles.

Y_{i,CO_2} = mass fraction of species i in CO_2.

Y_{CO_2} = mass fraction of CO_2 in the total volatiles.

Y_{i,H_2O} = mass fraction of species i in H_2O.

Y_{H_2O} = mass fraction of H_2O in the total volatiles.

Y_{FT} = mass fraction of combustible volatiles in the total volatiles.

The values of $Y_{i,CO2}$ and $Y_{i,H2O}$ are obtained by using basic chemistry. The value of Y_{CO2}, Y_{H2O} and Y_{FT} are calculated from the GC analysis results.

The values of $Y_{i,vol}$ are calculated by using the following formula:

$$Y_{i,vol} = \frac{\dot{m}_{i,vol}}{\dot{m}_{vol}}$$

$$= \frac{Y_{i,cell} - Y_{i,char}\,Y_{char}}{1 - Y_{char}} \qquad (5\text{-}3)$$

where $\dot{m}_{i,vol}$ = mass of species i in the total volatiles per unit time.

$\dot{m}_{vol}$ = mass of total volatiles per unit time.

$Y_{i,cell}$ = mass fraction of species i in the cellulose samples.

$Y_{i,char}$ = mass fraction of species i in char.

Y_{char} = mass fraction of char in the cellulose samples.

The values of $Y_{i,cell}$ are calculated for both pure and retarded cellulose samples, using the molecular formula $C_6H_{10}O_5$ for pure cellulose samples. The values of $Y_{i,char}$ are measured for both pure and retarded samples by using a elemental analyzer (Perkin-Elmer, 240 B); details about the measurement are given by Frendi (1986). The Y_{char} values for pure and retarded samples are obtained by making a special series of measurements. The cellulose samples are cut at the front end to make disks 2-3 mm thick and 1 in. (2.54 cm) in diameter. These disks are then attached to cellulose samples by a specially made holder. The cellulose samples with disks are pyrolyzed following the same procedure as in h_g measurements, except using an increased heating time in order to let the Section 3.3, except using an increased heating time in order to let the disks become completely charred. The values of Y_{char} are calculated by using the mass data of the disks before and after charring.

Once the C, H, O composition of the combustible volatiles becomes known, the values of ν_s are calculated by using the following stoichiometric equation for complete combustion:

$$C_xH_yO_z + nO_2 = x\ CO_2 + \frac{y}{2} H_2O$$

where $C_xH_yO_z$ is the combustible compound.

From the balance of the equation:

$$n = \frac{1}{2}\left(2x + \frac{y}{2} - z\right) = x + \frac{y}{4} - \frac{z}{2}$$

For a unit mass of $C_xH_yO_z$,

$$x = \frac{Y_{C,cv}}{12}\ , \quad y = Y_{H,cv}\ , \quad z = \frac{Y_{O,cv}}{16}$$

so that

$$n = \frac{Y_{C,cv}}{12} + \frac{Y_{H,cv}}{4} - \frac{Y_{O,cv}}{32}$$

and

$$\nu_s = 32\ n \tag{5-4}$$

The values of the heat of combustion per unit mass of combustible volatiles $h_{c,cv}$ can be calculated from

$$h_{c,cv} = \frac{h_{c,vol}}{Y_{FT}} \tag{5-5}$$

where $h_{c,\,vol}$, the heat of combustion per unit mass of total volatiles, has been measured by A. Frendi (1986) using a semi-microcalorimeter (Parr 1421), for pure and retarded cellulose samples ranging from $Y_R=0$ to 0.03.

The values for h_g, Y_{FT}, ν_s and $h_{c,cv}$ obtained, as described above, are used as inputs to a computer program to predict the burning behavior of cellulose.

It is interesting to look at the decomposition of cellulose into char, inert gases and combustible volatiles. The amount of char per unit mass of cellulose Y_{char} is from the measurements, as mentioned earlier. The amount of inert gases per unit mass of cellulose Y_{inert} and the amount of combustible volatiles per unit mass of cellulose $Y_{comb,vol}$ are calculated from the following formulas:

$$\begin{aligned} Y_{inert} &= \frac{m_{inert}}{m_{cell}} \\ &= (1 - Y_{FT})\,(1 - Y_{char}) \end{aligned} \tag{5-6}$$

and

$$Y_{comb,vol} = 1 - Y_{char} - Y_{inert} \tag{5-7}$$

The results are tabulated in Table 5.7 and plotted in Fig. 5.1.

5.2 Results and Discussion

During cellulose pyrolysis, a certain amount of char is produced. The values of mass fraction of char in the cellulose samples, Y_{char}, are obtained by charring the thin disks for pure and retarded cellulose samples, under the same conditions as described in Section 2.2. The results of these measurements are tabulated in Table 5.1. It is obvious from the table that the production of char from cellulose pyrolysis increases as the retardant concentration increases. However, the mass concentration of char in the cellulose samples, Y_{char}, does not increase linearly with the retardant concentration Y_R. As Y_R increases, Y_{char} increases rapidly and then slows down approaching a maximum value.

Table 5.2. gives the elemental composition values for cellulose according to the formula $C_6H_{10}O_5$. It can be seen that C and O are the major species in cellulose, each composing about 40% of the cellulose by mass.

The elemental composition of char are given in Table 5.3. The analysis are described in the last section. It was assumed that all Na remains in the char, the data for C and H were obtained from direct measurements, and the value for O was found by subtraction. The table shows that the mass fractions of C, H and O vary only a little as the retardant concentration increases from 0 to 0.03, and can be considered as nearly constant. As Y_R increases from 0 to 0.03, the values of mass fraction of C, H and O composition of char remain around 80%, 4% and 16%, respectively. Therefore the data in Table 6.3 lead to the conclusion that the retardant addition does not cause significant effects on the C, H and O composition in char.

The elemental compositions of the volatiles in Table 5.4. are obtained by using formula (5-3) shown in Section 5.1 and the data in Tables 5.1, 5.2 and 5.3. Table 5.4 shows that the values of the C, H and O composition of total volatiles change with the retardant concentration. As Y_R increases from 0 to 0.03, the mass fraction of C in the total volatiles decreases from 41% to 29%, an approximate decrease of 30% of the initial value, which is presumably because more of the original C ends up in the char, as shown in Table 5.1. On the other hand, the mass fraction of H and O increase with increasing Y_R. The total increases of the H and O in the total volatiles amount to 10% and 20% of the initial values, respectively. The fact that the C, H and O composition of the total volatiles changes with the increasing retardant concentration shows the effects of retardant addition on the elemental composition of total volatiles.

In order to obtain a better understanding of the physical mechanism by which the fire retardant NaOH acts to suppress flaming combustion, data on the noncombustible products of cellulose pyrolysis were obtained using the GC results. The details about the calculations of the mass fraction of CO_2 and H_2O in the total volatiles, Y_{CO2} and Y_{H2O}, are presented in Appendix D and shown in Figs. 4.4 and 4.5. The values of the mass fraction of combustible volatile in total volatiles Y_{FT} are calculated from formula (5-1) using the measured values of Y_{CO2} and Y_{H2O}. Table 5.5 gives the data on the noncombustible gaseous products of cellulose pyrolysis.

It shows that as Y_R increased from 0 to 0.03, Y_{CO2} increased 3 times (from 0.06 to 0.24), and Y_{H2O} nearly doubled (from 0.25 to 0.41). As a result, Y_{FT} decreased to half of its initial value (from 0.69 to 0.35). Therefore, Table 5.5 clearly indicates that redardant addition causes a decrease of gas phase "fuel" in volatiles.

Table 5.6 shows the elemental composition and the stoichiometric oxygen/fuel ratio of the combustible volatiles. The values of the mass fraction of C, H and O in the combustible volatiles are calculated by using formula (5-2) and the data in Tables 5.4 and 5.5, while the values of stoichiometric ratios of the combustible volatiles are calculated by using formula (5-4), as described in the previous section. It can be seen from the table that the C, H and O composition of the combustible volatiles changes with increasing retardant concentration in a different way from that for the total volatiles. The value of $Y_{C,cv}$ first increases as Y_R increases, reaches a maximum value at Y_R=0.015 which is 30% higher than the minimum one corresponding to Y_R=0, then decreases to a value which is about 10% higher than the minimum one. The value of $Y_{C,cv}$, on the other hand, continuously increases, from the initial value for Y_R=0, to a maximum value for Y_R=0.03, which is 40% higher than the initial one. While the $Y_{O,cv}$ value first decreases as Y_R increases, reaches a minimum value, which is just half of the initial value, at Y_R=0.015, then increases to the value, which is about 80% of the initial one, at Y_R=0.03. The effects of these three factors result in the ν_s data. Similarly to $Y_{C,cv}$, the ν_s value also first increases as Y_R increases, reaches a maximum value, which is about 44% higher than the initial one at Y_R=0.015, then decreases to a value which is 25% higher than the initial one at, Y_R=0.03. The very important fact here is that the value of ν_s increases with increasing Y_R, which implies that in an environment with certain concentrations of oxygen and combustible volatiles, the addition of retardant NaOH simply makes cellulose harder to burn.

As a summary, in order to give a clearer picture of the results of cellulose pyrolysis, the data on mass fraction of the major products of cellulose pyrolysis per unit mass of cellulose are tabulated in Table 5.7 and plotted against retardant concentration in Fig. 5.1. Table 5.7 and Fig. 5.1 can be used to explain how the retardant NaOH acts to suppress burning through two important factors. First, as retardant concentration increases, both the mass fraction of char and inert gases increase causing the mass fraction of combustible volatiles to decrease. Therefore, one can conclude that the retardant addition reduces the amount of the "fuel" in the volatiles, and, thereby, suppresses burning. Second, Fig. 5.1 shows that 90% of the mass fraction changes occurs as Y_R increases from 0 to 0.015. This suggests that retardant NaOH is acting as a catalyst to speed up and increase the formations of char, CO_2 and H_2O at the expense of combustible volatiles, as discussed in Section 1.1. Therefore, it appears that only a small amount of NaOH is needed for fire retardation of cellulose.

The overall effects of NaOH addition on cellulose pyrolysis and combustion are summarized in the next chapter.

CHAPTER 6

SUMMARY OF RETARDANT EFFECTS ON BURNING OF CELLULOSE

The motivation for this study of cellulose pyrolysis is related to its role as one of the processes in the burning of cellulose. In particular, the present study is directed toward determining the effects of the solid phase fire retardant, NaOH, on the burning of cellulose. The results are summarized as follows:

(1) The theory of diffusion flames shows that an important parameter relating gas-phase combustion and solid-phase pyrolysis is the heat of gasification h_g, which is the heat input per unit mass of volatiles. A new technique for the study of bulk cellulose pyrolysis has been developed to measure surface temperature, pyrolysis rate, (mass loss rate), and heat of gasification. The experimental results indicate that addition of a fire retardant (NaOH) to cellulose increases the surface temperature, which in turn decreases the net heat input, and also increases the pyrolysis rate, (while some previous researchers reported decreased pyrolysis rates after adding retardants); these effects result in a lower heat of gasification. Analysis of pyrolysis wave propagation in a char-forming material such as cellulose shows that there is no simple relationship between the heat of gasification and the heat of reaction. Numerical calculations for a pyrolysis wave propagating into cellulose using reasonable estimates of the material properties were performed to generate theoretical predictions for surface temperature, pyrolysis rate and heat of gasification. The experimental data

are in qualitative agreement with the theoretical results, but there is a significant difference in the magnitudes of the apparent heat of gasification.

(2) Diffusion flame theory also shows that the mass fraction of combustible volatiles in the total volatile products of pyrolysis, Y_{FT}, the stoichiometric oxygen/fuel ratio of the combustible volatiles, ν_s, and the heat of combustion per unit mass of combustible volatiles, $h_{c,cv}$, are the fuel-related material properties which must be determined to predict burning behavior. Based on the assumption that the only noncombustible gases in the volatile products of pyrolysis are CO_2 and H_2O, a GC was used, (together with the experimental apparatus for the h_g measurements) to determine the amount of CO_2 and H_2O in the volatiles. Calculations using the GC results show that the addition of NaOH lowers the Y_{FT} values. The data from the GC measurements and char analysis also show that the NaOH addition causes an increase in the ν_s values. Although Frendi (1986) has shown that the heat of combustion of the total volatiles, $h_{c,vol}$, decreases with increasing NaOH concentration, the combined effects of $h_{c,vol}$ and Y_{FT} lead to increased $h_{c,cv}$ values with NaOH addition.

(3) The previous experiments by Tewari (1985) showed that the retardant NaOH acts to suppress the burning of cellulose. In the present work, the retardant NaOH is found to have a dual effect on cellulose burning. Table 6.1 shows the material properties used in diffusion flame calculations. NaOH acts to retard (or suppress) burning by: (1) increasing surface temperature, thereby decreasing the net heat input to the solid fuel surface; (2) decreasing the mass fraction of combustible volatiles in the total

volatiles, thereby reducing the gas phase "fuel" during burning; and (3) raising the stoichiometric oxygen/fuel ratio of the combustible volatiles, thereby making cellulose harder to burn in certain oxygen-containing environments. On the other hand, NaOH acts to promote burning by: (1) lowering the heat of gasification, thereby increasing the production rate of combustible volatiles for a given amount of net heat input to the solid fuel surface; and (2) raising the heat of combustion per unit mass of combustible volatiles, thereby increasing the heat released per unit mass of gas phase "fuel".

In order to determine the complete effects of NaOH on the burning of cellulose and the detailed physical mechanisms by which solid phase fire retardants act to suppress flaming combustion, further studies regarding the physical and thermal properties of the char are needed.

APPENDIX A

SAMPLE PREPARATION

In order to obtain reproducible results for the pyrolysis of bulk samples of cellulose, first of all the samples have to be prepared by following a standard procedure precisely so that the properties will not very from one sample to another. On the other hand, a sample has to have the following principal characteristics:

1. A homogeneous structure to assure homogeneous properties.
2. A smooth and crack-free surface.
3. Sufficient mechanical strength to survive experimental operations without breaking.
4. For a retarded sample, the retardant should be distributed uniformly throughout the sample.

Based on Tewari's (1985) studies, it was decided that for a sample made of a total of 20 g of cellulose, a mix of 8g (2/5 by weight) of filter paper pulp (Schleicher and Schnell, No. 289, 0.01% ash content) and 12g (3/5 by weight) of cellulose powder, (Whatman, Type CF11, 0.015% ash content) is the most suitable combination in terms of surface smoothness and mechanical strength of the samples. For retarded samples, the amount of retardant, NaOH, is calculated by multipylying Y_A (retardant concentration in the cellulose slurry) by 20 g (total amount of cellulose), where Y_A can be obtained from the calibration curve in Fig. A.1 through Y_R (retardant concentration in the sample). It was also decided that the shape of the sample should be a cylinder, 2 in. (5.08 cm) long and 1 in. (2.54 cm) in diameter, with flat surfaces on both ends.

The apparatus for making the cellulose samples is shown in Fig. A.2. It consists of a plexiglass cylinder, 24 in. (61 cm) in length and 1 in (2.54 cm) in internal diameter, with a piston at the top. The piston can be pushed down by a pneumatic press at a controlled speed and pressure. There are two porous metal filters on the piston bottom and cylinder bottom, respectively. The cylinder is placed in a stainless steel cup.

A total of 300 ml of distilled water (including the wash water) is used in making each sample. The following procedure is adopted:

1) Weigh out 12 g of cellulose powder and 8 g of cellulose pulp on an electronic balance (Mettler, PR700). Put the two kinds of cellulose in a 500 ml beaker, add 200 ml (175 ml for retarded samples) of distilled water from a measuring flask, and stir the mixture with a stirrer. For retarded samples, weigh out the desired amount of NaOH on an electronic balance (Mettler, H80), place it in a 100 ml beaker, add 25 ml of distilled water, and dissolve the retardant by stirring.

2) Put 100 ml of distilled water in a wash bottle to wash the container surfaces which have been in contact with cellulose (or cellulose and NaOH) slurry and NaOH solution in order to collect all the original materials.

3) Pour cellulose slurry (or cellulose slurry and NaOH solution) into a blender, wash the beaker containing NaOH solution, and run the blender for 3 minutes to obtain a well-mixed cellulose (or cellulose and NaOH) slurry.

4) Pour the contents of the blender into the 500 ml beaker, and wash the sides of the blender. Then pour the cellulose (or cellulose and NaOH) slurry into the cylinder of the sample making apparatus, as shown in Fig. 2.1., wash the beaker containing the slurry and pour the remaining wash bottle water into the cylinder.

5) Adjust the control valves on the pneumatic press system to let the piston be pressed down with a pressure of 110 psig (8 kg/cm^2) and an average speed of 1 in/min (2.54 cm/min) to squeeze the water out into the cup.

6) Stop the piston at a calibrated height to produce a 3 in. (7.6 cm) long sample.

7) Drain all the water from the cylinder by inverting it, take the sample out of the cylinder with the help of a special jig.

8) Dry the sample in a laboratory oven (Blue M, SwW-11TA) for 5 hours at 85°C to remove moisture.

9) Cut the dried sample to 2 in. (5.1 cm) length and measure the density.

10) Spray the sample front surface with a black heat resistant enamel, (If the cellulose samples were pyrolyzed in their natural condition, the surface emissivity would change with time until the surface was fully charred. In order to have a known value of surface emissivity, the samples surface is sprayed with the high temperature black paint).

11) Dry the sample in the laboratory oven for 1 hour at 105°C to remove the final traces of moisture, and then keep it in a plastic dessicator (Bel-Art) filled with dessiccant. The sample is then ready for use.

The samples thus produced have a density of 0.55 ± 0.01 g/cm^3.

APPENDIX B

DATA ACQUISITION AND PROCESSING

B.1 Temperature Signal Conditioning

The voltage output from the pyrometer inputted into the ADA-AMP signal conditioner is digitized in an A/D convertor, which gives a running digital count of the input voltage. The following are the relations between the input voltage (V) and the digital count (DC).

$$V = \frac{\left[\frac{DC}{2047}\right] FS[2(GN+1)]}{(SW\ GN)(OP\text{-}AMP\ GN)} \tag{B-1}$$

which gives

$$DC = \frac{2047\ V(SW\ GN)(OP\text{-}AMP\ GN)}{FS[2(GN+1)]} \tag{B-2}$$

where:

V = Actual input voltage in volts; maximum ±10 volts; ± 4 volts in this case.

DC = Digital count of the input voltage; equals ±2047 at the peak of the full scale voltage range (±FS) in the ADA-LAB.

FS = Jumper selectable voltage range in the ADA-LAB; can be ±0.5 v, ±1 v, ±2 v and ±4 v. ±4 volts in this case.

GN = Programmable attenuation index in ADA-AMP; range from 0 to 9. 0 in this case.

SW GN = Switch selectable gain in the ADA-AMP; can be 0.1, 1, 10, and 100; 1 in this case.

OP-AMP GN = Operational amplifier gain in the ADA-AMP; continuously variable from 1 to 10; 2 in this case.

If the input voltage range is known approximately, a judicious selection of the above parameters can be made which allows the A/D convertor to use its full range, that is, DC as close to ±2047 as possible. For example, in the pyrolysis experiments, FS, GN, SW GN and OP-AMP GN are set as ±4 v, 0, 1 and 2, respectively, for the extreme case in which V could be the limited value of ±4 volts, the equation (A-2) gives:

$$\begin{aligned} DC &= 2047 \quad \frac{\pm 4 \times 1 \times 2}{\pm 4 \times 2} \\ &= 2047 \end{aligned}$$

It shows that the gain settings used lead to the maximum utilization of the A/D convertor.

B.2 Temperature and Mass Sampling

Fig. A.1 illustrates the way temperature and mass are sampled. It is essential to leave at least a one second margin between the previous mass sampling point (say 3 seconds) and the start of the temperature sampling point for the next mass sampling point (say 6 seconds). This is because whenever the SOFTWEIGH interface is activated to sample mass, the computer and hence all the peripheral interfaces (including Quick I/0), with the exception of the Quick I/0 timer, are disabled for about 1 second. This one second is the time required by the balance to digitize the analog signal into an 8 bit parallel signal, and then convert it into a serial signal to transmit it through the balance cable. Finally, the serial signal is converted again into an 8 bit parallel signal which then is processed by the SOFTWEIGH interface.

Although the computer code can handle arbitrary values of mass and temperature sampling rates, because of the reason above, there is a limited relationship between the two sampling rates, i.e., a 1 second time gap between the mass sampling point and the next temperature sampling point. Also, because of BASIC Language Software limitations, a sampling interval less than 0.2 seconds is not possible. Therefore, in minimum mass sampling time allowed is 3 seconds if 10 temperature samples are taken by using the minimum 0.2 seconds sampling interval. A shorter mass sampling time, e.g. 2 seconds is possible if only 5 temperature samples are taken at 0.2 seconds sampling interval.

B.3 Temperature and Mass Data Processing

Because of fluctuations in the mass readings as sent to the computer, it is not possible to calculate the mass-loss rate using the raw data. It was decided to run a least squares curve fit through the raw mass data, and calculate a curve fit to get the mass and mass loss rate at different times. The same strategy was adopted to smooth the raw temperature data obtained from the pyrometer, which also exhibits significant fluctuation.

To generate input data for the mass regression scheme (or curve fitting), mass values from the balance, along with corresponding time data, at 19 points (starting from 3 seconds) are taken. After fitting a second order curve through these points, a "smoothed" mass value is calculated at the midpoint of the data, and the corresponding mass loss rate is obtained by differentiating the curve fit at that point. Next, again mass and time data at 19 points, starting from 6 seconds this time, are chosen, a second order curve fit is done, and mass loss rates are calculated at the curve midpoint, i.e. at (6+60)/2 = 33 seconds. This process is continued and "smoothed" mass and mass loss rate values are obtained every three seconds, starting at 30 seconds, and ending at 270 seconds for a run of 300 seconds. The curves of mass and mass loss rate versus time are thus obtained.

The value of the temperature at each mass calculation point (30, 33, 36 seconds, etc.) is obtained by fitting a second order curve through 10 temperature raw data readings from the pyrometer. That is, in order to obtain a "smoothed" temperature value at 30 seconds, temperature readings from the pyrometer are collected at 0.2 seconds interval, starting at 28 seconds, and a second order curve is fitted through these 10 points. The temperature at 30 seconds is thus obtained (see Fig. B.1). This process is continued and a smooth curve of sample surface temperature versus time is obtained.

APPENDIX C

DSC MEASUREMENTS OF HEAT OF REACTION

Heat of reaction measurements were made for unretarded (Y_R = 0 and retarded (Y_R = 0.03) samples. A differential scanning calorimeter (DSC) was used (Dupont 9900 DSC/DTA system). The DSC was calibrated with a standard reference, indium, and the reference used during the measurements was an empty copper DSC pan.

Samples were pre-tested, by storing them in an oven at 80°C for two hours, and then immediately transferred to a dessicator. Pre-weighed samples were sealed in a DSC pan under pure N_2. During the measurements, the samples were heated from ambient temperature up to 600°C at the controlled heating rate of 40°C/min, and then weighed after completion of the reaction.

A typical DSC result is shown in Fig. C.1 for an unretarded sample. A downward peak corresponds to an endothermic reaction, while an upward peak means an exothermic reaction. The total values of heat flow into (or out of) the samples during the reaction were automatically integrated by the DSC data recording and processing system. Fig. C.2 shows a comparison of the DSC results for pure and retarded samples. It is apparent that the unretarded sample went through endothermic reaction, even though there is a minor endothermic reaction at the beginning.

The values of the heat of reaction per unit mass of volatiles were calculated by using the following formula:

$$h_r = \frac{q}{1-Y_c} \qquad \text{(C-1)}$$

where

q = heat flow per unit mass of sample, obtained from the DSC integrated value.

Y_c = mass fraction of char.

The average values of the heat of reaction obtained from the DSC measurements are 0.23×10^6 J/kg for the unretarded samples ($Y_R = 0$) and -0.10×10^6 J/kg for the retarded samples ($Y_R = 0.03$). They are used in the numerical calculations of cellulose pyrolysis.

APPENDIX D

CALIBRATION OF GAS CHROMATOGRAPH

The purpose of the GC measurements is to obtain the mass fraction of noncombustible volatiles in the total volatiles for cellulose pyrolysis. The results of the GC measurements are given by the integrator as an area in counts for each component. Therefore a calibration factor is needed for converting the area into the mass for each component.

A bottle of calibration gas (Alltech Associates, Inc., Scott Specialty Gases, Can Mix 217) is used to obtain the calibration factors for CO and CO_2. (The factors for O_2 and N_2 are also obtained at same time.) The bottle contains known volumetric percentages of CO, CO_2 and O_2 in an N_2 base. The formula for calculating the mass of each component derived by using the perfect gas equation is

$$m_i = \frac{P}{RT} V_s M_i X_i \qquad \text{(D-1)}$$

where m_i = mass of species i

P = pressure at which the calibration gas is sampled

= 1 atm

R = universal gas constant

= 8314 J/kg mol.K

T = temperature at which the calibration gas is sampled

= ambient temperature

V_s = volume of the calibration gas sample

= 1 mℓ

M_i = molecular weight of species i

X_i = volumetric fraction (i.e. mole fraction) of species i.

The mass is divided by the corresponding "counts" to give the calibration factors F_i in units of μg/count. Once the factor is known, the masses of CO_2 and CO for unknown samples can be calculated, simply by multiplying the total counts c_i by the calibration factor F_i.

A mixture of laboratory air and pure N_2 was used to calibrate for H_2O. During pyrolysis the H_2O contents for pure and fire retarded cellulose samples cover a wide range. Because the H_2O content in ambient air is limited by the ambient temperature and relative humidity, it was not possible to get a sufficiently small H_2O content from the ambient air. Therefore, it was decided to mix laboratory air with pure N_2. Thus the desired amount of H_2O can be obtained by adjusting the air and N_2 volume ratio which includes the pure laboratory air case. The formula for calculating the mass of H_2O in the mixture was obtained by using Van Wylen and Sonntag's equation (1985), which gives the mass of H_2O in air, and the ideal gas equation. It is as follows:

$$m_{H_2O} = 0.622 \, \frac{m_A}{m_m} \, \frac{V_m}{R_m \, T_m} \, p_{sat} \, \phi_m \qquad \text{(D-2)}$$

where m_{H_2O} = mass of water vapor in the mixture of laboratory air and N_2

m_A = mass of laboratory air

m_m = mass of the mixture of laboratory air and N_2

V_m = volume of the mixture of laboratory air and N_2

= 1 ml

R_m = gas constant of the mixture of laboratory air and N_2

≈ 292 J/kgK (for 90% of N_2)

T_m = temperature of the mixture of laboratory air and N_2

p_{sat} = saturated vapor pressure of steam at T_m

ϕ_m = relative humidity of the mixture of laboratory air and N_2

In the case of pure laboratory air, m_A=m_m, the Eqn. (D-2) becomes

$$m_{H_2O} = 0.622 \frac{V_A}{R_A\ T_A}\ p_{sat}\ \phi_A \qquad \text{(D-3)}$$

where V_A = volume of laboratory air

= 1 ml

R_A = gas constant for air

= 287 J/kg K

T_A = temperature of laboratory air

p_{sat} = saturated vapor pressure of steam at T_A

ϕ_A = relative humidity of laboratory air

According to the formulas, since $V_m(V_A)$, R_m and R_A are constants, and p_{sat} is a function of $T_m(T_A)$ at one atmosphere, the mass of H_2O is a function of $T_m(T_A)$ and $\phi_m(\phi_A)$. Because p_{sat} is a very sensitive function of temperature, a thermometer with 1/10°C divisions was used to measure $T_m(T_A)$. A relative humidity meter (Dikson Instant RH) was used to measure the ϕ_m (ϕ_A) values to 1 percent accuracy. The meter was calibrated against 0% and 75% standard relative humidity capsules.

After a number of calibration runs, the values of the mass of H_2O per unit volume were obtained as functions of a wide range of GC "counts". The calibration results of m vs. c of H_2O are shown in Fig. 5.3. Since the calibration factor $F_i \equiv m_i/c_i$, the results show that the calibration factor for H_2O is not a constant. A linear fit was run through the calibration data. The equation for the straight line was used for data reduction.

Once the calibration factors are known, the mass fractions of the noncombustible gaseous products of cellulose pyrolysis can be calculated as described below.

The mass fraction of species i in total volatiles is defined as the ratio of mass flow rate of species i to the total volatiles production rate (as measured by the electronic balance during the experiment), i.e.

$$Y_i = \frac{\dot{m}_i}{\dot{m}_{vol}} \qquad \text{(D-4)}$$

The basic assumption made for the calculation is that the mass fraction of species i in the total volatiles, as defined above, is a constant throughout the whole volatiles flow system (see Fig. 4.1 and Section 4.1) i.e.

$$Y_i = Y_{i,\,\text{Rotameter}} = Y_{i,\,\text{sample loop}} \qquad \text{(D-5)}$$

There are the following relations.

$$\dot{m}_i = Y_{i,\mathrm{Rotameter}} \quad \dot{m}_{\mathrm{Rotameter}}$$

$$= Y_{i,\mathrm{sample\ loop}}\ \dot{m}_{\mathrm{Rotameter}} \qquad \text{(D-6)}$$

$$Y_{i,\mathrm{sample\ loop}} = \frac{c_i F_i}{\sum_i (c_i F_i)} \qquad \text{(D-7)}$$

$$\dot{m}_{\mathrm{Rotameter}} = \dot{V}_{\mathrm{Rotameter}}\ \rho_{\mathrm{Rotameter}} \qquad \text{(D-8)}$$

The value of $\rho_{\mathrm{Rotameter}}$ is taken as the value of ρ_{N_2} at 1 atm and the measured value of T because it is found that there is about 99% N_2 in the total volatiles during the cellulose pyrolysis.

Therefore, the final formula is

$$m_i = \frac{\text{counts } F_i}{\Sigma\ (\text{counts } F_i)}\ \dot{V}_{\mathrm{Rotameter}} \quad \rho_{N_2} \qquad \text{(D-9)}$$

The $\dot{m}''_{vol}$ data are obtained by using the same balance-computer system. The data acquisation and processing procedure is exactly the same as in the h_g measurements.

At last, the data for m_i and m_{vol} are combined to get the Y_i values.

REFERENCES

Atreya, A., "Pyrolysis, Ignition and Fire Spread on Horizontal Surfaces of Wood", Ph.D. Thesis, Division of Applied Sciences, Harvard University (1983).

Bauer, R. G., "Fire Retardant Polymners: A Review", J. Fire Retardant Chemistry, **5**, 200 (1978).

Chan, W. -C. R., Kelbon, M. and Krieger, B. B., Product Formation in the Pyrolysis of Large Wood Particles", Fundamentals of Thermochemical Biomass Conversion, pp. 219-236, Elsevier Applied Science Publishers, New York (1985).

Cullis, C. F., Hirschler, M. M., Townsend, R. P. and Visanuvimol, V., "The Combustion of Cellulose under Conditions of Rapid Heating", Comb. and Flame, **49**, 249-254 (1983).

Drews, M. J. and Barker, R. H., "Pyrolysis and Combustion of Cellulose. Part VI. The Chemical Nature of the Char", J. Fire and Flammability, **5**, 116 (1974).

Emmons, H. W., "Scientific Progress on Fire", Ann. Rev. Fluid Mechanics, 223 (1980).

Encyclopedia of Polymer Science and Technology, Fire Retardancy, Interscience, Vol. 7 (1967).

Fire Safety Aspects of Polymeric Materials: State of the Art, National Academy of Sciences, Washington (1977).

Fremy, E., Compt. Rend., **66**, 456 (1968).

Frendi, A., "Heat of Combustion of the Combustible Gases of Cellulose", M.S. Thesis, Division of Engineering, Brown University (1986).

Heskestad, G., "A Fire Products Collector for Calorimetry into the Megawatt Range", Factory Mutual Research, J.I. (OC2E1.RA (1981).

Kansa, E. J., Perlee, H. E. and Chaiken, R. F., "Mathematical Model of Wood Pyrolysis Including Internal Forced Convection", Comb. and Flame, **29**, 311 (1977).

Kanury, A. M. and Blackshear, P. L., Jr., "Some Considerations Pertaining to the Problem of Wood-Burning", Comb. Sci. and Tech., **1**, 339-355 (1970).

Kashiwagi, T., Ohlemiller, T. J. and Werner, K., "Effects of External Radiant Flux and Ambient Oxygen Concentration on Nonflaming Gasification Rates and Evolved Products of White Pine", Comb. and Flame, **69**, 331-345 (1981).

Kilzer, F. J. and Broido, A., "Speculations on the Nature of Cellulose Pyrolysis", Pyrodynamics, **2**, 151-163 (1965).

Kung, H. C., "A Mathematical Model of Wood Pyrolysis", Comb. and Flame, **18**, 185 (1972).

Kung, H. C. and Kalelkar, A. S., "On the Heat Reaction in Wood Pyrolysis", Comb. and Flame, **20**, 91-103 (1973).

Lee, C. K., Chaiken, R. F. and Singer, J. M., "Charring Pyrolysis of Wood in Fires by Laser Simulation", 16th Internat'l Symp. on Comb., The Combustion Institute, 1459-1470 (1977).

Lee, C. K. and Diehl, J. R., "Combustion of Irradiated Dry and Wet Oak", Comb. and Flame, **42**, 123-138 (1981).

Lewin, M. and Basch, A., "Structure, Pyrolysis and Flammability of Cellulose", Flame-Retardant Polymeric Materials, Vol. 2, Plenum Press (1978).

Lipska, A. E. and Parker, W. J., "Kinetics of the Pyrolysis of Cellulose in the Temperature Range 250-300°C", J. Appl. Polym. Sci., **10**, 1439-1453 (1966).

Lipska, A. E. and Martin, S. B., "The Effect of Flame Retardants on Thermal Degradation of α-Cellulose in Nitrogen", SRI Project No. PYU-8150, Final Report, Stanford, CA (1971).

Mark, H. F., Atlas, S. M. Shalaby, S. W. and Pearce, E. M., "Combustion of Polymer and Its Retardation", Fire-Retardant Polymeric Materials, Vol. 1, Plenum Press (1975).

McCarter, R. J., "The Pyrolysis of Cellulose at Rates Approaching Those in Burning", Textile REsearch Journal, **42**, 709-719 (1972).

Mok, W. S.-L. and Antal, M. J., Jr., "Effects of Pressure on Biomass Pyrolysis. II. Heats of Reaction of Cellulose Pyrolysis", Thermochimica Acta, **68**, 165-186, 1983.

Nunn, T. R., Howard, J. B., Longwell, J. P. and Peters, W. A., "Studies of the Rapid Pyrolysis of Sweet Gum Hardwood", Fundamentals of Thermochemical Biomass Conversion, pp. 293-315, Elsevier Applied Science Publishers, New York, 293-315 (1985).

Ohlemiller, T. J., Kashiwagi, T. and Werner, K., "Wood Gasification at Fire Level Heat Fluxes", Comb. and Flame, **69**, 155-170 (1987).

Pagni, P. J., "Diffusion Flame Analyses", Fire Safety Journal, **3**, 273 (1980).

Parker, W. J. and Lipska, T. J., "A Proposed Mechanism for the the Decomposition of Cellulose and the Effect of Flame Retardants", NRDL-TR-69 (1969).

Roberts, A. F. and Clough, G., "Thermal Decomposition of Wood in an Inert Atmosphere", 9th Intern'l Symp. on Comb., The Combustion Institute, 158-166 (1963).

Roberts, A. F., "Problems Associated with the Theoretical Analysis of the Burning of Wood", 13th ntern'l Symp. on Comb., The Combustion Institute, 893-903 (1971).

Roberts, A. F., "The Heat of Reaction during the Pyrolysis of Wood", Comb. and Flame, **17**, 79-86 (1971).

Rogers, F. E. and Ohlemiller, T. J., "Cellulose Insulation Materials. I. Overall Degradation Kinetics and Reaction Heats", Comb. Sci. and Tech., **24**, 129-137 (1981).

Roy, C., DeCaumia, B., Brouillard, D. and Menard, H., "The Pyrolysis under Vacuum of Aspen Poplar", Fundamentals of Thermochemical Biomass Conversion, pp. 237-256, Elsevier Applied Science Publishers, New York (1985).

Seshadri, K. and Williams, F. A., "Structure and Extinction of Counterflow Diffusion Flames", J. Polym. Sci., **16**, 1755 (1978).

Shafizadeh, F., "Pyrolysis and Combustion of Cellulosic Materials", Advances in Carbohydrate Chemistry, **23**, 419-474 (1968).

Shafizadeh, F., Chin, P. S. and DeGroot, W. F., "Mechanistic Evaluation of Flame Retardants", J. Fire Retardant Chemistry, **2**, 195-203 (1975).

Sibulkin, M., Kulkarni, A. K. and Annamalai, K., "Burning on a Vertical Fuel Surface with Finite Chemical Reaction Rate", Comb. and Flame, **44**, 187-199 (1982).

Sibulkin, M. and Tewari, S. S., "Measurements of Flaming Combustion of Pure and Fire-Retardant Cellulose", Comb. and Flame, **59**, 31-42 (1985).

Sibulkin, M., "Heat of Gasification for Pyrolysis of Charring Materials", Fire Safety Science - Proc. of the First Intern'l Symp., pp. 391-400.

Tamanini, F., "A Numerical Model for One-Dimensional Heat Conduction with Pyrolysis in a Slab of Finite Thickness", Factory Mutual Research, Serial No. 21011.7, Appendix A, 220 (1976).

Tang, W. K. and Neill, W. K., "Effect of Flame Retardants on Pyrolysis and Combustion of α-Cellulose", J. Polym. Sci., Part C, 65-80 (1964).

Tewari, S. S., "An Experimental Study of the Burning of Pure and Fire Retarded Cellulose", Ph.D. Thesis, Division of Engineering, Brown University (1985).

Tewarson, A., "Physico-Chemical and Combustion/Pyrolysis Properties of Polymeric Materials", NBS-GCR-80-295, **26** (1980).

Van Wylen, J. and Sonntag, R. E., "Fundamentals of Classical Thermodynamics", pp. 421, John Wiley & Sons, 3rd Edition (1985).

Wodley, F. A., "Pyrolysis Products of Untreated and Flame Retardant-Treated a-Cellulose and Levoglucosan", J. Appl. Polym. Sci., **15**, 835-851 (1971).

Table 2.1

Reflectance of Sample Surface

λ (um)	Y_R	ρ
0.2-3.5	0	0.03
	0.03	0.05
2.5-25	0	0.03
	0.03	0.04

TABLE 3.1

Material Properties Used in Pyrolysis Calculations

Y_R	ρ_S (kg/m^3)	ρ_C (kg/m^3)	C_{pS} (J/kg °C)	C_{pC} (J/kg °C)	C_{pG} (J/kg °C)
0	550	55	1300	900	1700
0.03	550	165	1300	900	1700

Y_R	$k_{S,\infty}$ (w/m °C)	$k_{C,\infty}$ (w/m °C)	k^*_S (w/m °C)	k^*_C (w/m °C)	$h_{r,\infty}$ (J/kg)
0	0.1	0.027	4×10^{-4}	4×10^{-4}	-0.23×10^{6}
0.03	0.1	0.080	4×10^{-4}	4×10^{-4}	0.10×10^{6}

Y_R	E (J/kg mol)	A	$\bar{h}$ (W/m^2 °C)	ϵ_s	$q''_{ab,s}$ (kW/m^2)
0	1.5×10^{8}	1×10^{10}	13.5	0.96	40
0.03	1.5×10^{8}	1×10^{10}	13.5	0.96	40

TABLE 5.1

Mass Fractions of Char from Cellulose Pyrloysis

Y_R	Y_{char}
0	0.09
0.005	0.19
0.010	0.25
0.015	0.27
0.020	0.28
0.025	0.29
0.030	0.30

TABLE 5.2

Elemental Composition of Cellulose

$Y_{C,cell}$	$Y_{H,cell}$	$Y_{O,cell}$
0.44	0.062	0.49

TABLE 5.3

Elemental Composition of Char

Y_R	$Y_{C,char}$	$Y_{H,char}$	$Y_{O,char}$	$Y_{Na,char}$
0	0.80	0.039	0.16	0
0.005	0.81	0.041	0.14	0.015
0.010	0.75	0.044	0.18	0.024
0.015	0.76	0.042	0.17	0.032
0.020	0.77	0.040	0.15	0.040
0.025	0.77	0.041	0.14	0.050
0.030	0.76	0.036	0.14	0.056

TABLE 5.4

Elemental Composition of Total Volatiles

Y_R	$Y_{C,vol}$	$Y_{H,vol}$	$Y_{O,vol}$
0	0.41	0.064	0.53
0.005	0.36	0.067	0.58
0.010	0.34	0.067	0.60
0.015	0.32	0.068	0.61
0.020	0.31	0.069	0.62
0.025	0.30	0.069	0.64
0.030	0.29	0.071	0.64

TABLE 5.5

Mass Fractions of Non-combustible Gases in Total Volatiles

Y_R	Y_{CO_2}	Y_{HO_2}	Y_{FT}*
0	0.06	0.25	0.69
0.005	0.16	0.37	0.47
0.010	0.19	0.43	0.38
0.015	0.21	0.44	0.35
0.020	0.22	0.44	0.34
0.025	0.23	0.43	0.34
0.030	0.24	0.41	0.35

*$Y_{FT} \equiv 1 - (Y_{CO_2} + Y_{H_2O})$

TABLE 5.6

Elemental Composition of Combustible Volatiles and Stoichiometric Ratio

Y_R	$Y_{C,\,cv}$	$Y_{H,\,cv}$	$Y_{O,\,cv}$	ν_s
0	0.57	0.050	0.38	1.6
0.005	0.66	0.050	0.29	1.9
0.010	0.75	0.050	0.20	2.2
0.015	0.75	0.060	0.19	2.3
0.020	0.73	0.060	0.21	2.2
0.025	0.68	0.060	0.26	2.1
0.030	0.63	0.070	0.29	2.0

TABLE 5.7

Major Products of Cellulose Pyrolysis

Y_R	Y_{char}	Y_{inert}	$Y_{com,vol}$
0	0.09	0.28	0.63
0.005	0.19	0.43	0.38
0.010	0.25	0.47	0.28
0.015	0.27	0.47	0.26
0.020	0.28	0.48	0.24
0.025	0.29	0.47	0.24
0.030	0.30	0.46	0.24

TABLE 6.1

Material Properties Used in Diffusion Flame Calculations

Y_R	$h_g \times 10^{-6}$ (J/kg)	Y_{FT}	ν_s	$h_{c,cv} \times 10^{-6}$ (J/kg)
0	1.0	0.69	1.6	20
0.005	0.61	0.47	1.9	26
0.010	0.46	0.38	2.2	28
0.015	0.40	0.35	2.3	27
0.020	0.38	0.34	2.2	27
0.025	0.38	0.34	2.1	28
0.030	0.37	0.35	2.0	27

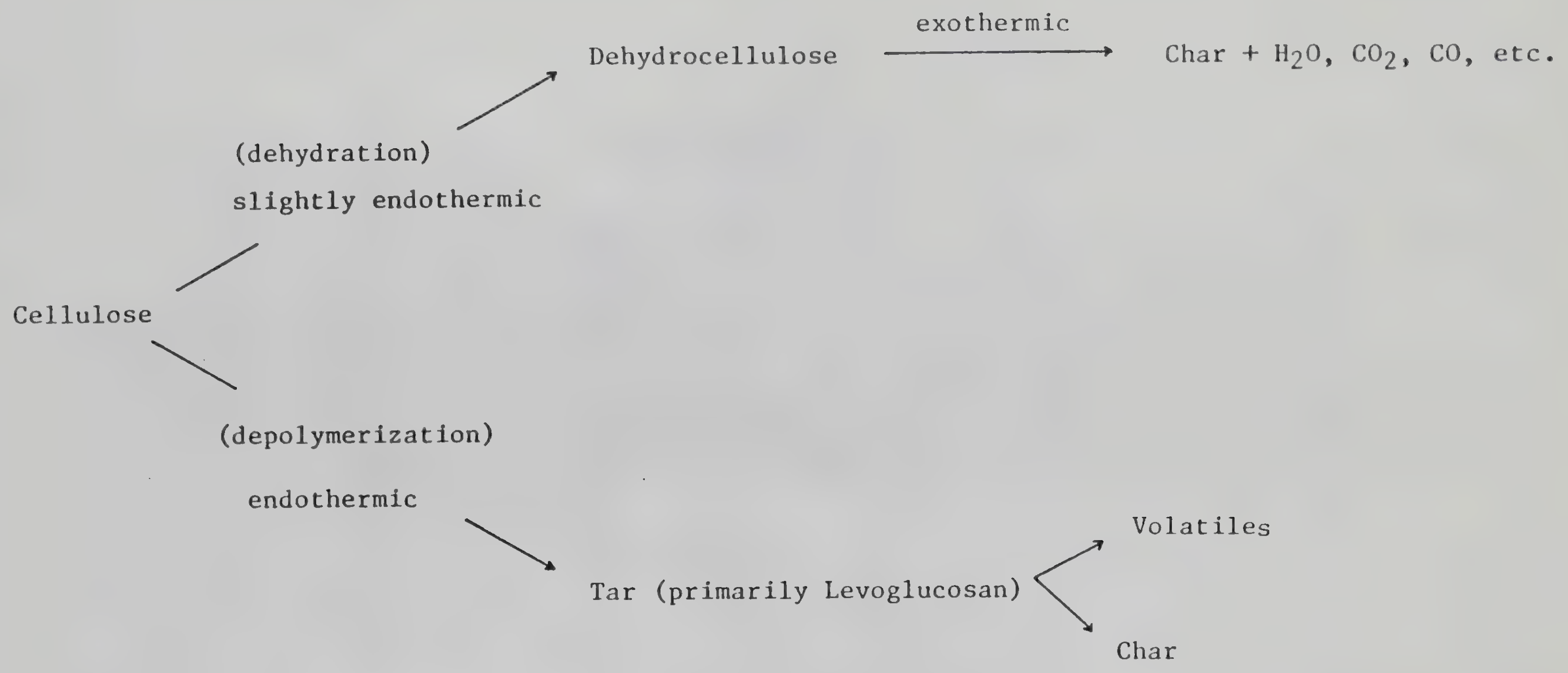

Figure 1.1 General scheme for cellulose pyrolysis.

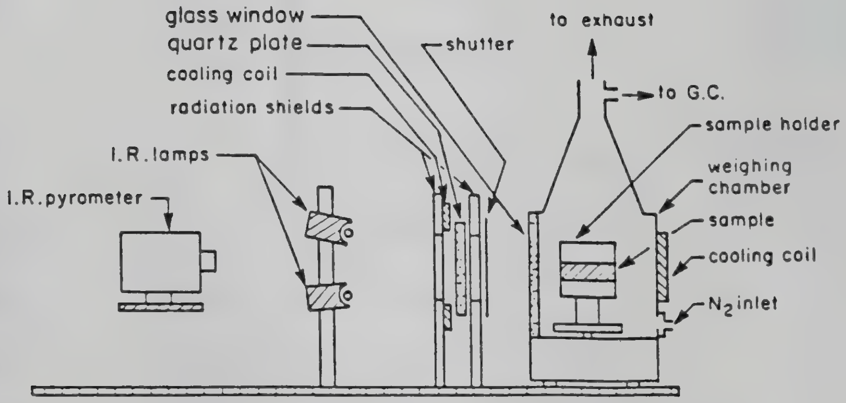

Figure 2.1 Schematic drawing of the apparatus used in heat of gasification measurements.

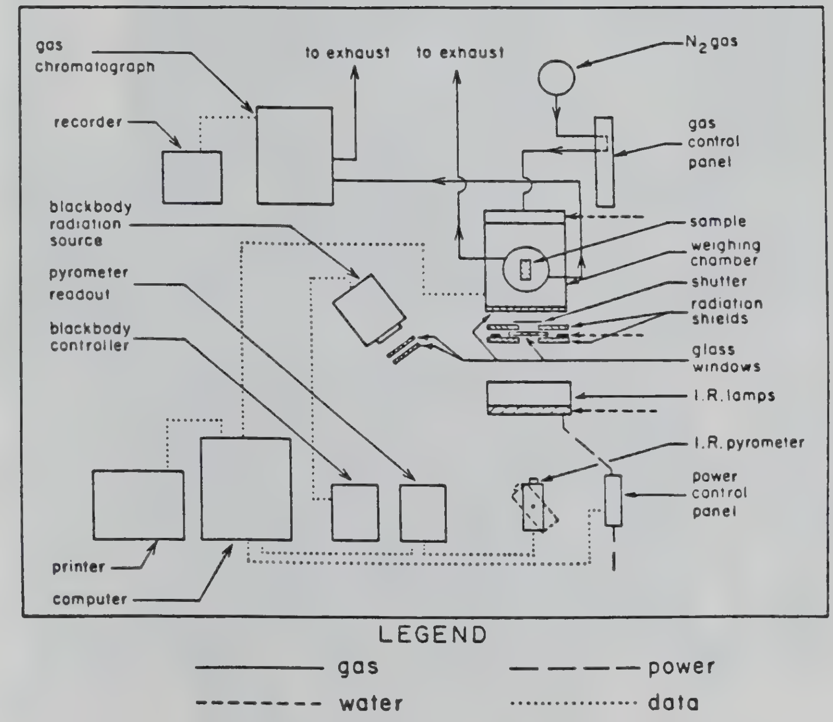

Figure 2.2 Schematic drawing (top view) of set-up for cellulose pyrolysis measurements.

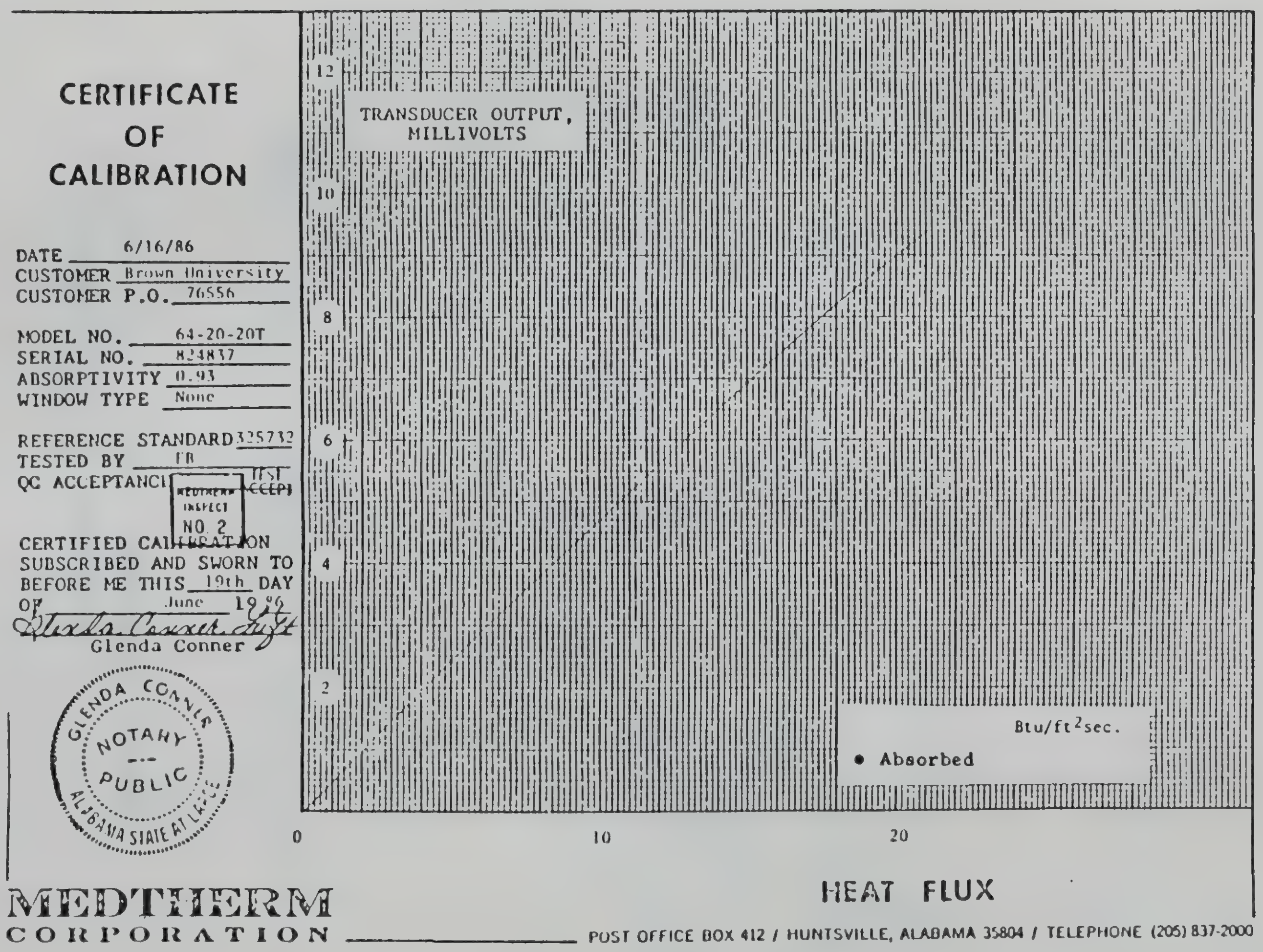

CERTIFICATE
OF
CALIBRATION

DATE 6/16/86
CUSTOMER Brown University
CUSTOMER P.O. 76556

MODEL NO. 64-20-20T
SERIAL NO. 824837
ABSORPTIVITY 0.93
WINDOW TYPE None

REFERENCE STANDARD 325732
TESTED BY FB
QC ACCEPTANC TEST CCEPT

MEDTHERM
INSPECT
NO. 2

CERTIFIED CALIBRATION
SUBSCRIBED AND SWORN TO
BEFORE ME THIS 19th DAY
OF June 1986
Glenda Conner

MEDTHERM
CORPORATION

POST OFFICE BOX 412 / HUNTSVILLE, ALABAMA 35804 / TELEPHONE (205) 837-2000

Figure 2.3 Heat flux gauge calibration curve.

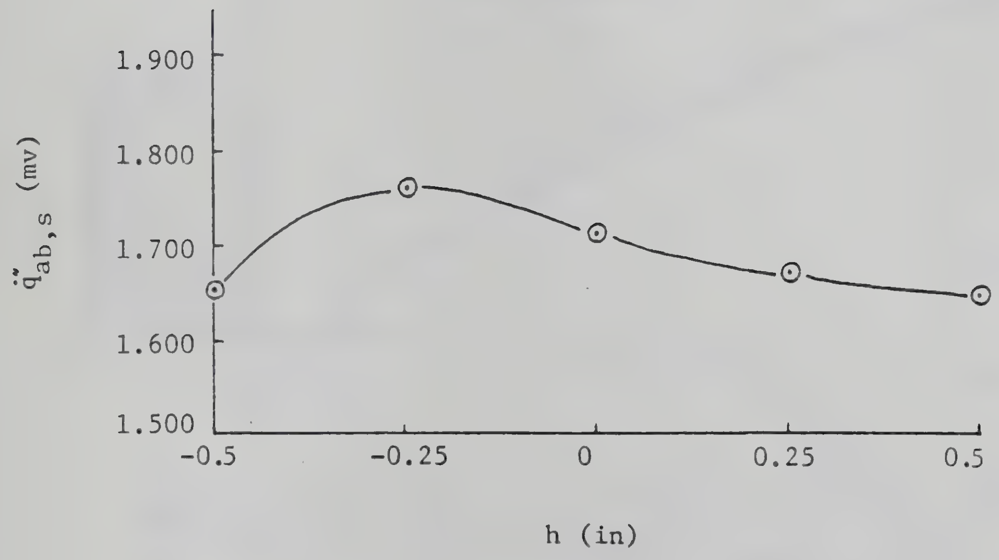

Figure 2.4 Vertical variation of absorbed heat flux over the sample height.

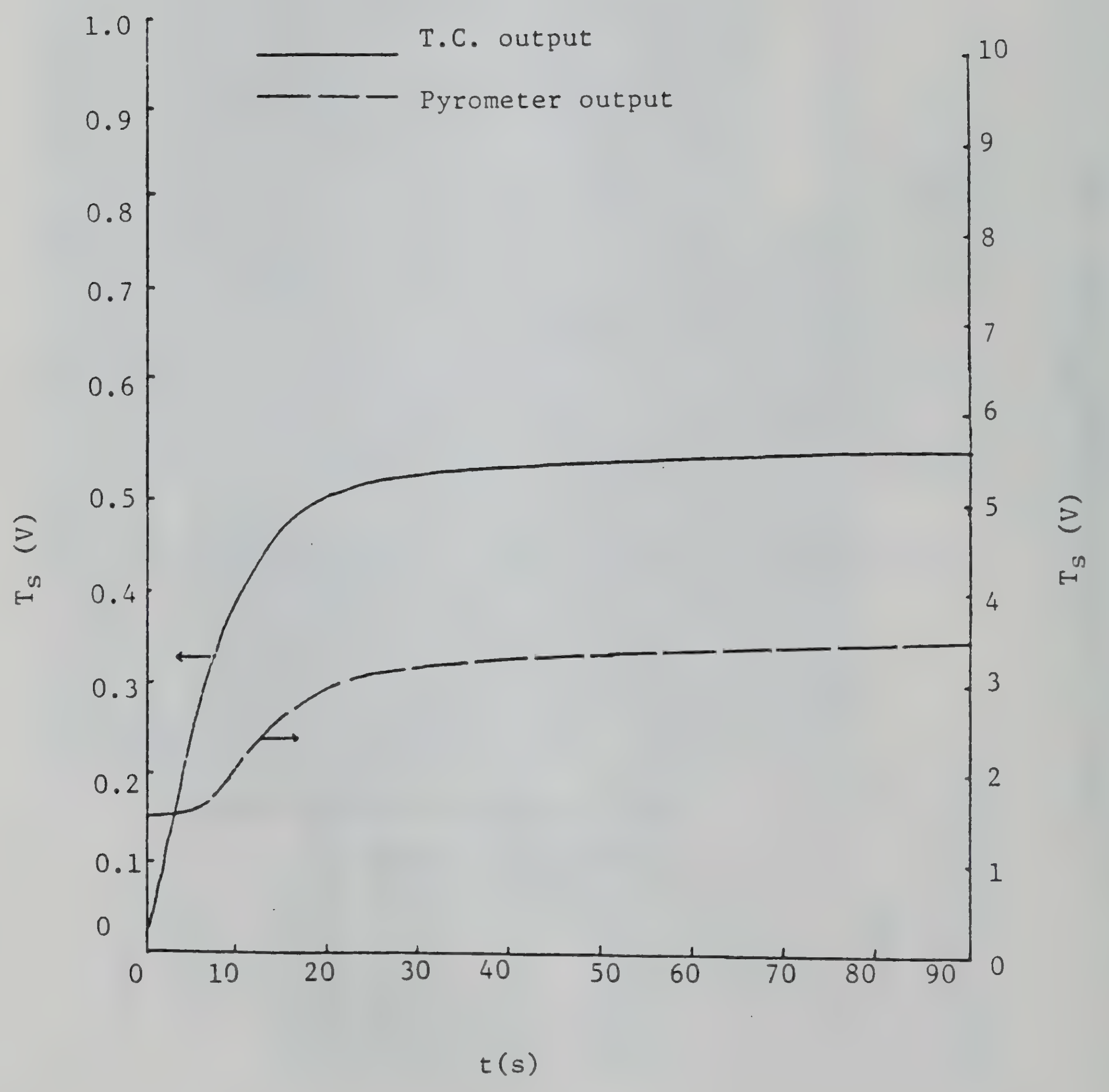

Figure 2.5 Voltage outputs of thermocouple and pyrometer vs. time.

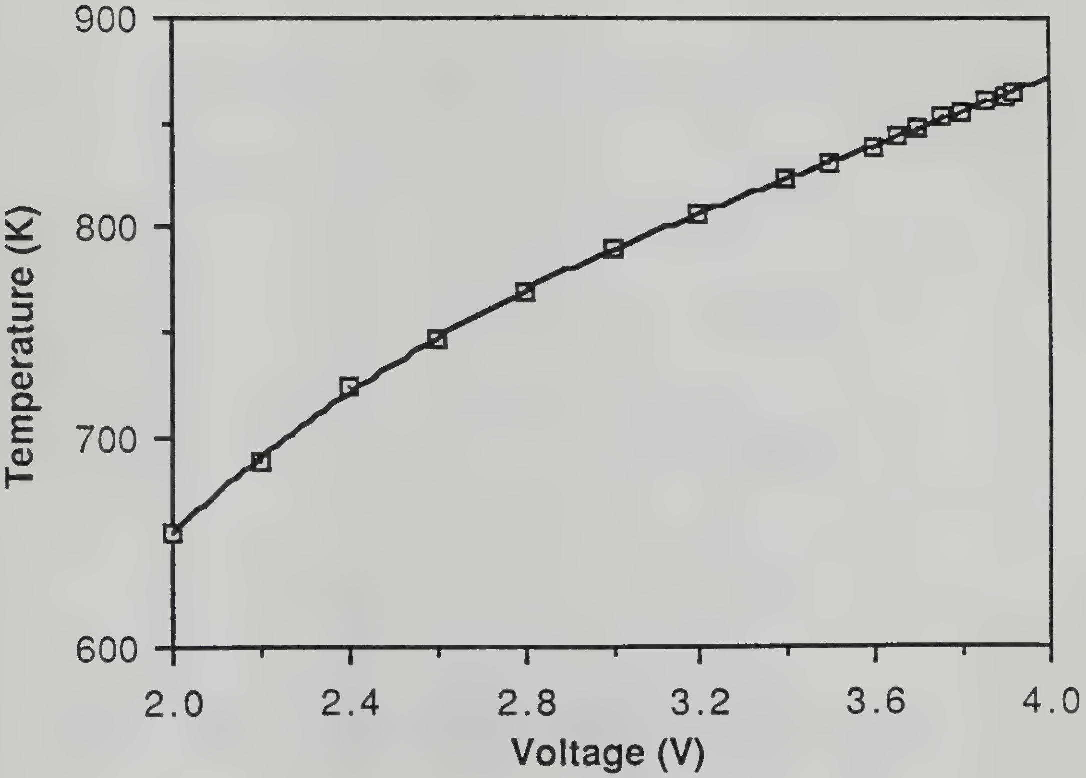

Figure 2.6 Calibration of surface temperature vs. pyrometer output voltage, the data is fitted by the polynomial $T = -116 + 641V - 157V^2 + 14.6V^3$.

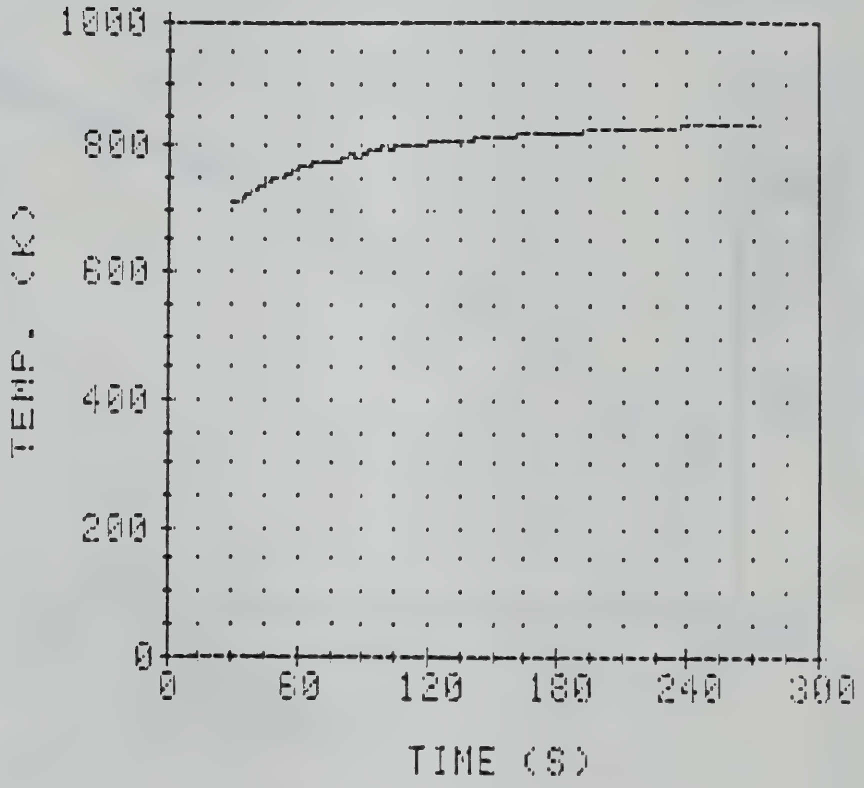

Figure 2.7(a) An example of computer output of surface temperature vs. time; $Y_R=0$; $\dot{q}''_{ab,s}=40$ kW/m^2.

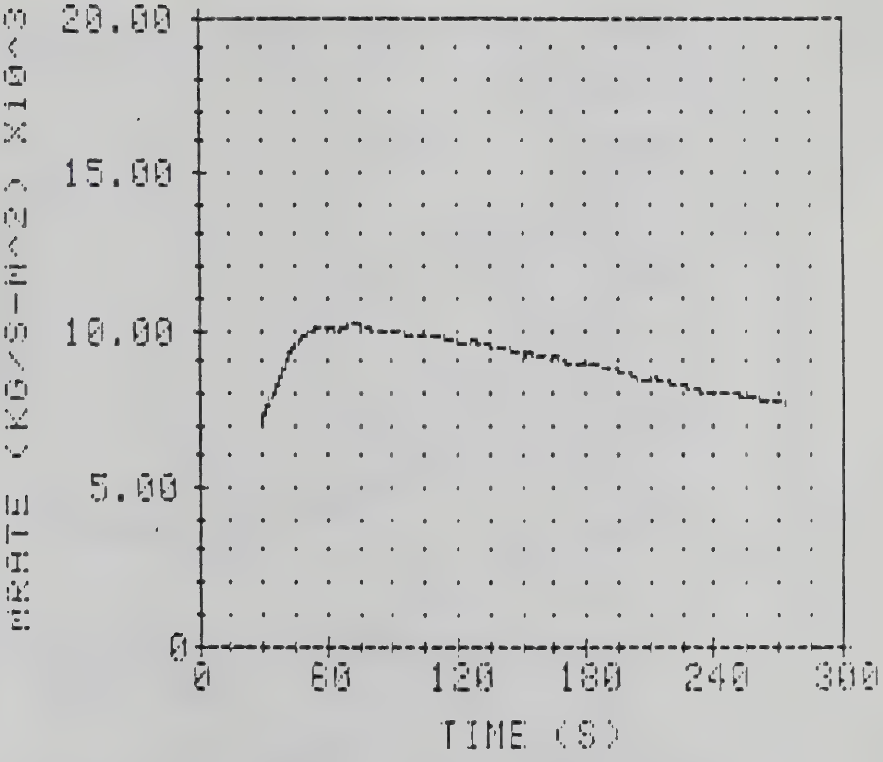

Figure 2.7(b) An example of computer output of mass loss rate vs. time; $Y_R=0$; $\dot{q}''_{a\ b,s}=40 kW/m^2$.

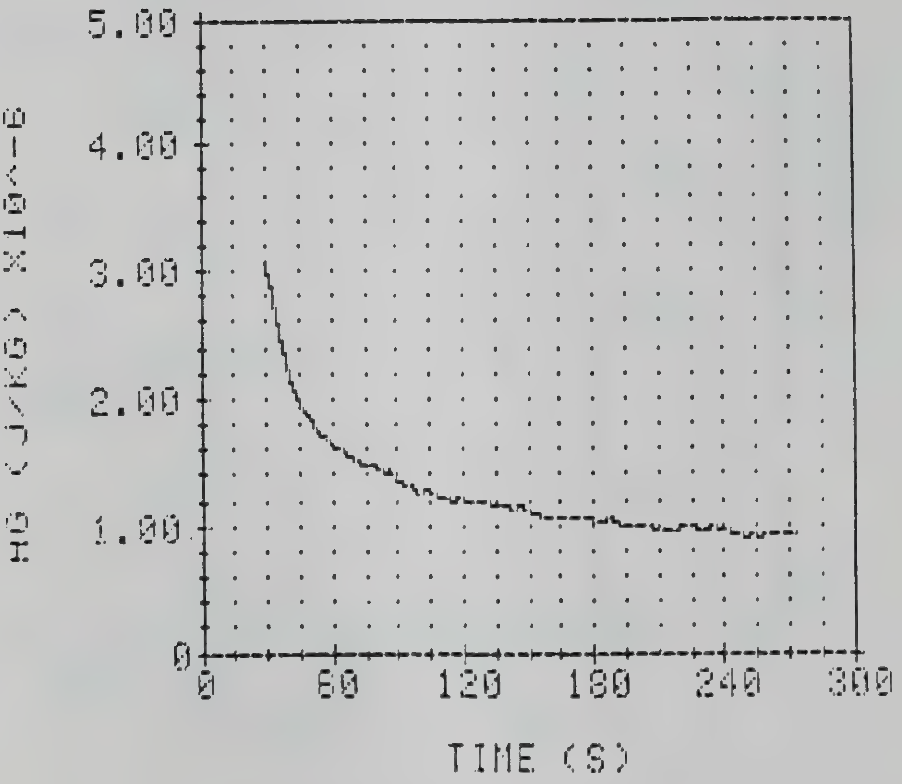

Figure 2.7(c) An example of computer output of heat of gasification vs. time; $Y_R=0$; $\dot{q}''_{ab,s}=40$ kW/m^2.

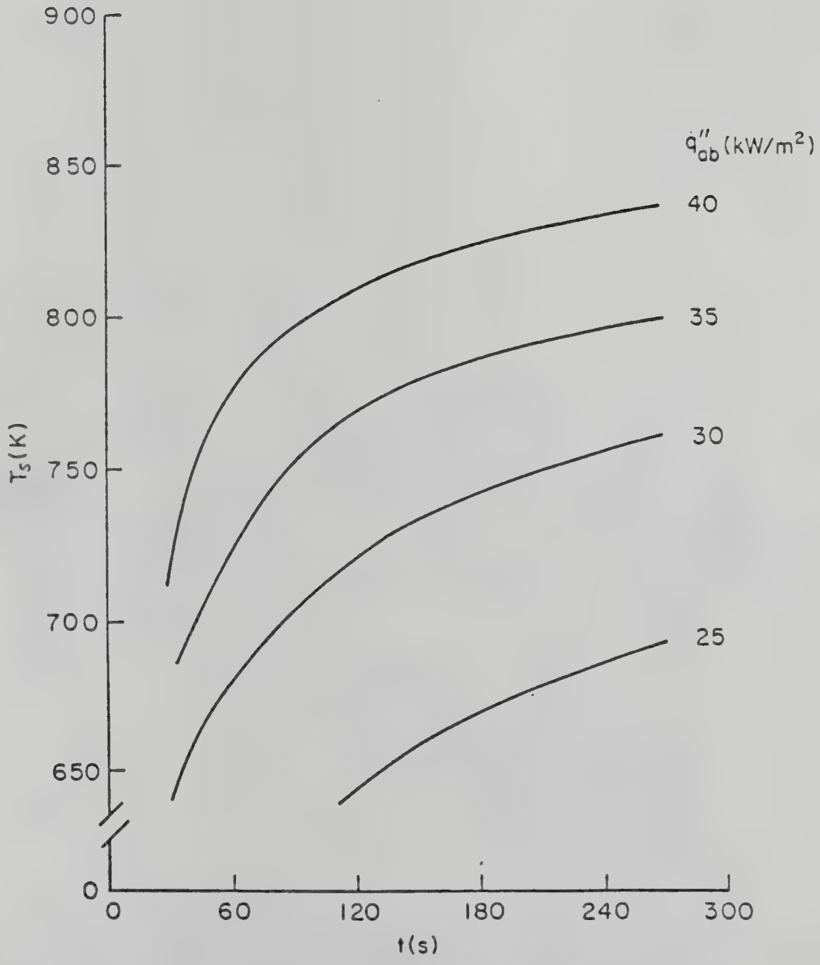

Figure 2.8 Surface temperature vs. time for different absorbed heat fluxes; Y_R=0.

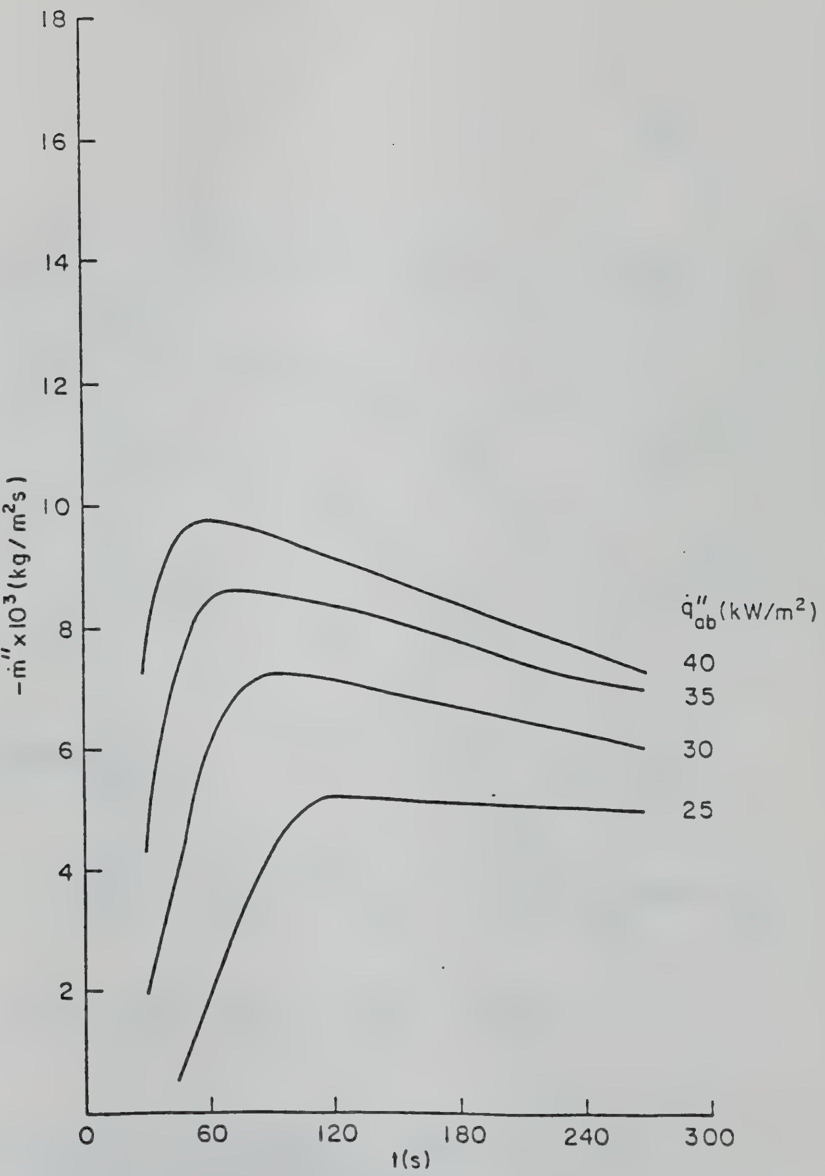

Figure 2.9 Mass loss rate vs. time for different absorbed heat fluxes; Y_R=0.

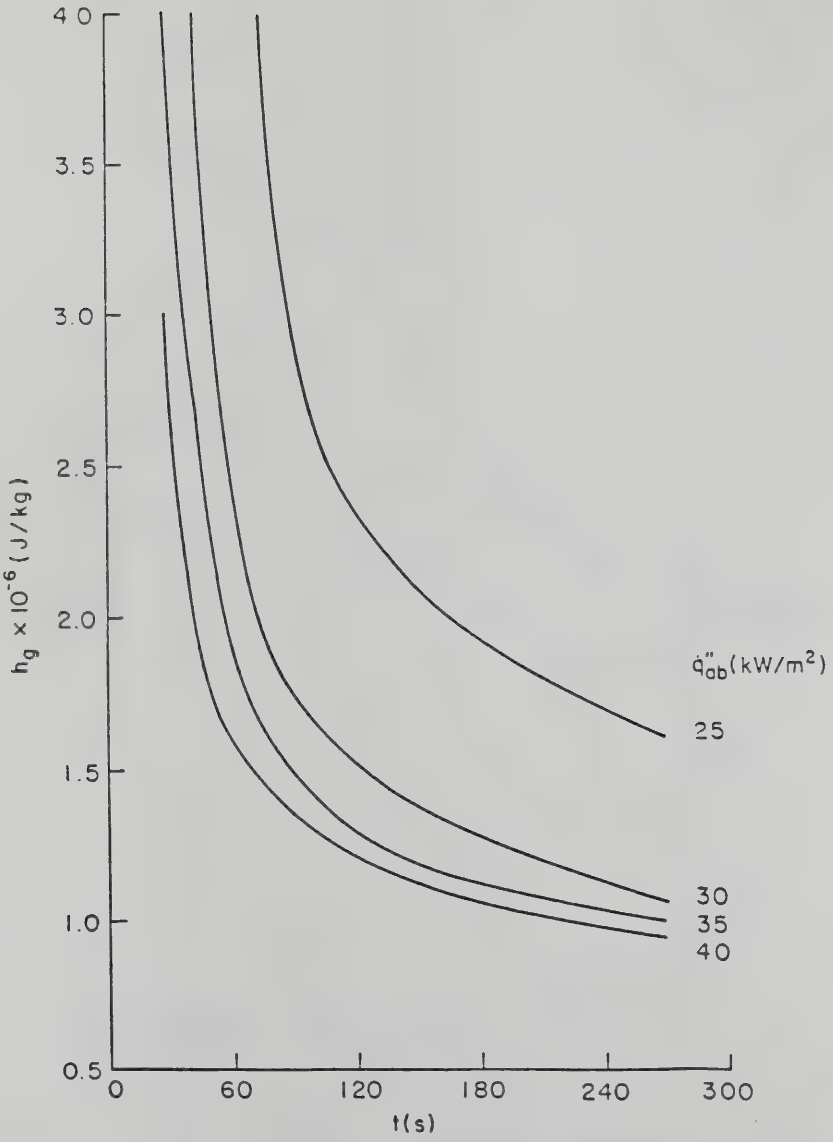

Figure 2.10 Heat of gasification vs. time for different absorbed heat fluxes; Y_R=0.

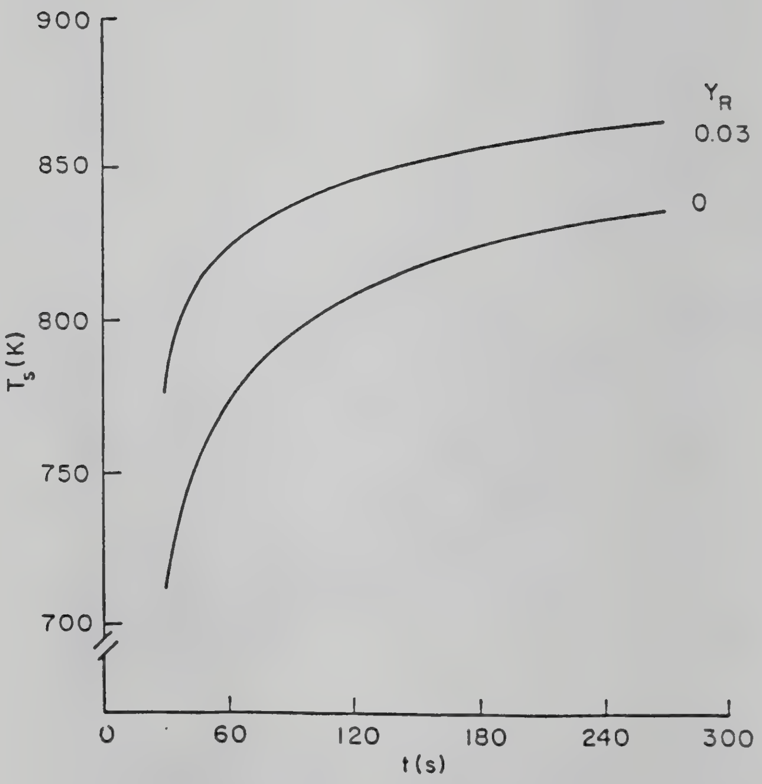

Figure 2.11 Surface temperature vs. time for pure and retarded cellulose samples; $\dot{q}''_{ab,s}$=40 kW/m^2.

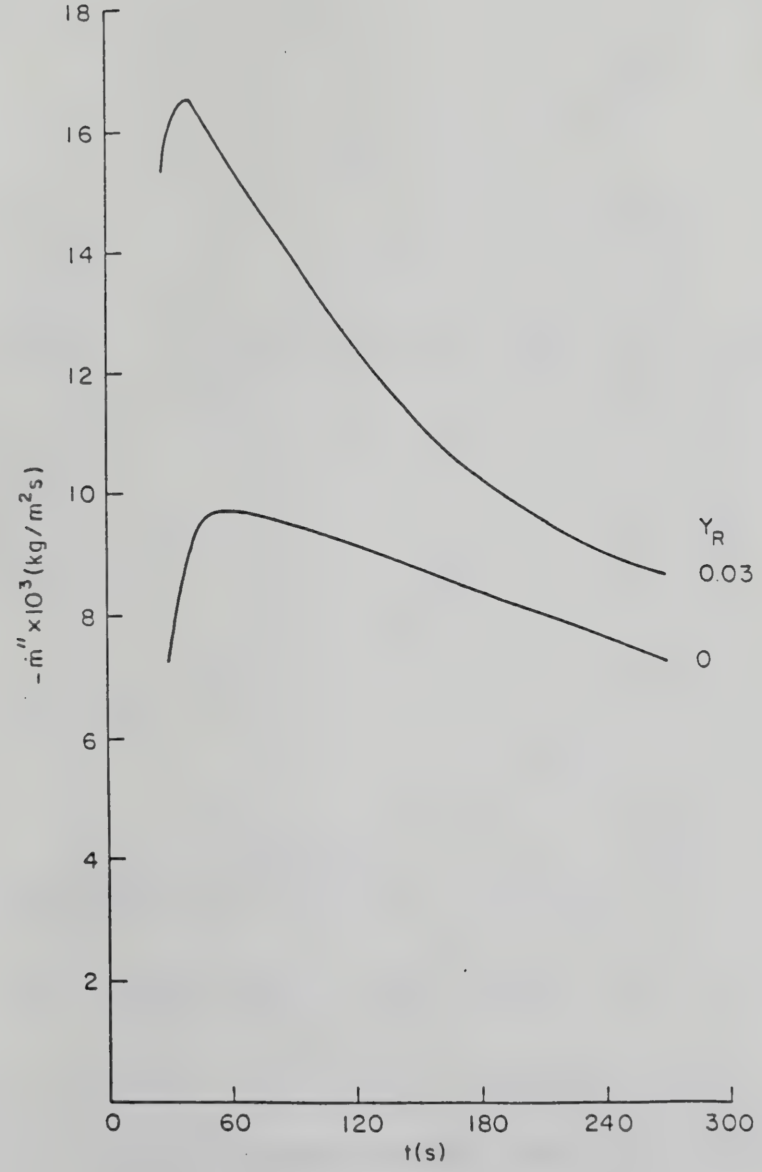

Figure 2.12 Mass loss rate vs. time for pure and retarded cellulose samples; $\dot{q}''_{ab,s}$=40 kW/m^2.

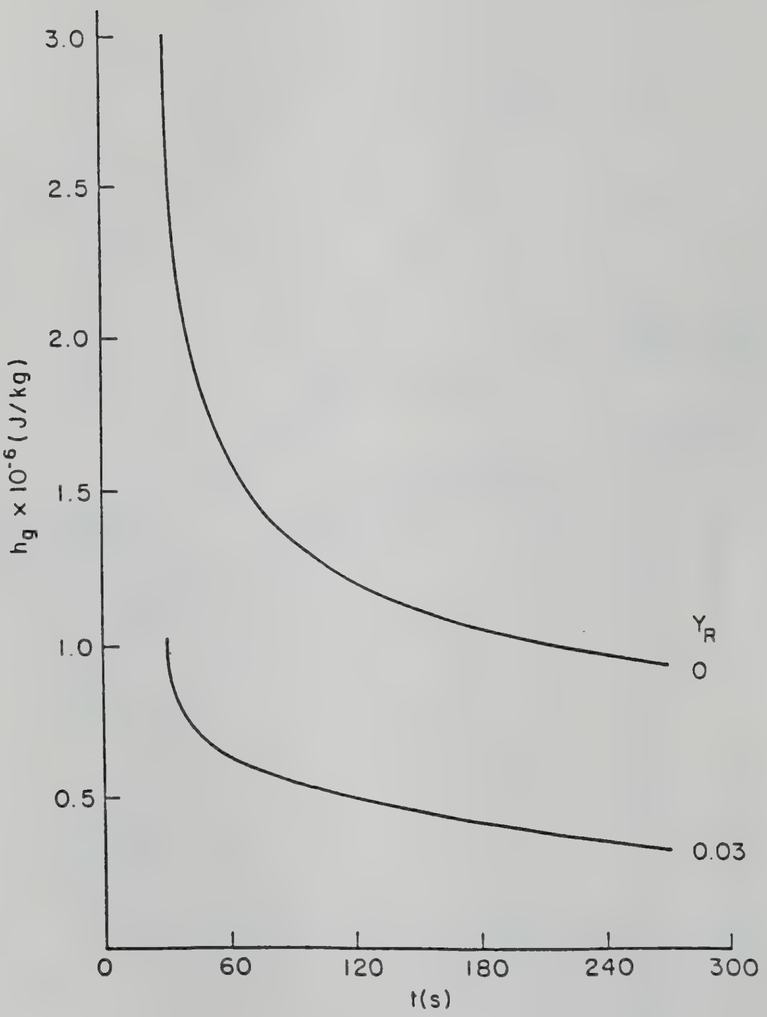

Figure 2.13 Heat of gasification vs. time for pure and retarded cellulose samples; $\dot{q}''_{ab,s}$=40 kW/m^2.

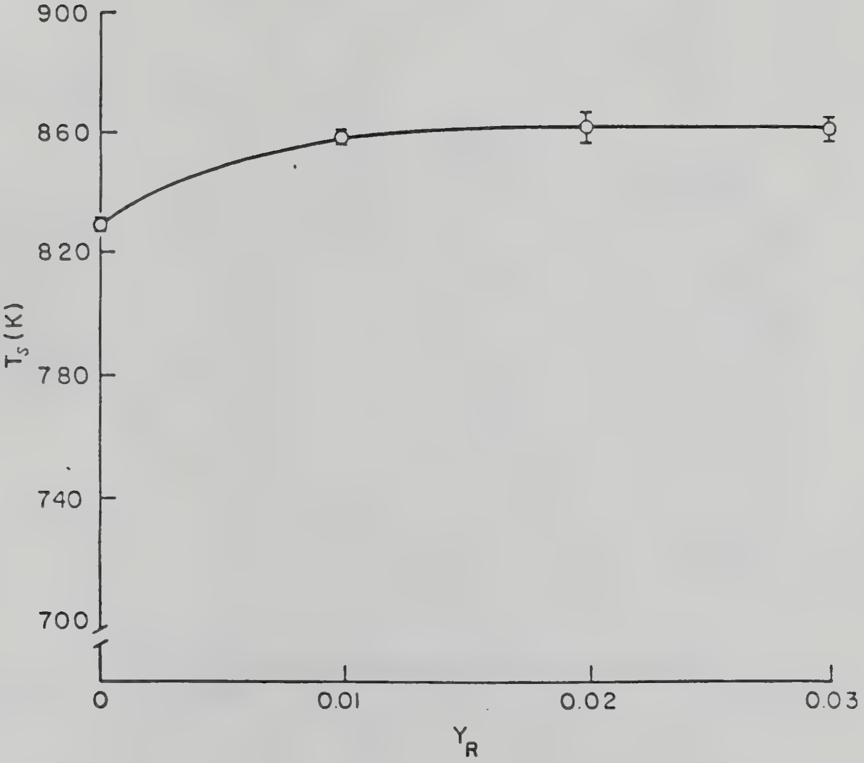

Figure 2.14 Surface temperature vs. retardant concentration; $\dot{q}''_{ab,s}$=40 kW/m^2; t=200s.

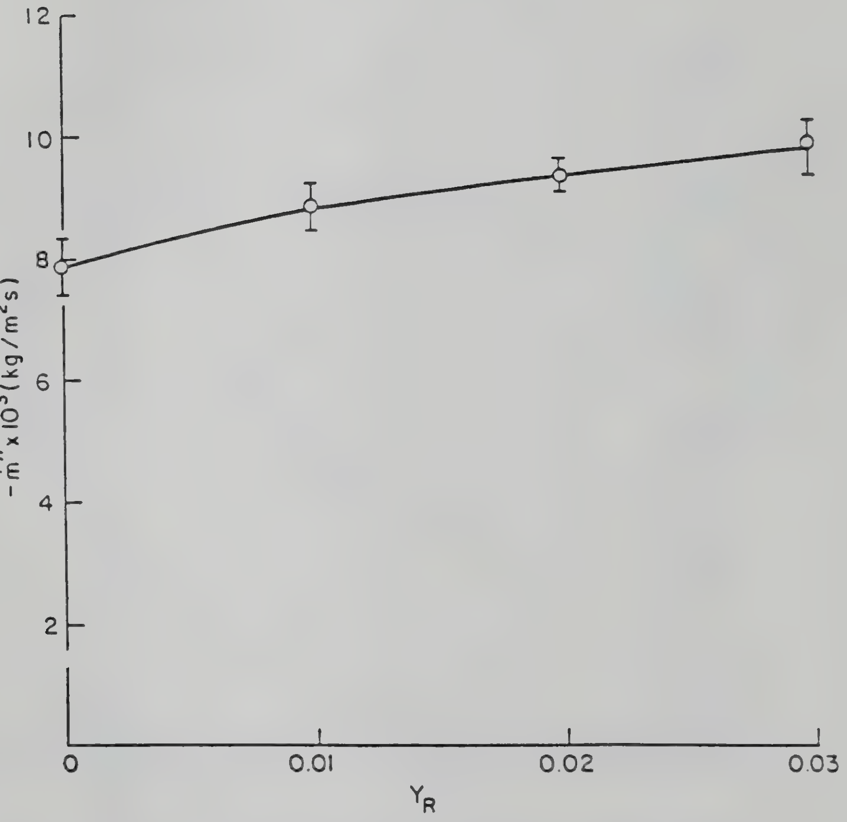

Figure 2.15 Mass loss rate vs. retardant concentration; $\dot{q}''_{ab,s} = 40$ kW/m^2; t=200s.

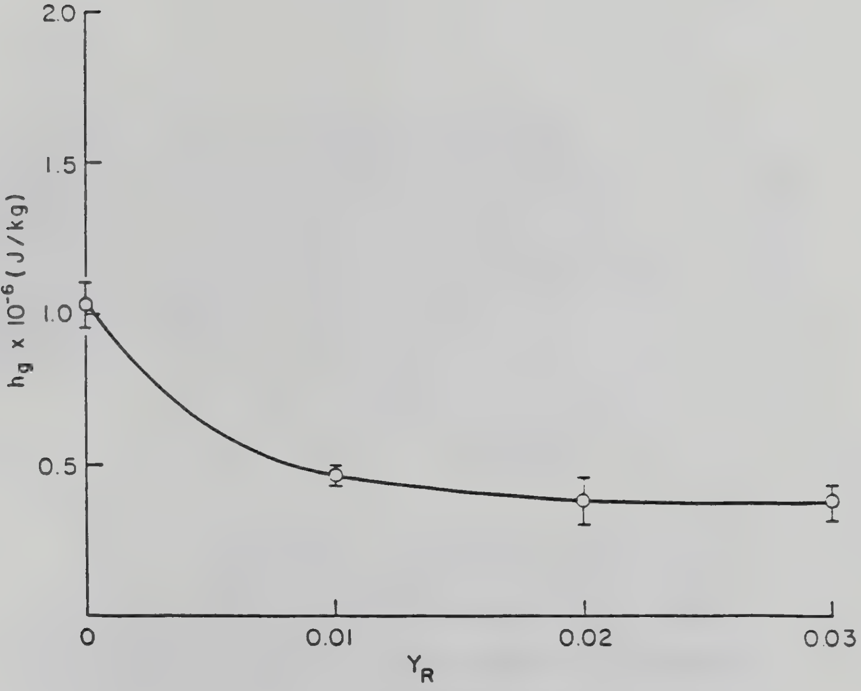

Figure 2.16 Heat of gasification vs. retardant concentration; $\dot{q}''_{ab,s}$ =40 kW/m^2; t=200s.

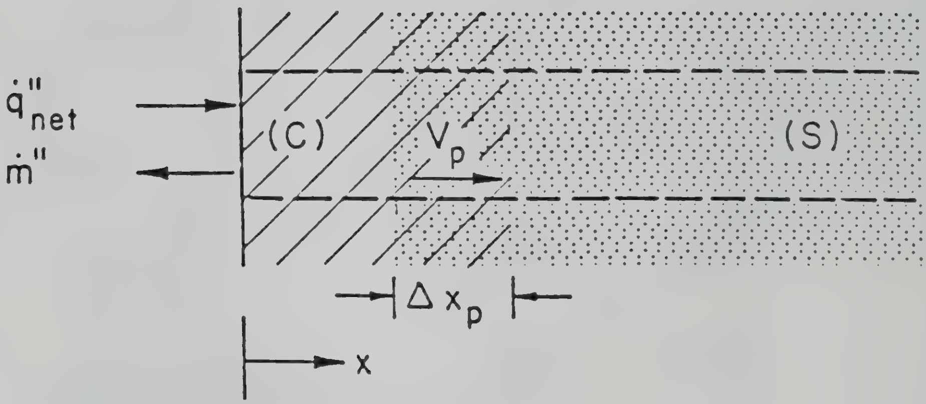

Figure 3.1 Control volume used in pyrolysis analysis of a charring fuel.

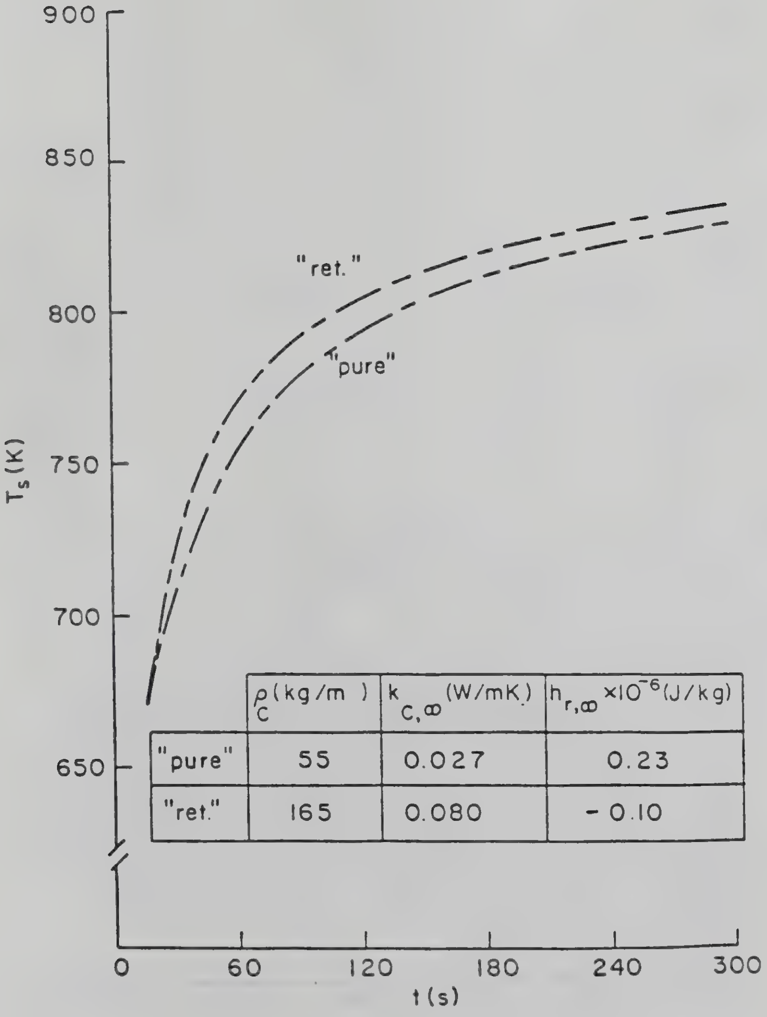

	ρ_C (kg/m)	$k_{C,\infty}$ (W/mK)	$h_{r,\infty} \times 10^{-6}$ (J/kg)
"pure"	55	0.027	0.23
"ret."	165	0.080	- 0.10

Figure 3.2 Theoretical surface temperature vs. time for pure and retarded cellulose.

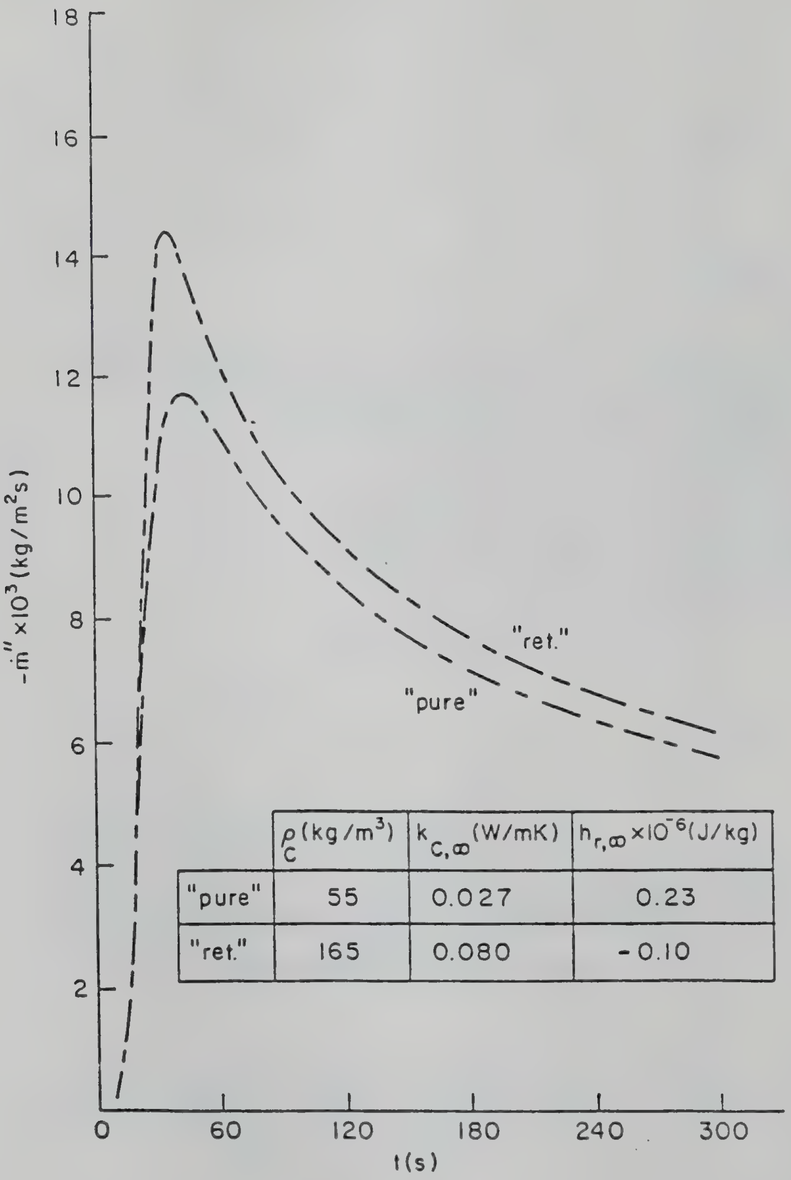

	ρ_C (kg/m^3)	$k_{C,\infty}$ (W/mK)	$h_{r,\infty} \times 10^{-6}$ (J/kg)
"pure"	55	0.027	0.23
"ret."	165	0.080	-0.10

Figure 3.3 Theoretical mass loss rate vs. time for pure and retarded cellulose.

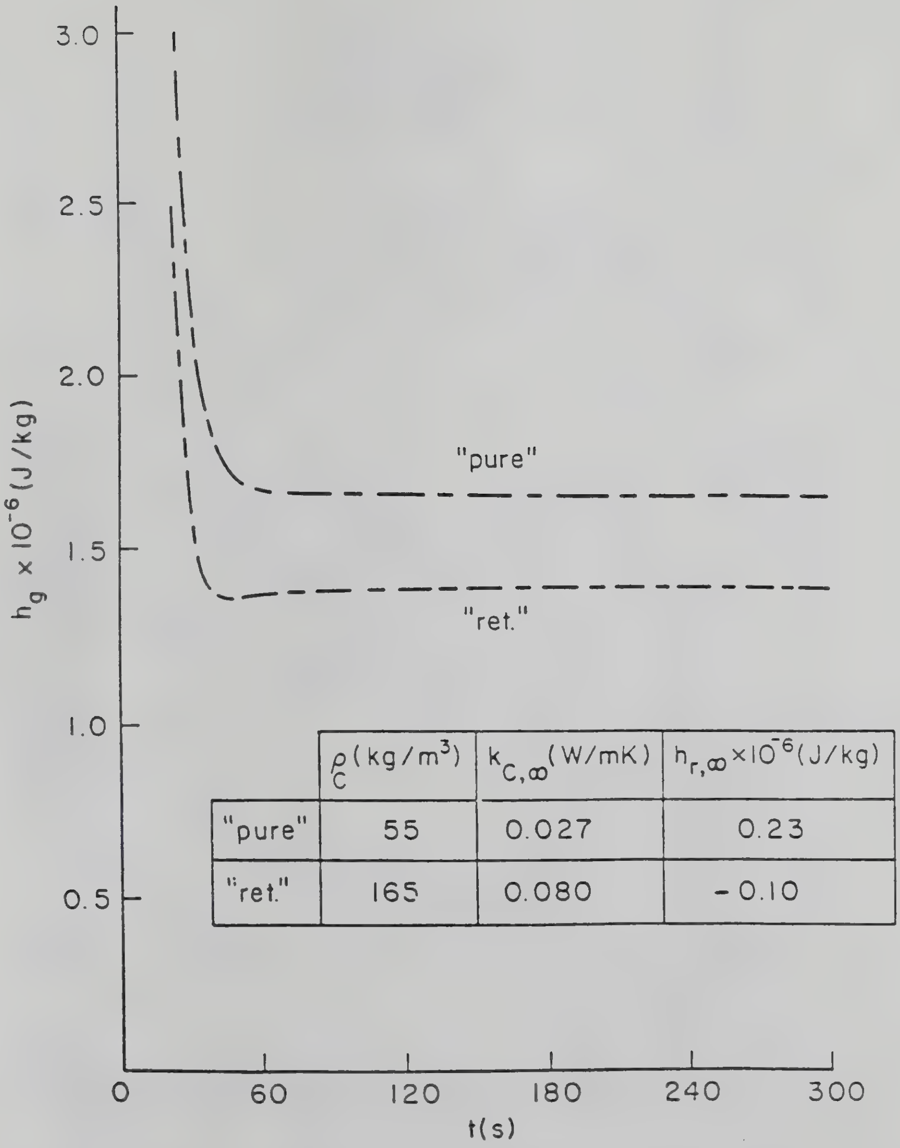

	ρ_C (kg/m^3)	$k_{C,\infty}$ (W/mK)	$h_{r,\infty} \times 10^{-6}$ (J/kg)
"pure"	55	0.027	0.23
"ret."	165	0.080	- 0.10

Figure 3.4 Theoretical heat of gasification vs. time for pure and retarded cellulose.

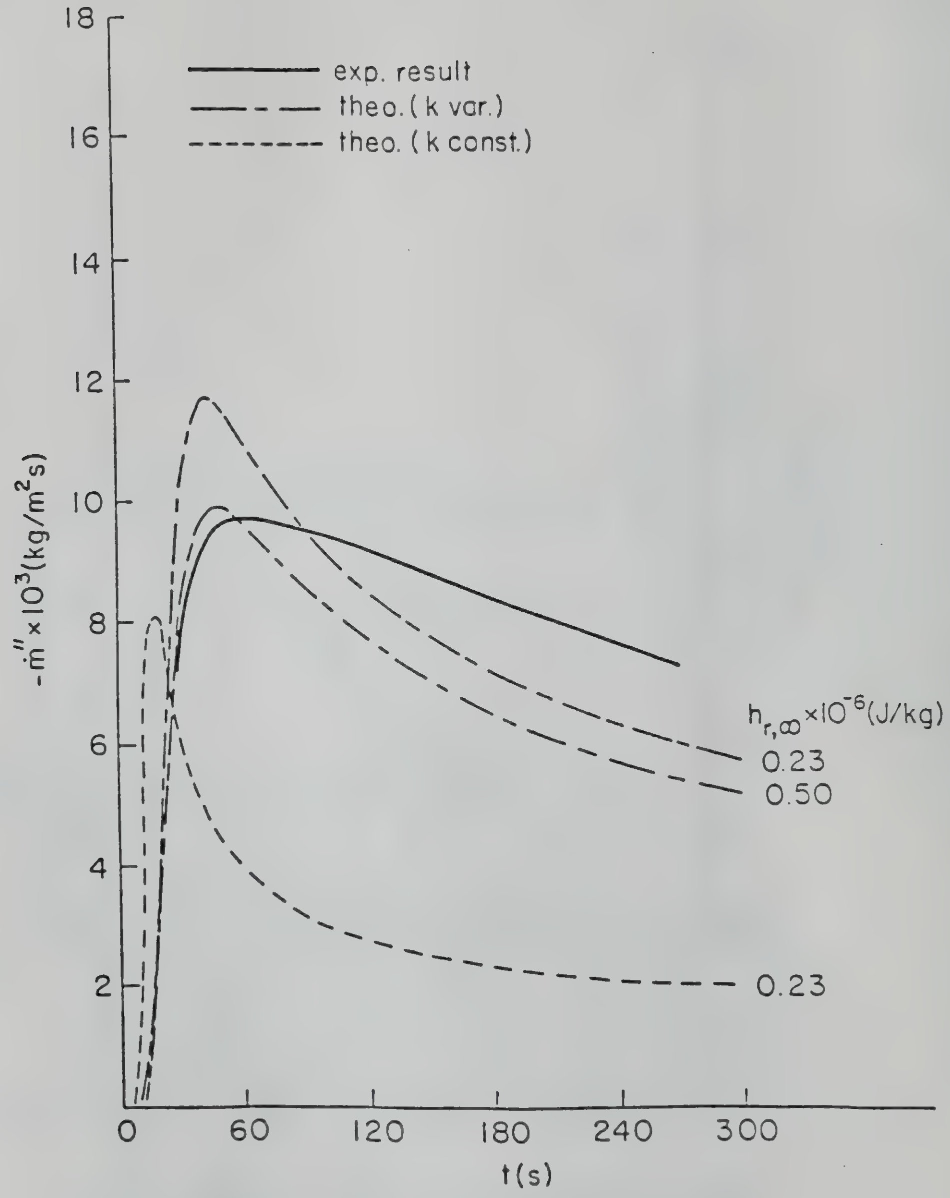

Figure 3.5 Experimental and theoretical mass loss rate vs. time for pure cellulose; Y_R=0.

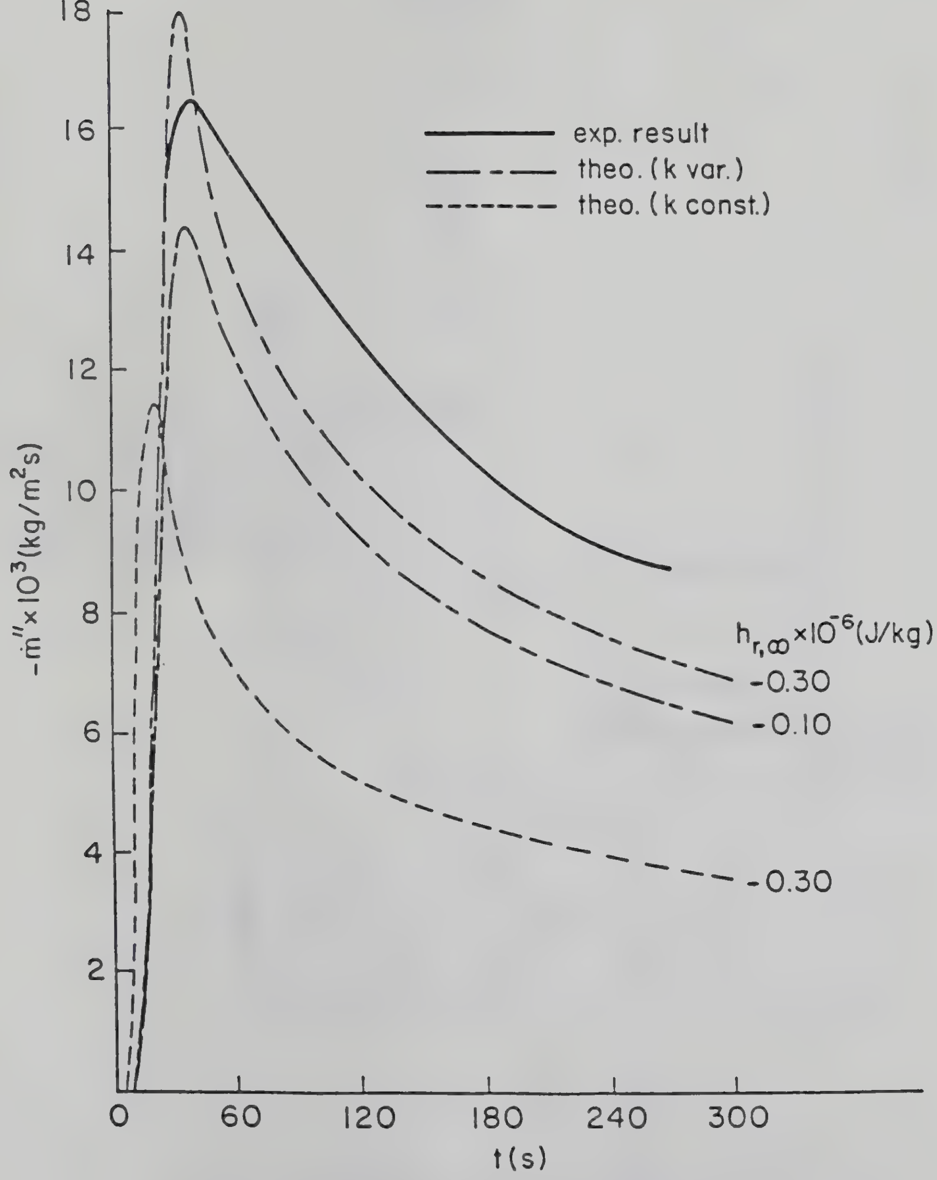

Figure 3.6 Experimental and theoretical mass loss rate vs. time for retarded cellulose; Y_R=0.03.

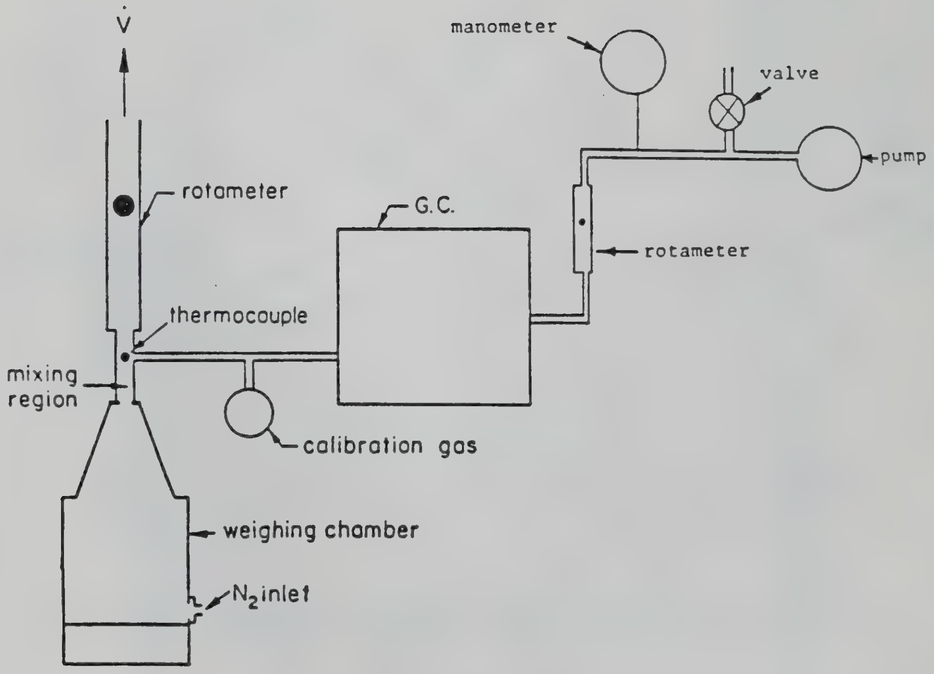

Figure 4.1 Schematic drawing of apparatus used in measurements of gaseous products.

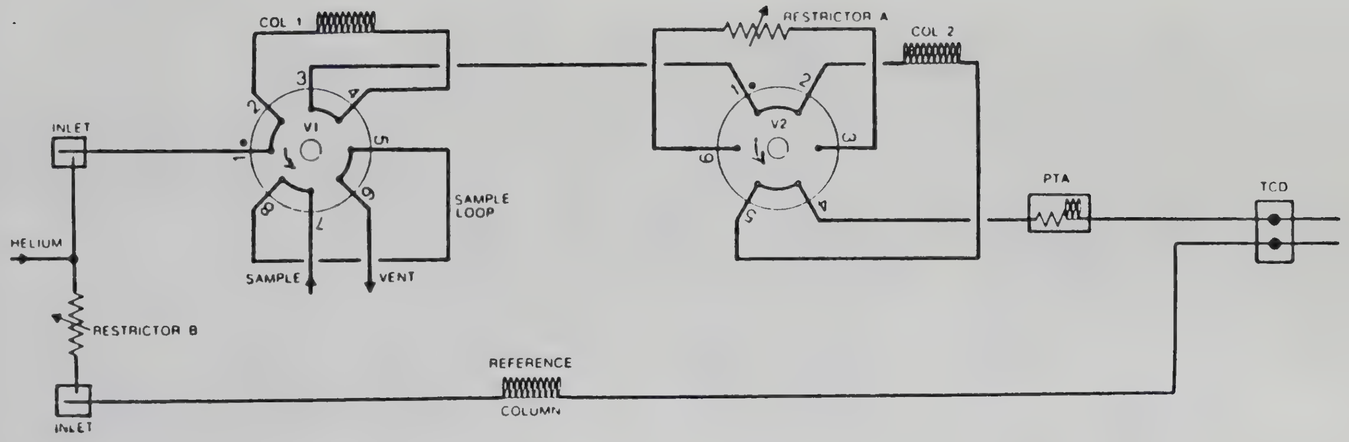

Figure 4.2 Schematic drawing of GC flow system.

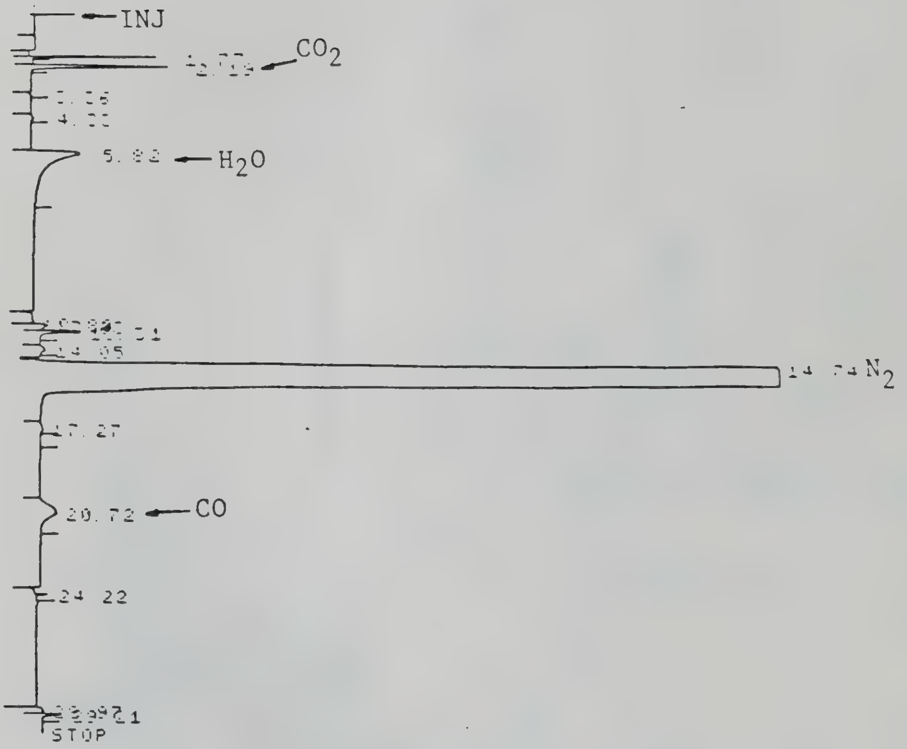

```
                              AREA %
  RT    TYPE       AREA
 1.77                491                 .096 02
 2.19               1063                 .207 9
 3.36                 10                 .001 956
 4.00                 49                 .009 582
 5.82               2244                 .438 8
12.80                241                  047 13
13.03     M          280                 .054 76
13.31     M          382                 .074 7
14.05                101                  019 75
14.74             505071               98.77
17.27     T           77                  015 06
20.72                714                  139 6
24.22                131                  025 62
28.97                298                  058 28
29.21     M          201                 .039 31
```

Figure 4.3 An example of output of GC analysis; Y_R=0.03; t=180s.

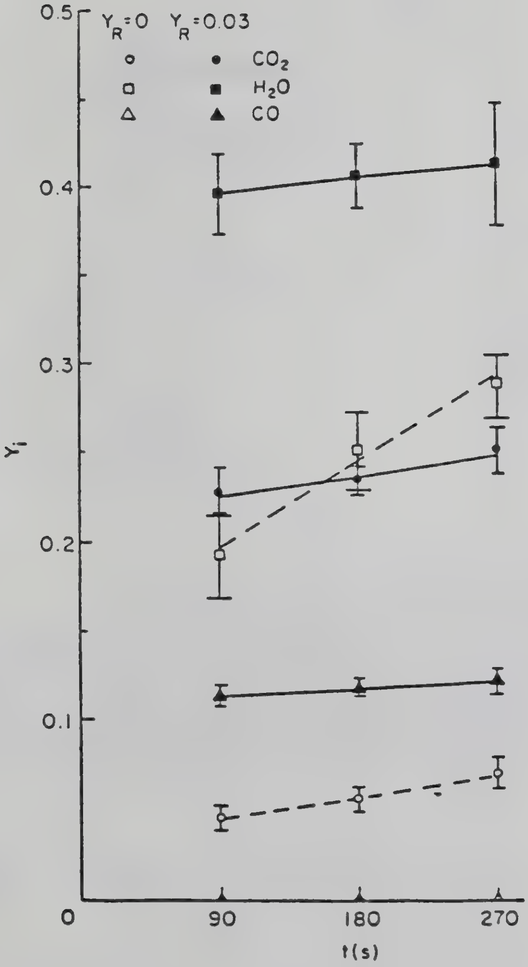

Figure 4.4 Mass fraction of CO_2, H_2O and CO vs. time for pure and retarded cellulose samples; $\dot{q}''_{ab,s}=40$ kW/m^2.

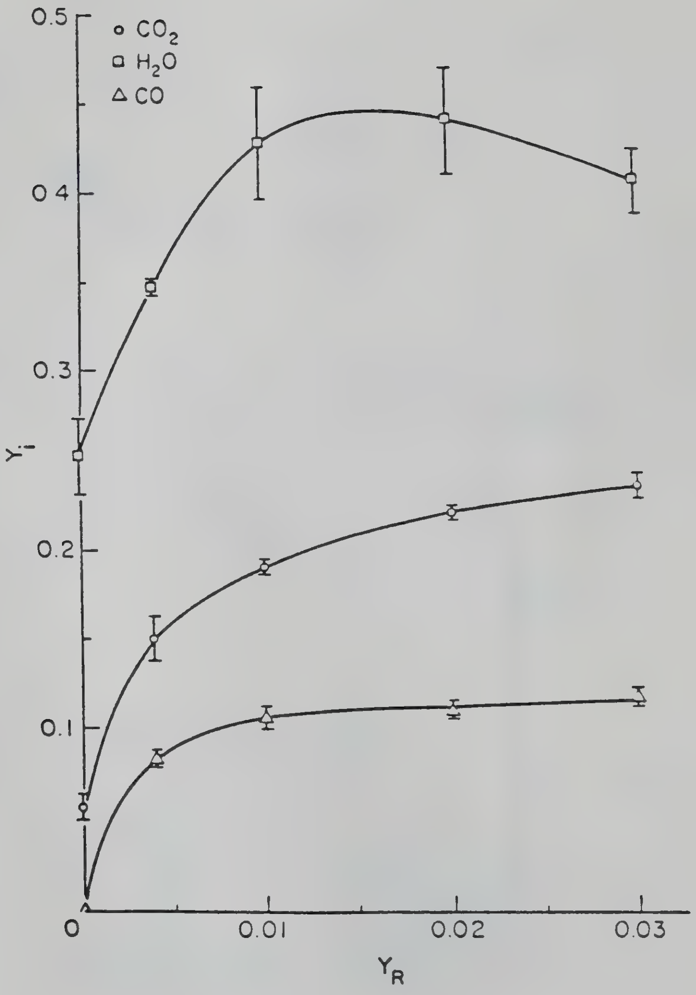

Figure 4.5 Mass fraction of CO_2, H_2O and CO vs. retarded concentration; $\dot{q}''_{ab,s}=40\ kW/m^2$; t=180s.

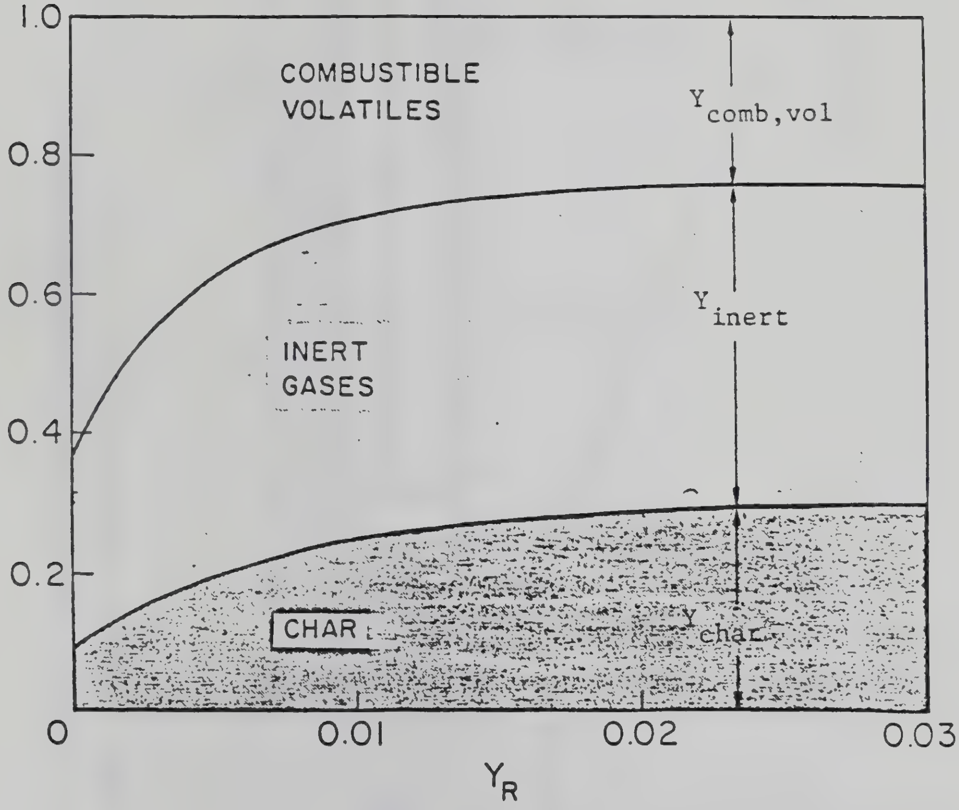

Figure 5.1 Effects of retardant concentration on major products of cellulose pyrolysis.

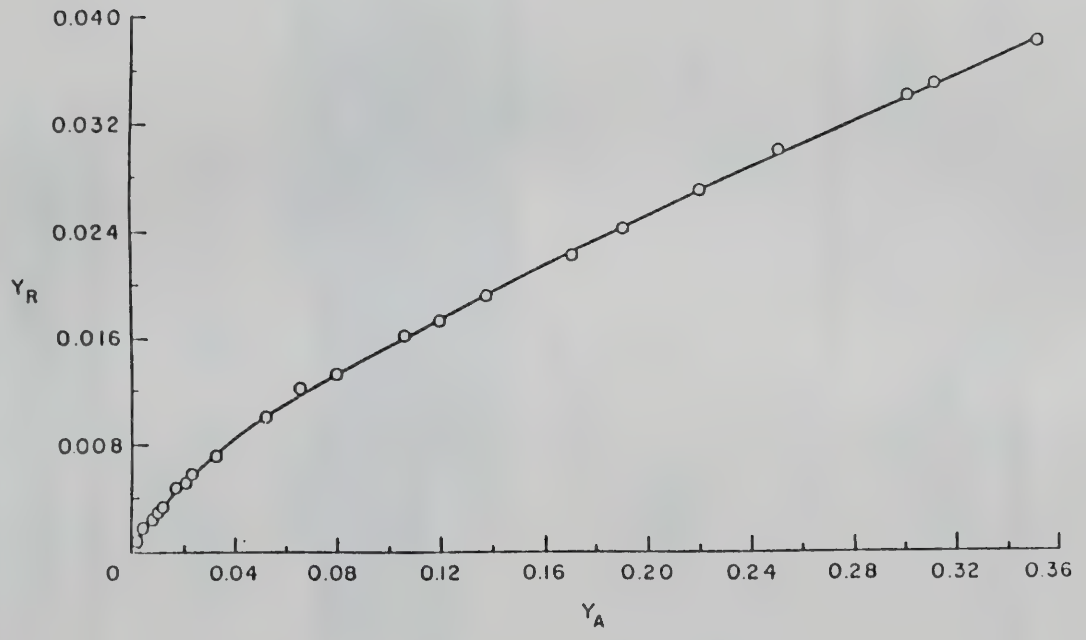

Figure A.1 NaOH retardant concentration in the sample, Y_R, as a function of retardant concentration in the cellulose slurry, Y_A.

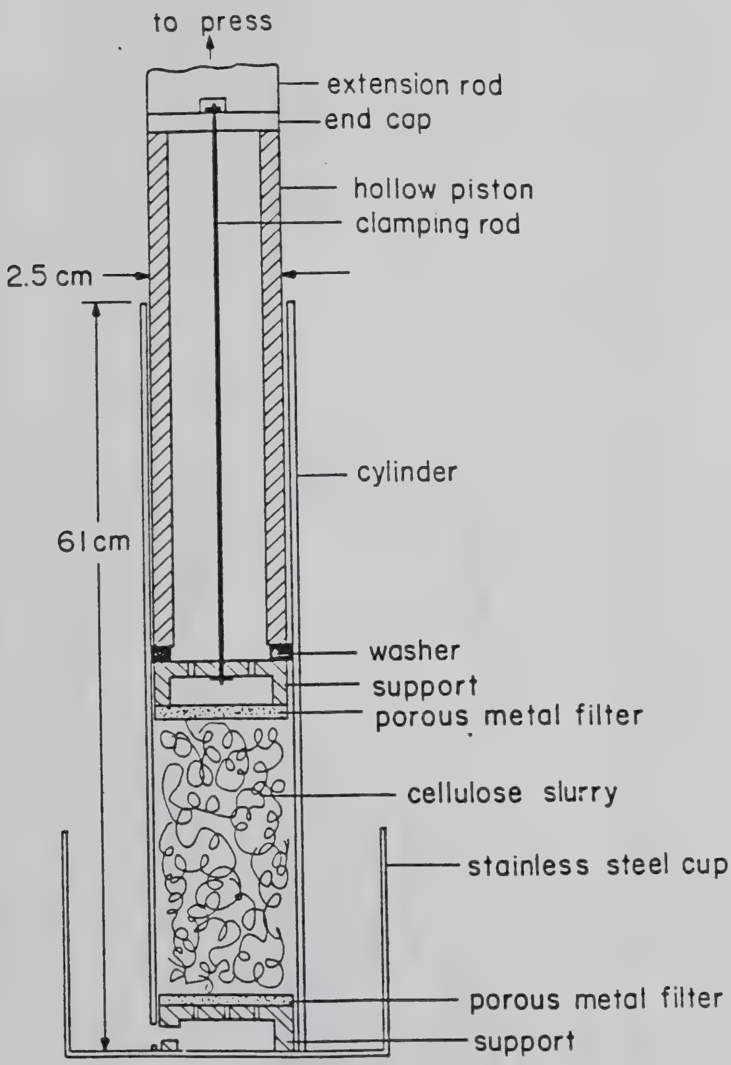

Figure A.2 Schematic drawing of the apparatus for making cellulose samples.

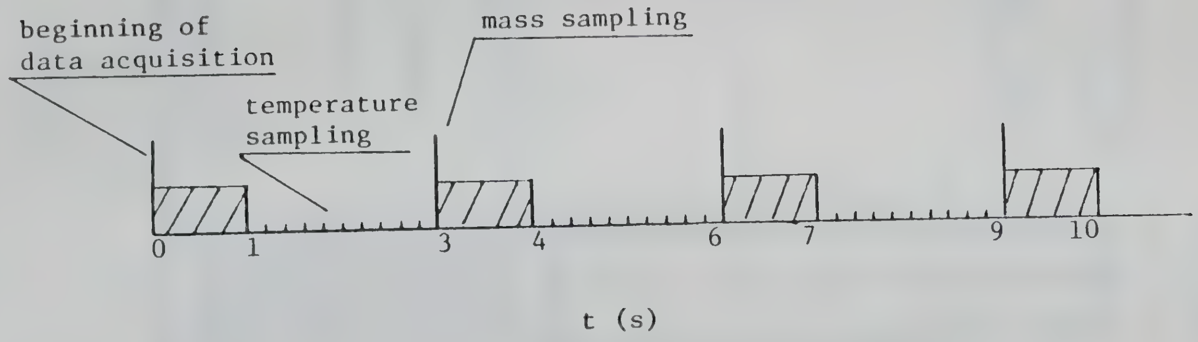

Figure B.1 Sequence of temperature and mass sampling times.

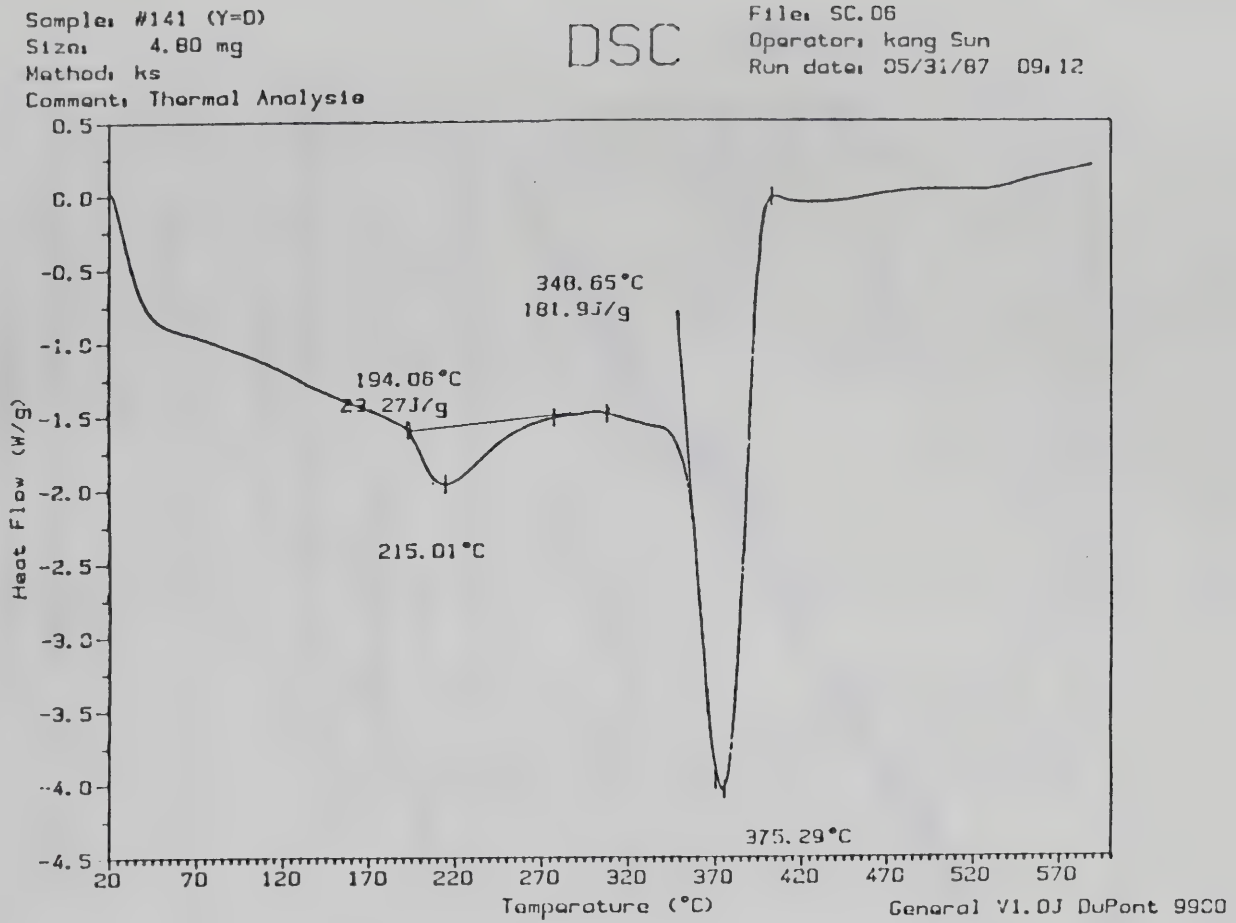

Figure C.1 An example of DSC output of differential heat flow vs. temperature.

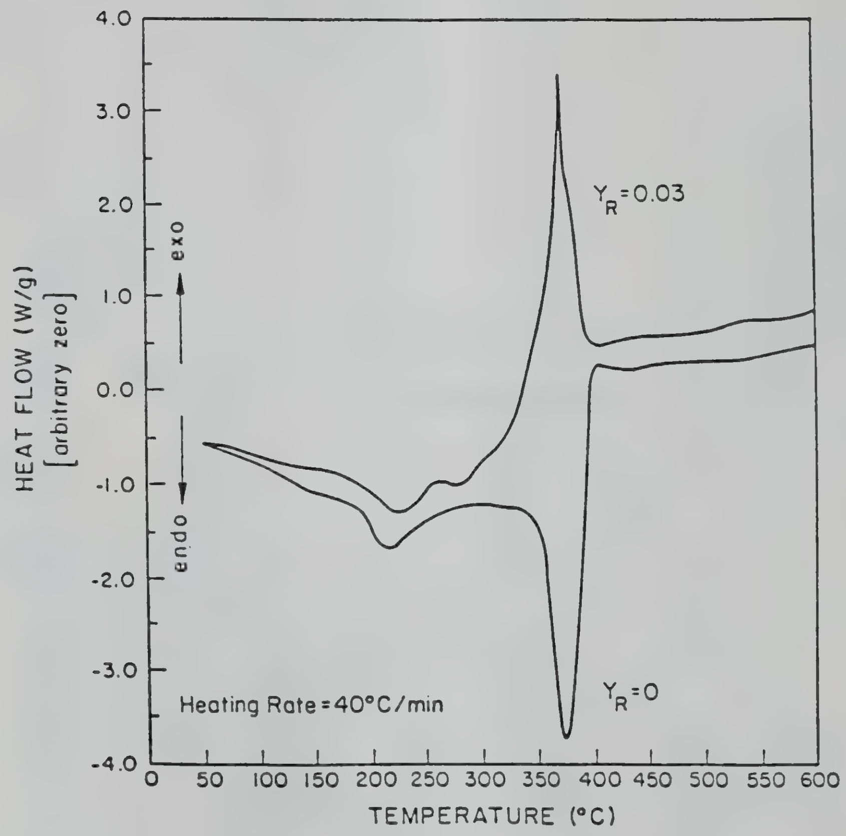

Figure C.2 Comparison of DSC results for pure and retarded cellulose samples.

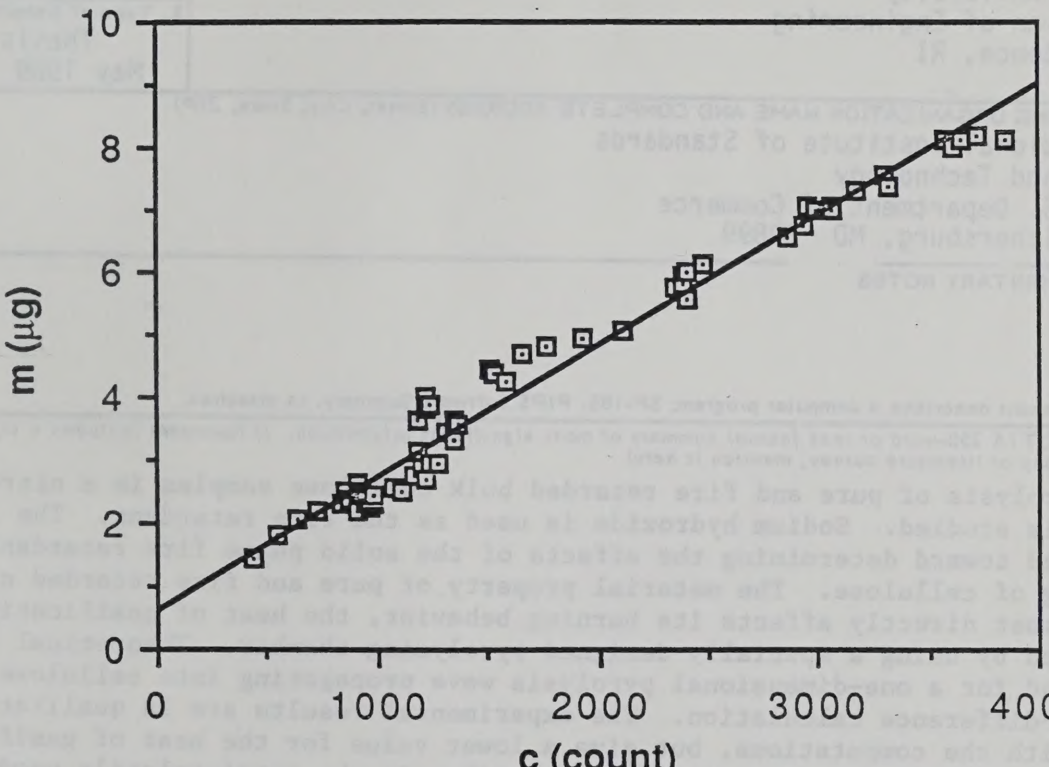

Figure D.1 Calibration curve of water mass vs. integrator count.

FORM NBS-114A (REV.11-84)

U.S. DEPT. OF COMM. **BIBLIOGRAPHIC DATA SHEET** *(See instructions)*	1. PUBLICATION OR REPORT NO. NIST/GCR-89/566	2. Performing Organ. Report No.	3. Publication Date June 1989

4. TITLE AND SUBTITLE

An Experimental Study of the Pyrolysis of Pure and Fire Retarded Cellulose

5. AUTHOR(S)

Yi Chen

6. PERFORMING ORGANIZATION *(If joint or other than NBS, see instructions)*

Brown University
Division of Engineering
Providence, RI

7. Contract/Grant No.

Grant No. 60NANB8D0851

8. Type of Report & Period Covered

Thesis
May 1989

9. SPONSORING ORGANIZATION NAME AND COMPLETE ADDRESS *(Street, City, State, ZIP)*

National Institute of Standards
and Technology
U.S. Department of Commerce
Gaithersburg, MD 20899

10. SUPPLEMENTARY NOTES

☐ Document describes a computer program; SF-185, FIPS Software Summary, is attached.

11. ABSTRACT *(A 200-word or less factual summary of most significant information. If document includes a significant bibliography or literature survey, mention it here)*

The pyrolysis of pure and fire retarded bulk cellulose samples in a nitrogen atmosphere is studied. Sodium hydroxide is used as the fire retardant. The study is directed toward determining the effects of the solid phase fire retardant on the burning of cellulose. The material property of pure and fire retarded cellulose which most directly affects its burning behavior, the heat of gasification, is measured by using a specially designed pyrolyzing chamber. Theoretical results are obtained for a one-dimensional pyrolysis wave propagating into cellulose by using a finite-difference calculation. The experimental results are in qualitative agreement with the computations, but give a lower value for the heat of gasification. The mass fraction of noncombustible volatiles in the total volatile products of pyrolysis, the stoichiometric oxygen/fuel ratio of the combustible volatile are also obtained as experimental results. These data have been obtained because they are needed as inputs in diffusion flame calculations. The experimental data show that sodium hydroxide acts as a catalyst in the pyrolysis of cellulose. Its addition leads to decreases in the heat of gasification and the mass fraction of noncombustible volatiles in the total volatiles, and to increases in stoichiometric ratio and the heat of combustion of combustible volatiles, thereby has a dual effect on cellulose burning.

12. KEY WORDS *(Six to twelve entries; alphabetical order; capitalize only proper names; and separate key words by semicolons)*

cellulose; flame resistant materials; flame retardants; gasification; pyrolysis; sodium hydroxides

13. AVAILABILITY

☒ Unlimited
☐ For Official Distribution. Do Not Release to NTIS
☐ Order From Superintendent of Documents, U.S. Government Printing Office, Washington, DC 20402.
☒ Order From National Technical Information Service (NTIS), Springfield, VA 22161

14. NO. OF PRINTED PAGES

146

15. Price

$19.95

USCOMM-DC 85-6006